Mechanisms of Stem Cell Regulation in Medulloblastoma

Mechanisms of Stem Cell Regulation in Medulloblastoma

A dissertation presented

by

Ronnie Yoo

to

The Division of Medical Sciences

in partial fulfillment of the requirements

for the degree of

Doctor of Philosophy

in the subject of

Biological and Biomedical Sciences

Harvard University

Cambridge, Massachusetts

April 2013

Advisor: Dr. Laurie Jackson-Grusby Ronnie Yoo

Mechanisms of Stem Cell Regulation in Medulloblastoma

Abstract

Medulloblastoma, the most common pediatric malignant brain tumor, is comprised of a heterogeneous group of tumors with distinct molecular subtypes and clinical outcomes. In particular, tumors with a cancer stem cell (CSC) population have been observed to be more resistant to conventional therapies, necessitating the elucidation of pathways important in this population. Work in our lab has shown that neurosphere culture-enriched cells from *Ptch1*$^{LacZ/+}$*;Trp53*$^{-/-}$ mouse medulloblastomas exhibit properties of self-renewal, expression of neural stem cell (NSC) markers and potent tumor-initiation. The pathway dependencies and mechanisms of self-renewal in these medulloblastoma neurospheres (MBNS) have not yet been characterized.

Reprogramming and dedifferentiation of tumor cells have been proposed as a mechanism for the establishment and maintenance of CSC. To test this, we asked if the endogenous genetic program of the *Ptch1*$^{LacZ/+}$*;Trp53*$^{-/-}$ MBNS was sufficient for the reprogramming of tumor cells into a pluripotent-like state *in vitro*. We observed that MBNS, unlike normal cerebellar stem cells (CbSC), were able to form embryonic stem (ES) cell-like colonies upon growth in ES culture conditions. *Klf4*, a reprogramming factor, was identified to be functionally important in maintaining both MBNS plasticity upon transfer to ES culture conditions and clonal self-renewal as neurospheres. Further, *Klf4* expression compensated for Stat3 inhibition in a Stat3-

independent manner for the maintenance of survival gene expression, thus identifying a novel compensatory transcriptional mechanism enhancing the survival of CSC.

We further characterized *Sox2*, a NSC marker highly expressed in the MBNS, as a definitive marker for the isolation of self-renewing CbSC from postnatal day 7 wild-type (WT) animals. Moreover, *Sox2* expression was maintained in the cerebella of 3-week-old *Ptch1*$^{LacZ/+}$*;Trp53*$^{-/-}$ animals and the prospective isolation of the *Sox2*-positive cells enriched for the aberrantly persisting, self-renewing cells, which are absent in by 3 weeks in WT animals. Thus, we have validated an endogenous *Sox2-GFP* reporter system that allows for the prospective isolation of the aberrant tissue stem cells from *Ptch1*$^{LacZ/+}$*;Trp53*$^{-/-}$ animals, which will be valuable for furthering our understanding of stem cell regulation during medulloblastoma tumorigenesis.

Table of Contents

List of Abbreviations

Acute myeloid leukemia	AML
Adenomatous polyposis coli	APC
Alkaline phosphatase	AP
Basic fibroblast growth factor	bFGF
Beta-catenin	CTNNB1
Beta-galactosidase	LacZ
Cancer stem cells	CSC
Cerebella	Cb
Cerebellar stem cells	CbSC
Cre-recombinase	Cre
Embryonic stem	ES
Epidermal growth factor	EGF
External granule layer	EGL
Extreme limiting dilution assay	ELDA
Fetal bovine serum	FBS
Fluorescence-activated cell sorting	FACS
Glial fibrillary acidic protein	GFAP
GLI-Krüppel family member	GLI
Granule cell progenitor	GCP
Green fluorescent protein	GFP
Hairy and enhancer of split-1	Hes1
Hematopoietic stem cells	HSC
Hematoxylin and eosin	H&E
Induced pluripotent cells	iPS
Janus kinase	Jak
Knockdown	kd
Krüppel-like factor 4	Klf4
Large cell anaplastic	LCA

Leukemia inhibitory factor	LIF
Mammalian target of rapamycin	mTOR
Medulloblastoma neurosphere	MBNS
Mitogen-activated protein kinase	MAPK/Erk
Mitogen-activated protein kinase kinase	Mek
Mouse embryonic fibroblast	MEF
Myelocytomatosis oncogene	MYC
Myeloid/lymphoid leukemia	MML
Neural stem cell	NSC
Neurosphere	NS
Non-obese diabetic/severe combined immunodeficiency	NOD/SCID
Octamer-binding transcription factor 4	Oct4
Oligodendrocyte transcription factor 2	Olig2
Patched-1	PTCH1
Phosphoinositide 3-kinase	PI3K
Retinoblastoma protein	Rb
Short hairpin RNA	shRNA
Smoothened	SMO
Sonic hedgehog	SHH
Suppressor of cytokine signaling 3	Socs3
Suppressor of fused	SUFU
Transcriptional start site	TSS
Transformation related protein 53	Trp53
Wild-type	WT
Wingless	WNT

List of Figures

List of Tables

Acknowledgements

My graduate studies would not have been possible without the support of many people. Words cannot describe my gratitude for everyone who has encouraged and helped me along the way. Firstly, I would like to thank Dr. Laurie Jackson-Grusby, my thesis advisor, for allowing me the opportunity to work in her lab. I am greatly appreciative for her guidance, patience and mentorship throughout my time in the lab. I am grateful for my DAC members, Drs. Ramesh Shivdasani, David Frank and Richard Mass, for being insightful, supportive, encouraging throughout the years. I would also like to extend my appreciation to the Examination Committee members, Drs. David Langenau, David Breault, and Charlotte Kuperwasser. Thank you to all past and present members of the Jackson-Grusby lab. My project would not have been possible without the efforts of Chewie Lin, Juliana Brown, and Chris Kanner in establishing the Ptc;p53 tumor system. I am greatly appreciative for their teaching, training, and advice. I thank Bernd Zetsche and Ann Ran for their company and all the laughter. I also greatly appreciate all the help provided by Guangwen Wang, Leah Liu, Daniel Park, David Dai and the guidance provided by my collaborator Suhu Liu (Frank lab). I would also like to extend my gratitude to Giri Buruzula and Joyce Lavecchio at the Joslin Flow Core and Ronald Mathieu at the CHB Flow Core for technical support and expertise; Konrad Hochedlinger lab for the collaboration (*Sox2-GFP* mice and construct); David Sabatini lab for reagent support (Rapamycin, Torin). Thank you to all of the members of the Pathology Department on Enders 11, the BBS office (including Tucker), friends and colleagues in BBS/DMS. I am deeply grateful to my lifelong support network of friends, both near and far. Thank you Harrison for just everything. And lastly my family- Mom, Luther, and Dad, whom I miss very, very much. Thank you for your endless love, support and encouragement. I would not have made it without you.

Chapter 1 : Introduction

Medulloblastoma Overview

Medulloblastoma, a primitive neuroectodermal tumor arising in the cerebellum, is the most common malignant childhood brain cancer and accounts for about 20% of pediatric brain tumors (Ellison *et al.*, 2003). Peak incidences occur in children from ages 3-4 and ages 8-9 and about 10% of cases occur in infants (Crawford *et al.*, 2007). While overall survival rates of medulloblastoma patients are about 80%, aggressive and non-specific conventional treatment strategies usually result in long-term cognitive deficits and neuroendocrinal abnormalities (Ellison *et al.*, 2003). Furthermore, aggressive tumor subtypes with a disseminated phenotype are associated with a higher frequency of relapse and have poor prognoses (Zeltzer *et al.*, 1999; Northcott *et al.*, 2011b). Such relapse mechanisms have been attributed to a subset of cancer stem cells (CSC) in the bulk tumor (Clarke *et al.*, 2006), which have, in fact, been identified in human medulloblastomas (Singh *et al.*, 2004). In the recent decade, immense advances have been made in the elucidation of the molecular underpinnings of medulloblastoma tumorigenesis (Taylor *et al.*, 2012), while the understanding of the tumor-initiating cells remains relatively sparse. As such, the identification of molecular pathways involved in CSC homeostasis could have potential ramifications for better risk-stratification and allow for the development of targeted therapeutic strategies to increase efficacy and reduce long-term sequelae in patients.

Clinical features of human medulloblastoma

The World Health Organization (WHO) classifies all medulloblastomas as malignant and invasive grade IV tumors. Based on the WHO classification, there are five histological variants of human medulloblastoma: classic, desmoplastic/nodular, extensive nodularity, large cell, and

anaplastic (Louis *et al.*, 2007). Classic medulloblastomas, which make up about ~70% of all cases (Ellison *et al.*, 2011) are characterized by sheets of undifferentiated cells with high nuclei to cytoplasm ratios. Desmoplastic/nodular and extensive nodularity tumors are closely related variants, both characterized by nodules (pale islands) of tumor cells undergoing neuronal differentiation, interspersed with stroma composed of reticulin (type III collagen) fibers. The internodular, reticulin regions are reduced in the extensive nodularity tumors compared to the desmoplastic tumors. The last two variants, the anaplastic and large cell medulloblastomas, which are cytologically similar, are marked with high mitotic activity and atypical nuclear pleomorphisms and are the most aggressive and treatment-resistant tumors.

Current risk stratification of patients is based on age, extent of surgical resection, and metastatic status. Standard risk patients include those greater than 3 years of age, with complete or near complete surgical resection of the tumor (<1.5cm^2 residual tumor) and absence of leptomeningeal dissemination; all other patients are classified as high risk (Zeltzer *et al.*, 1999). Long-term survival rates of standard risk patients are 60-80%, but surviving patients are often subject to a variety of long-term sequelae such as cognitive decline and neuroendocrinal defects, due to the non-specific and aggressive nature of standard treatment modalities, which entail post-operative radiation and chemotherapy (Dennis *et al.*, 1996; Crawford *et al.*, 2007). While efforts have been made to reduce the doses of irradiation, this has been associated with a subsequent increase in the risk of relapse (Thomas *et al.*, 2000). Furthermore, in the most recently published study of long-term effects of patients treated for standard-risk medulloblastoma, lower doses of radiospinal therapy than the standard dose (24Gy vs. 36Gy), nevertheless resulted in progressive decline in intellectual and academic scores (Ris *et al.*, 2013). Currently, young age at diagnosis is consistently the most important risk factor in determining if neurocognitive defects will follow a

standard treatment regime (Ris *et al.*, 2013). Given the non-specific modalities of the current therapies and their significant developmental impact, especially in young patients, a better understanding of specific molecular pathways involved in medulloblastoma tumorigenesis is crucial for the development of targeted therapies and improved risk stratification.

Cerebellar development

The cerebellum has been referred to as the "coordination center" of the brain, playing a role in balance and the fine tuning of motor movements (Wang and Zoghbi, 2001). In addition to the well-established role of the cerebellum in motor control, it has also been implicated in higher cognitive functions including spatial memory, speech and sensory motor learning (Hatten and Roussel, 2011; Marino, 2005). In humans and mice, the formation of the mature cerebellum is a protracted developmental process that continues postnatally for months after birth in humans and weeks in mice. Abnormalities during cerebellar development lead to developmental defects affecting balance and coordination such as Chiari malformations and Dandy-Walker syndrome or may lead to malignant transformation, resulting in medulloblastoma (Wang *et al.*, 2003). Therefore, an understanding of the genetic pathways regulating cerebellar development and the cell types present during the process is crucial in studying the mechanisms of tumorigenesis.

During mouse embryogenesis, the cerebellum arises from two embryonic germinal zones, the ventricular zone (VZ) and the rhombic lip (RL) (Figure 1-1a). In mice, by embryonic day 14 (E14), early progenitors in the ventricular zone, marked by *Ptf1* expression (Hoshino *et al.*, 2005), cease proliferation and begin to differentiate to give rise to calbindin-positive Purkinje neurons. Between E14-E17, the postmitotic Purkinje neurons subsequently migrate radially along glial fibers to establish the cerebellar field (Hatten and Heintz, 1995), by secreting Sonic

Hedgehog (SHH), a factor important for the proliferation and differentiation of granule neurons (Wechsler-Reya and Scott, 1999). In addition to Purkinje neuron fate determination, the *Ptf1*-expressing cells from the ventricular zone are also thought to give rise to other GABAergic neurons in the cerebella including the Golgi, basket, and stellate cells (Hoshino *et al.*, 2005).

The granule neurons of the cerebella are derived from another germinal epithelium, known as the rhombic lip (Figure 1-1a), located in between the neural tube and the fourth ventricle. Around E13, *Math1*-positive cells migrate out of the rhombic lip and coat the surface of the developing cerebellar field to form the external granule layer (EGL) (Hatten and Heintz, 1995; Ben-Arie *et al.*, 1997), which by postnatal day 0 (P0) is composed of a single layer of undifferentiated cells (Figure 1-1b). Beginning around postnatal day 7 (P7), the majority of the *Math1*-positive cells in the EGL form a zone of proliferating granule cell progenitors (GCP) that are driven by SHH secreted by the Purkinje neurons (Figure 1-1b, c) (Wechsler-Reya and Scott, 1999). This large clonal expansion continues until P15, after which the post-mitotic granule cells exit the cell cycle, downregulate *Math1* expression and move inwards from the EGL along the radial fibers of Bergmann glia cells to form the internal granule layer (IGL) (Hatten and Heintz, 1995; Hatten *et al.*, 1997). In normal development, cerebellar development is largely complete by P21, when the EGL diminishes as the mature granule neurons migrate into the IGL, leaving the trailing processes in the molecular layer (Wechsler-Reya and Scott, 2001). Dysregulated granule cell proliferation during cerebellar development results in the formation of an abnormally thickened EGL, containing aberrantly proliferative "rests", which may subsequently lead to tumorigenesis upon acquisition of additional mutations (Kim *et al.*, 2003).

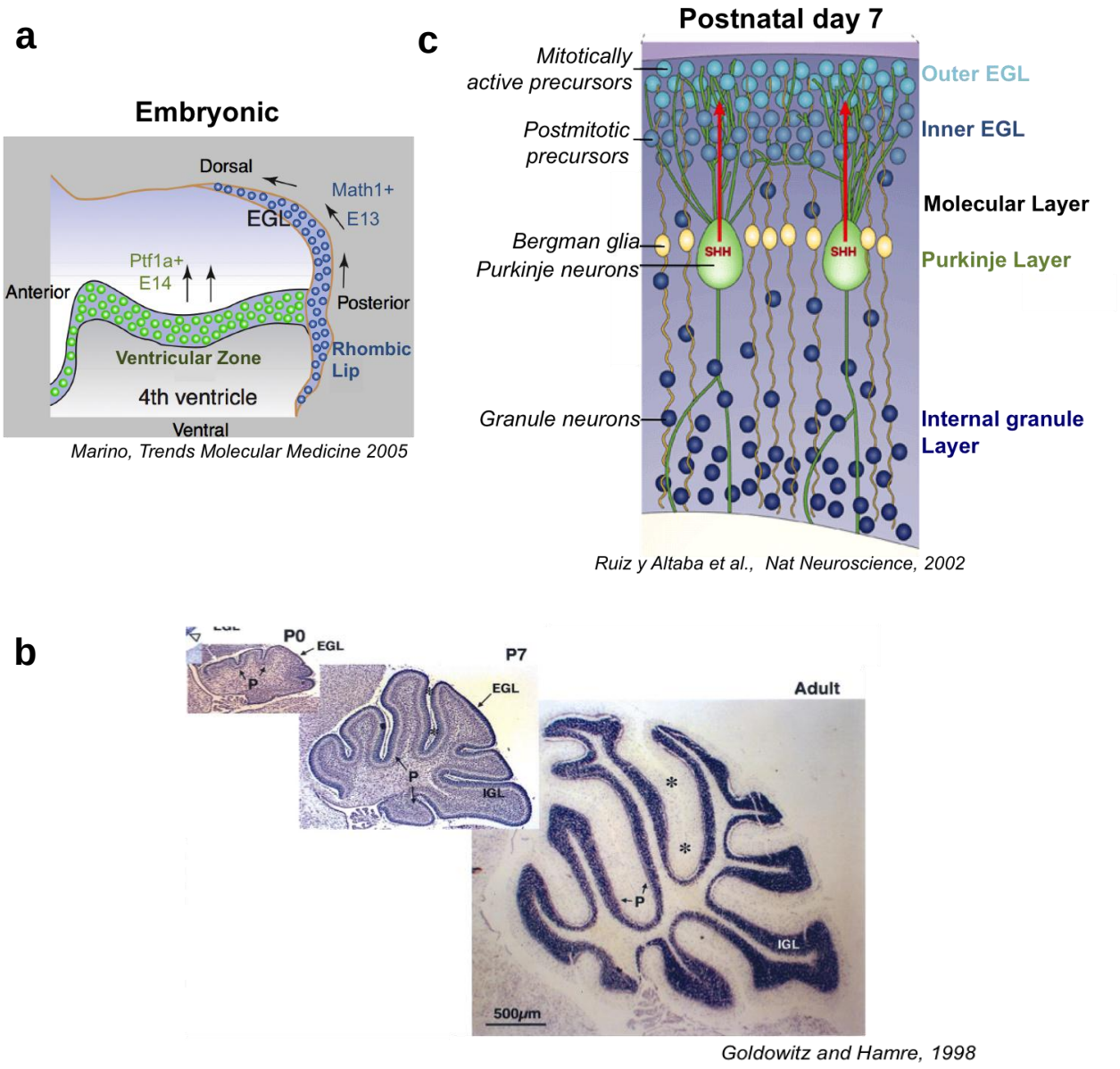

Figure 1-1 Overview of mouse cerebellar development through embryonic and postnatal development

(a) Around E13, *Math1*-expressing cells from the rhombic lip migrate rostrally over the surface of the cerebellum to form the external granule layer (EGL). Purkinje cells are derived from the *Ptf1*-expressing progenitors from the ventricular zone around E14 and migrate radially. (b) Histology of sagittal sections of mouse cerebella corresponding to the different stages during cerebellar development: postnatal day 0 (P0), day 7 (P7), and adult. "P" denotes the Purkinje cell layer. Images are taken from Goldowitz and Hambre, 1998. (c) During the large clonal expansion and differentiation of the granule cell progenitors that occur during the first 2-3 weeks, postmitotic granule neurons migrate inwards to form the internal granule layer (IGL). They move past the Purkinje layer, which secrete SHH to regulate the proliferation of the progenitors, leaving behind processes in the molecular layer. Non-neuronal cell types in the cerebellum include the Bergmann glia and oligodendrocytes (not shown). Figures are modified from Marino 2005 and Ruiz y Altaba et al., Nat Neuroscience 2002.

Cerebellar Stem Cells

In addition to the granule neurons and Purkinje cells, which are the two major neuronal cells in the cerebellum, other cell types of the cerebellum include the Golgi, stellate and basket interneurons, the Bergmann glia (located at the border of Purkinje cell layer and the IGL) and oligodendrocytes (found in the white matter). Unlike the granule neurons and the Purkinje cells, whose cells of origin have been well characterized as the GCP of the EGL and the progenitor cells of the ventricular zone, respectively, the developmental origins of the interneurons, glial cells and the oligodendrocytes are much less clear.

A multipotent cerebellar stem cell population with the ability to give rise to neurons, astrocytes, and oligodendrocytes *in vitro* and *in vivo* has, in fact, been isolated from the postnatal day 7 (P7) mouse cerebella (Lee *et al.*, 2005). Prospective isolation of prominin 1 (*Prom1*)-positive (also known as CD133) cells leads to the enrichment of these multipotent stem cells, which also exhibit self-renewal and high expression of NSC genes, SRY-box containing gene 2 (*Sox2*) and nestin. This suggests that the different cell types of the cerebellum can arise from a common multipotent stem cell population, revealing another potential cell population for transformation during medulloblastoma tumorigenesis.

Molecular classification of human medulloblastoma

Early insights into the molecular basis of medulloblastomas were drawn from the identification of developmental pathways altered in hereditary tumor syndromes and the examination of their roles in cerebellar development (Wechsler-Reya and Scott, 2001). The role

of the SHH signaling pathway in medulloblastoma was first appreciated when individuals with Gorlin's syndrome, which is characterized by heterozygous *PTCH1* mutations, were observed to display a predisposition to develop medulloblastomas (Hahn et al, 1996). PTCH1, a receptor for SHH, functions as a negative regulator of SHH signaling by inhibiting smoothened (SMO), which activates the downstream GLI transcriptional factors. Upon SHH binding to the PTCH1 receptor, SMO inhibition is relieved and the downstream GLI transcription factors are released from inhibitory complexes, which include the protein SUFU, to activate target gene expression (Figure 1-2) (Huse and Holland, 2010). Sporadic mutations in components of the SHH-PTCH1 signaling pathway, including *PTCH1*, *SUFU* and *SMO* have been reported in 25% of medulloblastomas (Ellison *et al.*, 2003). Similarly, the role of the WNT signaling pathway, known to be crucial during the embryonic development of the cerebellum and the midbrain (McMahon and Bradley, 1990; Thomas and Capecchi, 1990), was recognized by studying patients with Turcot's syndrome. Turcot's syndrome is characterized by the concomitant occurrence of multiple colorectal adenomas and a primary brain tumor, in particular medulloblastoma (Hamilton *et al.*, 1995). These patients were identified to harbor germline mutations in the adenomatous polyposis coli (*APC*) gene, a tumor suppressor that regulates the activity of the transcriptional co-activator beta-catenin *(CTNNB1)*, a key regulator of the WNT pathway (Figure 1-2). Mutations in the *CTNNB1*, *APC*, and *AXIN*, another component of the APC complex, have also been observed to occur in about 20% of sporadic medulloblastomas (Huse and Holland, 2010).

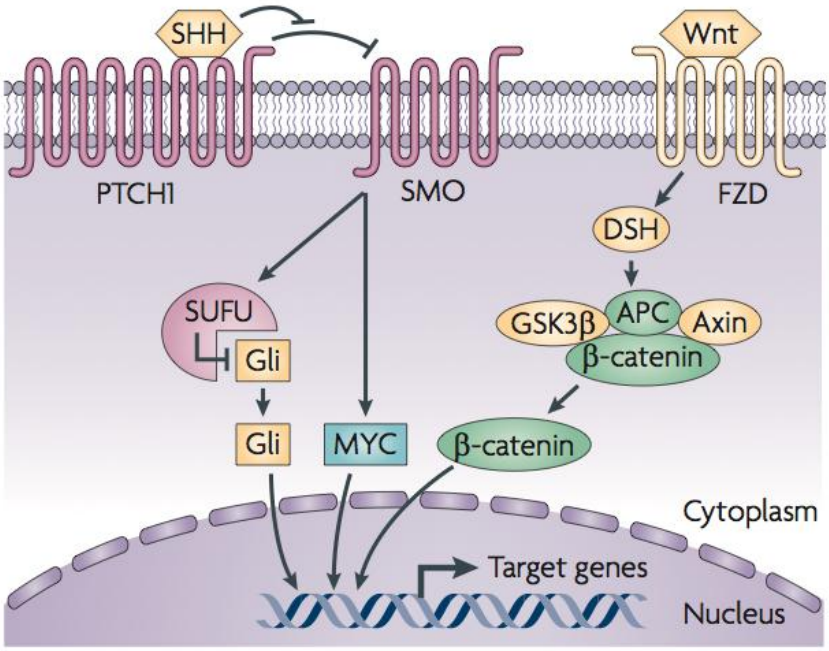

Figure 1-2 Developmental pathways implicated in medulloblastoma tumorigenesis

Both germline and sporadic mutations in components of the SHH and WNT signaling pathways have been identified to occur in human medulloblastomas. Figure taken from Huse and Holland (2010).

Four subtypes of human medulloblastoma

While candidate gene approaches have been crucial to our early understanding of the molecular basis of medulloblastoma and the development of early mouse models, genome-wide expression analyses are critical for further identification of potential prognostic markers and elucidation of other pathways important in tumorigenesis. An early expression profiling study established that different tumor types and histological variants within the same tumor (ie. classic vs. desmoplastic medulloblastoma) are molecularly distinct and furthermore, gene expression signatures can serve as predictors of patient outcome (Pomeroy *et al.*, 2002). Following this study, multiple transcriptional profiling studies have identified four to six subclasses of human medulloblastoma, highlighting medulloblastoma as a collection of tumors with distinct clinical features and outcomes, molecular underpinnings, and demographics and not a single-entity

disease (Kool *et al.*, 2008; Northcott *et al.*, 2011b; Cho *et al.*, 2010). The current consensus as determined by the multiple groups that conducted the genome-wide analyses of the human tumors, identifies four distinct molecular subtypes; WNT, SHH, Group 3 (*MYC*), and Group 4 tumors (Taylor *et al.*, 2012) (Figure 1-3). Meta-analyses of the expression profiling data from seven independent studies show consistency in the tumor grouping, further validating the four consensus classes (Kool *et al.*, 2012).

The WNT and SHH subtypes show clear activation of the corresponding signaling pathways by target gene expression and make up the two groups that have the most favorable clinical outcomes, with survival rates of 80-90%. Group 3 and Group 4 have lower survival rates and while they have overlapping gene signatures, Group 3 tumors have an increased proportion of metastases and the worst prognosis (Northcott *et al.*, 2011b). Given the molecular variation and differences in clinical outcomes, recent efforts have focused on developing and validating tumor subtype-specific mouse models of human medulloblastoma (Figure 1-3). As reviewed in the following sections, subtype-specific medulloblastoma models have also identified different putative subtype-specific tumor-initiating cells and cell of origins.

WNT subtype:

WNT tumors, which are characterized by the expression of genes present during activated WNT signaling (*WIF1*, *DKK1*, *DKK2*, etc.), constitute the subtype with the most favorable clinical outcome, with survival rates of over 95% in children and up to 100% in adults (Kool *et al.*, 2012). The WNT tumors are a well-defined subclass characterized by distinct features, including mutations in beta-catenin (*CTNNB1*), loss of chromosome 6, and

Subtypes	WNT	SHH	Group 3	Group 4
Prognosis/ Survival	Very good/ 95%	Infants good, others intermediate/75%	Poor/ 50%	Intermediate/ 75%
Gene expression profile	Wnt signaling	Shh signaling	Myc signature	Neuronal signature
Histology	Classic; rarely LCA	Classic;Desmoplastic; LCA	Classic; LCA	Classic LCA
Metastases (at diagnoses)	5-10%	15-20%	40-50%	35-40%
Mutations	CTNNB1/APC	PTCH1/Smo/SUFU; Gli2; TP53	MYC amplification	MYCN amplification
Mouse Models	Beta-catenin overexpression	Ptch inactivation, Smo activation, Sufu deletion	cmyc overexpression	Mycn overexpression
Proposed cell of origin	Lower rhombic lip	Granule neuron progenitors, SVZ neural stem cells	Cerebellar stem cells; GNP	Unknown

Figure 1-3 The four molecular subtypes of human medulloblastoma

Each subtype displays distinct clinical, genetic, and histological features. Subtype-specific mouse models have identified differences in the putative cell of origin. LCA=large cell anaplastic; SVZ=subventricular zone; GNP=granule neuron progenitors. Figure adapted from Northcott et al., 2012 and Lau et al. 2012.

immunopositivity for beta-catenin (Clifford *et al.*, 2006). Metastases are rare in the WNT tumors and given the favorable clinical outcome of these tumors, efforts have begun to stratify patients with WNT tumors for consideration in reducing treatment intensities (Northcott *et al.*, 2012).

The WNT subtype was recently established in a mouse model with a stabilizing mutation of beta-catenin (*Ctnnb1)* (Gibson *et al.*, 2010), which led to the abnormal accumulation of cells from the embryonic dorsal brainstem persisting into adulthood. However, tumors did not form without the inactivation of *Trp53*. *Ctnnb1;Trp53* mutant tumors recapitulated the characteristics and gene expression of human WNT tumors. In this model, the cell of origin of the WNT subtype has been suggested to be the dorsal brainstem progenitor cell (Gibson *et al.*, 2010).

SHH subtype:

SHH tumors exhibit activation of the SHH signaling pathway, a pathway critical for the proliferation and differentiation of the granule cell neurons, and are marked by expression of genes such as *HHIP, ATOH1 (MATH1),* and *SFR1* as well as the SHH pathway-dependent transcription factors *GLI1, GLI2,* and *GLI3* (Northcott *et al.*, 2011b). Mutations associated with the SHH subtype include *PTCH1* and *SUFU,* both negative regulators of SHH signaling. Overall survival rates are good, with 5 or 10 year survival rates of ~80%. However, further stratification of the group by age indicates that the overall survival of children and adults are worse (10 year survival of 51% and 34%, respectively) than infants, suggesting the need for further subcategorization.

The SHH subtype has the most well-established mouse models of medulloblastoma. Various models with activating mutations or overexpression of *Smo* (Hatton *et al.*, 2008) or

inactivating mutations (Goodrich *et al.*, 1997; Wetmore *et al.*, 2001) or deletion (Yang *et al.*, 2008b; Schüller *et al.*, 2008) of *Ptch1* have been validated to recapitulate SHH human tumors. From the study of SHH subtype mouse models, it has been shown that both granule cell progenitors (GCP) and multipotent neural stem cells (NSC) can initiate medulloblastoma tumorigenesis following the inactivation of *Ptch1*. Cre-mediated deletion of *Ptch1* in the granule lineage-committed *Math1*-expressing cells in E14.5 to postnatal day 10 (P10) mice result in tumor formation, indicating that both embryonic and postnatal GCP can function as tumor-initiating cells (Yang *et al.*, 2008b). *Ptch1* deletion in GFAP-expressing multipotent NSC at E14.5 led to an expansion of the NSC in the embryonic cerebella, resulting in an abnormally thick EGL at birth and was soon followed by rapid tumor formation. However, no abnormalities were observed in astrocytes, oligodendrocytes and other non-granule neurons, suggesting that the oncogenic effects of the *Ptch1* deletion are only evident in cells that have committed to the granule cell lineage (Yang *et al.*, 2008b). Similarly, Schuller *et al*. (2008) showed that activation of *Smo* in *Math1*-expressing lineage-restricted progenitors, as well as early multipotent $hGFAP^{+}$ and $Olig2^{+}$ progenitors led to GCP-activated medulloblastomas. No other tumor types were observed, despite the multipotency of the progenitors, consistent with the observation that acquisition of the granule cell lineage is critical for the development of SHH-induced tumors (Schüller *et al.*, 2008).

As a result of the well-characterized nature of the SHH pathway and its role in tumorigenesis, various mouse models have been used in preclinical studies to test inhibitors of the SHH pathway for potential therapeutics (Lau *et al.*, 2012). In particular, SMO antagonists, such as Cyclopamine and HhAntag, have shown promise in *Ptch1* models (Berman *et al.*, 2002; Romer *et al.*, 2004). Notably, a SMO antagonist (GDC-0449) resulted in rapid, albeit transient,

tumor regression in a patient with a SHH-activated tumor displaying widespread dissemination (Rudin *et al.*, 2009). Nevertheless, further understanding of disease relapse and drug resistance mechanisms will be necessary for the development of effective treatments against SHH tumors.

Group 3

Group 3 human tumors, molecularly characterized by MYC overexpression or amplification, are more likely to exhibit metastases at time of diagnosis and have the poorest prognoses, with overall survival rates of 30-50% (Northcott *et al.*, 2011b; Kool *et al.*, 2012). Recently, two independent studies have validated the functional role of MYC overexpression in medulloblastoma tumorigenesis. Transformation of the postnatal cerebellar stem cells (CbSC) at P5-P7 with a stabilizing mutant of *c-myc* and dominant-negative *Trp53* leads to highly aggressive tumor formation (Pei *et al.*, 2012). While overexpression of *c-myc* and *Trp53* in *Math1-GFP* GCP can also lead to tumor formation with lower penetrance and longer latency, the tumors that develop no longer express GFP, indicating that the expression of *Math1*, a key marker for granule lineage commitment is lost during tumorigenesis. Tumors arising from this model exhibit gene expression profiles that overlap with NSC, suggesting that the *c-myc* and *Trp53*-induced transformation may, in fact, be leading to the dedifferentiation to more primitive cell types during tumorigenesis (Pei *et al.*, 2012; Kawauchi *et al.*, 2012). While these recent studies have been significant in providing the first validated models for the Group 3 tumors, one must keep in mind that these models are generated by the *ex vivo* transformation of CbSC by retroviral overexpression. Establishment of an endogenous system for targeting CbSC will be important to further examine the potential role for CbSC in medulloblastoma tumorigenesis.

Group 4

While Group 4 tumors are the most common subtype, it is by far the least characterized subtype of medulloblastoma (Kool *et al.*, 2012). Group 4 tumors display overlapping gene expression profiles with Group 3 tumors, but are distinguished by the amplification of proto-oncogene *MYCN* (Kool *et al.*, 2012) and have better overall survival rates (~75%) (Northcott *et al.*, 2012). In one model, the overexpression of *Mycn* in the postnatal day 0 cerebella led to the formation of SHH-independent tumors with LCA and classic histology, as typically observed in Group 4 tumors. Furthermore, these tumors, although infrequently, displayed leptomeningeal metastases and contain transplantable tumor-propagating cells (Swartling *et al.*, 2010). However, this model still remains to be validated for recapitulation of the human Group 4 subtype tumors.

Cancer Stem Cells

Background

A cancer stem cell is defined as a cell present in a tumor that possesses 1) the capability for self-renewal and 2) the ability to differentiate and give rise to the variety of heterogeneous progeny that make up the bulk of the tumor (Reya *et al.*, 2001; Clarke *et al.*, 2006). A self-renewing cell must be able to generate a daughter cell that retains its ability for self-renewal and differentiation and occurs either by symmetrical (generating two stem cells) or asymmetrical cell division (generating one stem cell and one differentiated cell) (Clarke *et al.*, 2006). The cancer stem cell hypothesis states that it is this rare population of cells with stem-like properties that drive the initiation and progression of the tumor and establish hierarchically organized,

differentiated tumor progeny. Therefore, akin to normal development, tumor heterogeneity is a result of the multipotent differentiation of the stem-like cell. By contrast, in the clonal, or stochastic model of tumorigenesis, any cell within the tumor that acquires the appropriate genetic and/or epigenetic alterations can gain the potential for tumor initiation (Shackleton *et al.*, 2009; Dick, 2009).

Cancer stem cells were first identified and characterized in human acute myeloid leukemia (AML). Drawing from the well-established markers of hematopoietic stem cells (HSC), Dick et al. (1994) observed that human AML cells with cell surface profiles ($CD34^+CD38^-$) typical of immature cells in the bone marrow were also able to regenerate leukemia and recapitulate the original tumor when serially transplanted into irradiated NOD/SCID mice. In contrast, the $CD34^+CD38^+$ or $CD34^-$ cells failed to initiate leukemia (Lapidot *et al.*, 1994; Bonnet and Dick, 1997). However, a CSC population is not necessarily derived from the transformation of the corresponding tissue stem cell. Increasing evidence has supported the notion that differentiated tissue progenitors, through oncogenic mutations, can dedifferentiate and acquire characteristics of CSC to initiate tumorigenesis (Passegué *et al.*, 2003). For example, the expression of the *MLL-ENL* and *MLL-AF9* fusion oncogenes can bestow properties of self-renewal in committed progenitors in myeloid/lymphoid leukemia (Cozzio *et al.*, 2003; Krivtsov *et al.*, 2006). The extensive lineage maps and validated cell surface markers for each distinct cell lineage have made it feasible to study the role of each cell population during hematopoietic tumorigenesis. The challenge remains in solid tumors, as the surface markers of stem cells and their progeny or even the developmental cellular hierarchies are not well defined in solid organs. However, mounting evidence has shown that CSC are, in fact, present in solid tumors, as will be discussed in the following section.

Isolation of cancer stem cells in solid tumors

The first demonstration that a specific, identifiable population of cells within a solid human tumor was able to isolate the tumor-initiating activity in a xenograft transplantation assay occurred in breast cancers (Al-Hajj *et al.*, 2003). In this study, FACS sorting based on the expression of cell surface markers CD44 and CD24 demonstrated that only the $CD44^{+}/CD24^{-/low}$ population of cells possessed the capability for self-renewal and tumor-initiation by serial transplantation. The transplanted tumors initiated by the $CD44^{+}/CD24^{-/low}$ population further exhibited differentiation into heterogeneous cell types to regenerate the phenotypic complexity observed in the primary tumor. Following this study, CSC have been further identified in other solid tumors of the brain (Singh *et al.*, 2004), colon (O'Brien *et al.*, 2007; Ricci-Vitiani *et al.*, 2007) and pancreas (Li *et al.*, 2007; Hermann *et al.*, 2007) by the prospective isolation with cell surface markers. Cell surface markers utilized for isolation of the tumor-initiating, stem-like cells in the variety of solid tumors include CD133 (also known as prominin 1) for brain, colon and pancreatic cancers, CD44/CD24/ESA (epithelial-specific antigen) for pancreatic cancer, and ALDH1 (aldehyde dehydrogenase) as an additional marker for breast cancers (Ginestier *et al.*, 2007). As observed in AML, the CSC surface markers in solid tumors include those that have also been characterized as markers for tissue stem cells present in the corresponding disease organ, such as CD133, a marker for NSC (Uchida *et al.*, 2000) and ALDH1 for mammary stem cells (Ginestier *et al.*, 2007).

The gold standard assay for determining CSC activity is the *in vivo* transplantation assay, in which the putative CSC population is orthotopically injected into immunocompromised mice (Clarke *et al.*, 2006). Animals are monitored for tumor formation and secondary tumors are

analyzed for differentiation capacity and recapitulation of the primary tumor. Serial transplantation further validates the self-renewal capability of the CSC present in the tumor (Clarke *et al.*, 2006). Limiting dilution transplantation assays can also be carried out to determine the number of fractionated cells required for cancer-initiation *in vivo* (Ginestier *et al.*, 2007; O'Brien *et al.*, 2007). Nonetheless, the xenograft assay is not without caveats and limitations. Importantly, there are major concerns about the separation of the tumor cells from the endogenous stroma, which may prevent engraftment in a foreign microenvironment (Clarke *et al.*, 2006). While this issue may be circumvented if the CSC population is niche-independent, the frequency of tumor-initiation has been shown to vary greatly depending on the genetic background of the recipient mouse (Quintana *et al.*, 2008). The role of the niche is further highlighted in cancers that may be induced by an endogenous tumorigenic niche itself (Walkley *et al.*, 2007). In addition, the xenograft assays have the technical disadvantage of being slow and may take months for tumors develop *in vivo* following transplantation.

The prospective isolation of CSC has largely been dependent on cell surface markers using markers of normal stem cells, mainly CD133 and CD44/CD24 (Visvader and Lindeman, 2008), but concerns about the purity of FACS isolated cell populations due to subjective factors such as gating or variability in reagents such as antibodies must be considered and marker expression may also not be a stable characteristic of the CSC. One possible method for circumventing these issues is by increasing specificity by using a combination of markers (Medema, 2013).

Non-adherent sphere formation assays, developed for the isolation of NSC (Reynolds and Weiss, 1996), have been a standard assay in isolating and maintaining the growth of brain tumor cell stems *in vitro* (Dirks, 2008). Tumors maintained in serum-free sphere cultures have been

shown to represent the characteristics of the original tumor more accurately than serum cultured lines (Lee *et al.*, 2006). It has also been reported that neurospheres are not necessarily derived from stem cells (Pastrana *et al.*, 2011) and intra-clonal heterogeneity is observed within a neurosphere, that may contain stem cells, as well as, more differentiated progenitors (Suslov *et al.*, 2002). One must consider the caveats of utilizing a culture-based isolation method, as tissue culture-induced alterations may also occur. Nonetheless, *in vitro* propagation and expansion of stem-like cells by sphere formation assays prove to be a valuable method for rapid examination of pathways and amenable for genetic manipulation.

Tracking cancer stem cells in vivo

An ideal method to avoid the concerns of separating CSC from its endogenous niche, which may lead to culture-induced changes or loss of activity, is by tracking cells *in vivo* in an unperturbed system with viral tagging strategies or knock-in reporter models. (Clevers, 2011). While this is not feasible in humans for obvious ethical reasons, *in vivo* lineage tracing of genetically marked cells allows for the observation of progeny derived from a single cell in mouse models. Recently, three independent studies demonstrated the presence of endogenous tumor-initiating cells by marking a putative stem cell population and tracking the tumor growth *in vivo*, in colon, skin, and brain cancers (Schepers *et al.*, 2012; Driessens *et al.*, 2012; Chen *et al.*, 2012). Particularly, in the brain tumor study, *Nestin-ΔTK-IRES-GFP* expressing stem cells in a mouse model of glioblastoma (*hGFAP-Cre;Nf1*$^{fl/+}$*;P53*$^{fl/fl}$*;Pten*$^{fl/+}$), which mark the adult NSC in the subventricular zone, were also demonstrated to identify the glioma-initiating stem cells *in vivo* (Chen *et al.*, 2012). Furthermore, ablation of this cell population by treatment with ganciclovir led to arrested tumor growth, showing that the *hGFAP*-expressing stem cells

maintained tumor growth. Importantly, following the regression of the tumor with chemotherapeutic agent temozolmide (TMZ), tumor regrowth was observed to be initiated by the *Nestin-ΔTK-IRES-GFP cells*. Together, the results from the three independent lineage tracing studies provide a convincing demonstration of an endogenous CSC population in solid tumors, as the CSC were identified in an unperturbed system in which cells are not removed from endogenous niche and transplanted to another species. A question that remains is whether the cells being tracked *in vivo* with the lineage tracing methods are, in fact, the same populations being functionally assayed in the xenograft transplantation assays. This will be important in determining the validity of transplantation assays that have been being utilized as the gold-standard method.

Treatment resistance of cancer stem cells

Chemo- and radiotherapy preferentially kill rapidly dividing, cycling cells. If a CSC is derived from a rare cell that infrequently enters the cell cycle, such therapies would be relatively inefficient or unable to target these cells (Clarke *et al.*, 2006). In fact, normal stem cells exhibit properties such as quiescence, expression of ABC (ATP-binding cassette) transporters, active DNA-repair, and resistance to apoptosis, rendering them resistant to radiation and toxins (Dean *et al.*, 2005). In particularly, high expression of ABC transporters, known for their role in multi-drug resistance, results in a "side-population" phenotype characterized by efflux of the Hoechst dye. In bone marrow, the "side population" contains HSC that are able to reconstitute the hematopoietic system. Utilization of the Hoechst dye has also allowed for the early isolation of cells with stem-like characteristics from tumor samples (Dean *et al.*, 2005). However, this

method isolates a heterogeneous population and subsequent studies have focused on the characterization of specific cell-surface markers for the prospective isolation of CSC.

Both chemo- and radioresistance mechanisms have been observed in the cancer stem-like population in hematopoietic cancers and solid tumors. In human AML, the $CD34^{+}CD38^{-}$ leukemia stem cells were more resistant to the chemotherapeutic Ara-C and a greater fraction of these cells were found to be quiescent in G0 compared to the $CD34^{+}CD38^{+}$ or $CD34^{-}$ cells. Secondary transplantation of the Ara-C-surviving $CD34^{+}CD38^{-}$ cells suggests that these chemoresistant cells can be responsible for tumor relapse (Ishikawa *et al.*, 2007). In breast tumors, standard chemotherapy treatment led to an increase in the fraction of $CD44^{+}CD24^{-/low}$ breast CSC and a concurrent increase in mammosphere formation (Li *et al.*, 2008; Yu *et al.*, 2007) and this was mediated by the reduction of miRNA let7 expression by the breast CSC.

Several mechanisms have been implicated in the resistance of CSC to ionizing radiation. In human glioblastoma primary and xenograft tumors, $CD133^{+}$ glioma stem cells displayed increased resistance to ionizing radiation compared to $CD133^{-}$ cells and the $CD133^{+}$ cells that survived the radiation were able to initiate tumors with similar potency as untreated cells. This survival was mediated by enhanced DNA damage checkpoint activation by the $CD133^{+}$ cells (Bao *et al.*, 2006). $CD133^{+}$ cells in medulloblastoma cell lines exhibited greater radioresistance than the $CD133^{-}$ counterparts and displayed an increase in CD133 expression in hypoxic conditions (Blazek *et al.*, 2007). In a breast cancer model, CSC-enriched populations also exhibited less DNA damage after radiation and this was be attributed to lower levels of reactive oxygen species (ROS), mediated by the increased expression of antioxidant or anti-ROS genes (Diehn *et al.*, 2009).

In several mouse models of medulloblastomas, a population of radioresistant CSC was identified to be present in the perivascular niche (Hambardzumyan *et al.*, 2008). Upon radiation treatment, the bulk of the tumor underwent *Trp53*-dependent apoptosis. However, a subset of nestin-positive cells in the vascular niche was able to survive radiation and undergo cell cycle arrest, until they re-entered the cell cycle 72 hours post-treatment and proceeded to proliferate and cause tumor recurrence (Hambardzumyan *et al.*, 2008).

Significance and Controversy

The CSC hypothesis emerged in part from observations that tumors with stem cell-like properties have greater resistance to conventional chemo- or radiotherapy, resulting in disease recurrence following tumor resection. There are great implications if the CSC hypothesis is true and there exists a rare population of cells that are refractory to standard treatments. While standard therapies can effectively target the bulk of the tumor, therapies targeting the CSC population specifically may be necessary for effective elimination of the tumor and the prevention of tumor relapse (Clarke *et al.*, 2006). Therefore, it is crucial to study the mechanisms of CSC survival and maintenance. However, this has not been straightforward and controversies have been raised regarding the validity of the CSC hypothesis.

Controversies involving CSC are manifold and reasons include, but are not limited to methods of isolation, assays for measuring activity, confusion regarding the definition of CSC and whether or not it must be derived from transformed tissue stem cell. Recently, the controversy of CSC was fueled by a study showing that a very high frequency (1 in 4) of tumor-initiating cells were actually present in melanomas when more severely immunocompromised recipient animals were utilized (Quintana *et al.*, 2008). This is contrary to the notion that only a rare population of cells possesses the capability for tumor-initiation. This would argue that the

xenograft transplantation assays have been underestimating the frequency of human CSC when, in fact, a much larger proportion of cells have the tumorigenic potential when the appropriate environment is provided. This highlights the concerns and caveats regarding the use of xenograft transplantation assays as the gold standard for measuring functional CSC activity. Syngeneic transplantation assays carried out in mouse models of B and T- cell lymphomas, driven by *c-myc* and *N-ras* expression by the *Eu* enhancer also concluded that the tumor-initiating population is not as rare as initially expected (>10%) (Kelly *et al.*, 2007). However, in other tumor models of leukemia and breast cancer that examined CSC activity with the syngeneic transplantation of the prospectively isolated tumor stem cells, the results were consistent with the xenograft studies, identifying the tumor-propagating population as a rare population (Guo *et al.*, 2008; Zhang *et al.*, 2008). These studies demonstrate the variability that occurs depending on the experimental context, or alternatively, may be reflecting the biological variability in the frequency that occurs between different tumor types or even between individual tumors of the same type. In fact, the frequency of leukemia initiating cells can vary up to 500 fold between patients (Bonnet and Dick, 1997).

Current methods of CSC isolation are largely based on FACS isolation with cell surface markers. But further complexities in the characterization and the interpretation of CSC populations may arise if the CSC are not a stable population, but demonstrate a phenotypic plasticity allowing for interconvertibility between CSC and non-CSC (Gupta *et al.*, 2009). If CSC are maintained in a stable state with defined properties and pathway dependencies, targeting CSC specifically may be a feasible strategy. However if CSC demonstrate "plasticity" during the progression of tumorigenesis or during therapeutic challenge, this will have important implications for treatment strategies (Jordan, 2009). For example, if dedifferentiation of non-

stem cancer cells can also lead to the generation of a CSC population, this necessitates the need for targeting both the bulk and the stem cell compartment.

Other controversies have arisen due to confusions regarding the term cancer "stem cell", which have led to the assumption about the cellular origin of these cells, the name suggesting that the precursors of CSC are normal tissue stem cells. While it is true that in some cases of leukemia, the cell of origin is a transformed stem cell, the assays used to identify CSC are purely based on functional tests for tumor-initiation and not intended to imply that they are derived from normal stem cells (Jordan, 2009). Despite the many controversies, the CSC hypothesis has remained a topic of immense interest and efforts continue to further validate and characterize the population of CSC in various tumor types.

Brain tumor stem cells

As previously described, mouse and human NSC when cultured as neurospheres in the presence of bFGF and EGF have been shown to maintain the characteristics of clonogenic self-renewal *in vitro* and engraftment and multipotent differentiation *in vitro* and *in vivo* (Reynolds *et al.*, 1992). These methods for studying normal NSC have been employed for the initial identification and isolation of human brain tumor stem cells in astrocytomas, glioblastomas and medulloblastomas (Singh *et al.*, 2004; Hemmati *et al.*, 2003). Culturing human brain tumors as neurospheres in serum-free culture has been shown to better retain and recapitulate the characteristics of the primary tumor (Lee *et al.*, 2006), further supporting the neurosphere culture as an important method for the characterization and isolation of potential brain tumor stem cells, especially in the absence of cell surface markers allowing for the prospective isolation from primary tumors.

Prospective isolation of tumor cells using NSC markers, such as CD133, has also been successfully utilized for the isolation of brain tumor stem cell activity. Specifically, in medulloblastoma, as low as 100 CD133-positive cells was shown to initiate a tumor upon xenograft transplantation and both classic and desmoplastic histologies have been recapitulated, while CD133-negative cells lacked this activity (Singh *et al.*, 2004). Furthermore, nestin^{+}/CD133^{+} brain CSC have been identified in the perivascular niche, interacting with the endothelial cells for maintenance of their stem cell state (Calabrese *et al.*, 2007). A recent lineage-tracing study marking nestin^{+}-expressing NSC in a glioblastoma model demonstrated the ability of these NSC to initiate tumors and importantly, reinitiate tumor formation following chemotherapeutic treatment (Chen *et al.*, 2012). An endogenous population of medulloblastoma stem cells has yet to be examined with lineage tracing studies. While an embryonic stem (ES) cell gene expression profile is enriched in the high grade tumors, which have poor prognoses (Ben-Porath *et al.*, 2008), the correlation between the presence of endogenous stem cell populations in brain tumors and overall survival has also not been studied.

Ptch1$^{LacZ/+}$;Trp53$^{-/-}$ mouse model of disseminated medulloblastoma with self-renewing, tumor-initiating cells

Despite the recent advances in the development of subtype-specific tumors, few models have examined the phenotypes of dissemination or the population of CSC specifically. This is important given that dissemination/metastases is an indicator for poor prognosis and there is evidence suggesting CSC can exhibit metastatic capabilities (Hermann *et al.*, 2007). Specifically, in pancreatic cancers, the subpopulation of CD133^{+} cells co-expressing CXCR4 (C-X-C chemokine receptor type 4) were located at the invasive front of the tumors and exhibited

migratory and metastatic characteristics (Hermann *et al.*, 2007). In all tumor subtypes except the WNT tumors, which have an overall high rate of survival, in general, patients exhibiting dissemination have worse overall survival compared to those without disseminated tumors (Kool *et al.*, 2012). A relatively small proportion of patients with SHH tumors exhibit metastases (13% in SHH tumors), however, it will be valuable to have models that represent the metastatic phenotype given the poor survival of patients with metastases. Although the SHH tumor models are well established, the smaller subset of SHH tumors with the metastatic phenotype may not be captured in these models and may not uncover the underlying genetic pathways important in dissemination and treatment resistance. In one activated *Sm*o model, a homozygous *SmoA1* mutation was shown to result in highly aggressive tumors with leptomeningeal dissemination to the brain and spine and the ability to form secondary tumors transplantation, suggestive of a tumor-initiating population (Hatton *et al.*, 2008).

In other models of medulloblastoma-initiating cells, consistent with the identification of human CSC in the perivascular niche, a *Nestin*-positive, radioresistant stem cell population was also observed in the perivascular niche in mice (Hambardzumyan *et al.*, 2008). Furthermore, the survival of these stem cells following radiation was dependent on activation of the Akt pathway, suggesting the inhibition of this pathway as a potential avenue for treatment. Recently, postnatal self-renewing CbSC overexpressing *c-myc* (Pei *et al.*, 2012) or with inactivating mutations of *Rb* and *Trp53* (Sutter *et al.*, 2010) have been shown to initiate tumors upon transplantation, suggesting the potential role for CbSC transformation for medulloblastoma tumorigenesis.

$Ptch1^{LacZ/+};Trp53^{-/-}$ mouse model of medulloblastoma

In mice, *Ptch1* homozygosity results in embryonic lethality at around E9.0-E10.5, but heterozygous *Ptch1* mutants develop medulloblastomas histologically similar to human

medulloblastomas (Goodrich *et al.*, 1997). The combination of *Trp53*$^{-/-}$ with the *Ptch1*$^{LacZ/+}$ mutation results in a more malignant tumor, accelerating medulloblastoma formation from 10 months (in *Ptch*$^{LacZ/+}$ mice) to 12 weeks and increasing tumor penetrance from 14% to greater than 95% (Wetmore *et al.*, 2001). Histological differences are also observed, as the *Ptch1*$^{LacZ/+}$ genotype represents a more benign and focal tumor with no dissemination and the *Ptch1*$^{LacZ/+}$*;Trp53*$^{-/-}$ tumors are more diffuse (C.Lin thesis). Recently, Sleeping Beauty transposon mutagenesis in the *Ptch1* heterozygous background accelerated tumorigenesis and also led to tumors exhibiting leptomeningeal dissemination (Wu *et al.*, 2013), suggestive that additional mutations are required for dissemination in the *Ptch1* model.

Our lab further determined that there was a difference in the endogenous stem cell activity between the *Ptch1*$^{LacZ/+}$ and *Ptch1*$^{LacZ/+}$*;Trp53*$^{-/-}$ tumors using the serum-free *in vitro* neurosphere assay for self-renewal. *Ptch1*$^{LacZ/+}$*;Trp53*$^{-/-}$ tumor cells have been reported to undergo changes during adherent, serum-enriched tissue culture, such as downregulation of SHH signaling, highlighting concerns that serum-cultured cells *in vitro* cells may be not representative of the original tumors (Sasai *et al.*, 2006). Thus, our lab sought to culture the tumor cells in neurosphere conditions to better preserve the *in vivo* characteristics of the *Ptch1*$^{LacZ/+}$*;Trp53*$^{-/-}$ medulloblastomas, including the potential stem cell population, as the addition of serum leads to differentiation or NSC. As described above, this neurosphere culture method is commonly utilized for the enrichment of brain tumor stem-like cells. While the prospective isolation of tumor stem cells directly from the primary tumor is crucial for further characterization of this population, additional markers may need to be identified for the isolation of *Ptch1*$^{LacZ/+}$*;Trp53*$^{-/-}$ tumors stem cells. In the *Ptch1* heterozygous mouse model, CD133, the most commonly used marker for brain tumors, does not enrich for tumor-initiating capability (Read *et al.*, 2009). One

additional marker, CD15, a marker of embryonic and NSC, was previously shown to fractionate the cells with tumor-propagating capability (Read *et al.*, 2009; Ward *et al.*, 2009).

Ptch1$^{LacZ/+}$*;Trp53*$^{-/-}$ tumors display robust neurosphere formation at a frequency of approximately 1/50 in clonal growth conditions (C.Lin thesis). In contrast, *Ptch1*$^{LacZ/+}$ tumors only displayed sporadic, if any, self-renewal activity. In addition, the long term culture of the *Ptch1*$^{LacZ/+}$*;Trp53*$^{-/-}$ medulloblastoma neurospheres (MBNS) led to the enrichment of self-renewing cells, with high expression of NSC markers, *Sox2* and nestin. Furthermore, tumor-propagation capability of these *Ptch1*$^{LacZ/+}$*;Trp53*$^{-/-}$ MBNS was demonstrated by injections of both bulk tumor and neurosphere lines into the cerebella of nude mice (n=5), all of which developed cerebellar tumors. Tumor-initiation occurred more rapidly in the MBNS and their clonally derived subclones compared to the bulk tumors, suggestive of an enrichment for tumor-initiation activity. The transplanted tumors displayed dissemination within the brain and migration to the olfactory bulb and to the spinal cord. Together, these observations demonstrated that a self-renewing, tumor-propagating population can be enriched with *in vitro* neurosphere culture in the disseminated *Ptch1*$^{LacZ/+}$*;Trp53*$^{-/-}$ medulloblastoma model.

The *Ptch1*$^{LacZ/+}$*;Trp53*$^{-/-}$ model suggests that there may be an alternate cell of origin for the tumor-initiating cells within SHH-type tumors (C.Lin thesis), distinct from the granule cell progenitors, which have been characterized as the cell of origin in this subtype (Schüller *et al.*, 2008; Yang *et al.*, 2008b). In the *Ptch1*$^{LacZ/+}$*;Trp53*$^{-/-}$ animals, self-renewal activity was also present at 3 weeks (at a frequency of approximately 1/100), which is beyond the normal developmental window for self-renewal, as evident by the lack of neurosphere formation in wild-type (WT) 3 week animals. These aberrant CbSC, persisting beyond the stages of normal cerebellar development in the mutant p53 background, may also result in a tumor-initiating cell

population. While normal NSC depend on bFGF and EGF for the maintenance of proliferation and self-renewal, the growth factor responsiveness and pathway dependencies of the MBNS identified in the *Ptch1*$^{LacZ/+}$*;Trp53*$^{-/-}$ model have not been characterized. Data from our lab, however, suggest differences in the growth factor dependencies between the MBNS and the aberrant CbSC. When the growth factors bFGF and EGF were withdrawn from 3 week old *Ptch1*$^{LacZ/+}$*;Trp53*$^{-/-}$ aberrant CbSC cultures, the expression of the NSC marker *Sox2* was reduced. The MBNS, however, are not dependent on exogenous bFGF and EGF, and short-term growth factor withdrawal did not affect the expression of *Sox2*. These data indicate that further elucidation of pathways involved in the maintenance of the MBNS enriched from the *Ptch1*$^{LacZ/+}$*;Trp53*$^{-/-}$ tumors is necessary. In addition, pathways allowing for the aberrant persistence of self-renewing, premalignant cells in 3 week *Ptch1*$^{LacZ/+}$*;Trp53*$^{-/-}$ animals will shed light on the early progression of the tumors.

Research Objectives

In my dissertation, we sought to ask about the mechanisms of stem cell regulation and the pathways dependencies of medulloblastoma neurospheres and premalignant tissue stem cells in the *Ptch1*$^{LacZ/+}$*;Trp53*$^{-/-}$ model. The discovery of reprogramming mechanisms for converting somatic cells to a pluripotent embryonic state demonstrated that directed de-differentiation can occur through ectopic expression of the transcription factors, *Oct4, Sox2, c-myc, and Klf4* (Takahashi and Yamanaka, 2006); the latter two being notable oncogenes expressed in many types of human cancer (Rowland and Peeper, 2006). The intrinsic genetic program of NSC can be reprogrammed to an embryonic state with the induction of a single transcription factor, *Oct4* (Kim *et al.*, 2009), possibility because of endogenous expression of *Sox2, c-myc and Klf4* (Kim

et al., 2008b), as well as reprogramming markers SSEA-1 (CD15) and alkaline phosphatase (Kim *et al.*, 2009). In Chapter 2, we show that MBNS are able to rapidly adapt to embryonic stem cell culture selection in an *in vitro* assay for reprogramming. This led to the characterization of pluripotency gene *Klf4* as a crucial factor in MBNS plasticity and self-renewal, which was regulated in a *Stat3*-independent manner during clonogenic self-renewal.

While the culture-enriched *Ptch1*$^{LacZ/+}$*;Trp53*$^{-/-}$ MBNS exhibit properties of CSC, including as long term, clonal self-renewal *in vitro* and robust tumor-propagation *in vivo*, the lack of a prospective marker for isolation of the tumor-initiating activity precludes us from terming these cells as definitive CSC endogenously present in the primary tumors. In Chapter 3, we sought to isolate *Sox2*-expressing cells and characterize *Sox2* as a potential marker for the prospective isolation tumor stem cells in the *Ptch1*$^{LacZ/+}$*;Trp53*$^{-/-}$ model.

We prospectively isolated the aberrant tissue stem cell population from the *Ptch1*$^{LacZ/+}$*;Trp53*$^{-/-}$ animals using a fluorescent reporter allele of *Sox2*, a NSC marker, with the goal of characterizing pathways involved in the developmental persistence of these cells during tumorigenesis.

Chapter 2 : *Klf4* maintains the plasticity and self-renewal of medulloblastoma neurospheres in a *Stat3*-independent manner

Ronnie Yoo[1,2,3,5], ChieYu Lin[1,2,3,5], Suhu Liu[4], Leah Liu[3],
David Frank[4], Mark D. Fleming[1] and Laurie Jackson-Grusby[1,2]

[1]Pathology Department and [2]Kirby Center for Neuroscience, Boston Children's Hospital, [3]Biological and Biomedical Sciences Graduate Program, Harvard University, [4]Medical Oncology, Dana-Farber Cancer Institute, Boston, MA 02115
[5]These authors contributed equally

Author Contributions

RY acquired and analyzed results, wrote the manuscript and prepared figures. CYL contributed to the development of the methodology and acquired results for Figure 2-1. SL and DF contributed to the conception and design of experiments. LL contributed to the preparation of reagents. MDF contributed to the analyses of the histopathology. LJG contributed to the conception and design of experiments, analyzed results, wrote the manuscript and supervised the study.

Introduction

The cancer stem cell hypothesis suggests that only a small subpopulation of stem-like cells within a tumor have the capability for tumor-initiation and self-renewal. This population of cells is associated with greater resistance to conventional therapy, resulting in disease recurrence following tumor resection (Clarke *et al.*, 2006). Indeed, brain tumor-initiating cells displaying self-renewal and secondary tumor initiation in orthotopic xenografts have been identified in high grade human medulloblastomas and glioblastomas (Singh *et al.*, 2003; Galli *et al.*, 2004; Hemmati *et al.*, 2003). In mouse medulloblastoma models, while rational pathway inhibitors are able to slow tumor growth, they are unable to completely eliminate tumor cells, resulting in tumor regrowth (Lau *et al.*, 2012). Consistent with a role for tumor-initiating cells in disease relapse, a small population of stem-like cells resistant to radiotherapy has been identified in the cerebellar perivascular niche in primary human medulloblastomas (Calabrese *et al.*, 2007) and medulloblastoma-prone mice (Hambardzumyan *et al.*, 2008). Therefore, characterization of the mechanisms and pathways involved in the maintenance and survival of the population of medulloblastoma-initiating cells is critical for the development of effective targeted therapeutics.

Examination of the common genetic programs and signaling pathways utilized in stem cells and cancer cells provide important insights into mechanisms governing cancer stem cells (CSC) (Krizhanovsky and Lowe, 2009). For example, in AML, high expression of hematopoietic stem cell signatures directly predicts patient survival (Eppert *et al.*, 2011). A study by Kho *et al.* comparing human medulloblastoma gene profiles with expression signatures from the developing mouse cerebella observed a high correlation between metastatic human medulloblastomas and the postnatal day 5 through day 7 mouse cerebella (Kho *et al.*, 2004), a developmental timepoint when the cerebellum is largely undifferentiated and cerebellar stem

cells (CbSC) are the most abundant (Lee *et al.*, 2005). Selection for prominin 1 (also known as CD133) enriches for a CbSC population co-expressing pluripotency genes *Oct4, Nanog,* and *Sox2* and the NSC factors nestin and *Bmi1* (Po *et al.*, 2010). Notably, the comparison of gene expression profiles of cancers and embryonic stem (ES) cells have also revealed correlations between ES cells and poorly differentiated, high-grade human tumors (Wong *et al.*, 2008; Ben-Porath *et al.*, 2008), including brain tumors (Ben-Porath *et al.*, 2008; Holmberg *et al.*, 2011). Together, these studies reveal coordinated patterns of expression of pluripotency factors in CbSC and cancers; however the extent to which medulloblastoma-initiating cells rely upon these pathways has not been determined.

Oncogenic reprogramming and dedifferentiation of tumor cells has been proposed as a mechanism for generating and maintaining CSC (Krizhanovsky and Lowe, 2009; Hanahan and Weinberg, 2011). We were interested to test whether medulloblastoma neurospheres (MBNS) from metastatic medulloblastomas exhibit signs of endogenous reprogramming and dependency on these pathways. To approach this question, we studied the highly malignant $Ptch1^{LacZ/+};Trp53^{-/-}$ mouse medulloblastoma model (Wetmore *et al.*, 2001). $Ptch1^{+/-}$ medulloblastoma cells have previously been shown to undergo reprogramming following somatic nuclear transfer into mouse oocytes (Li *et al.*, 2003), showing that the cancer genomes can be epigenetically reprogrammed by the oocyte to reverse the tumorigenic activity and restore normal early development. Self-renewing, tumor-initiating neurospheres enriched from $Ptch1^{LacZ/+};Trp53^{-/-}$ tumors were used in an *in vitro* assay for reprogramming to assess adaptation to embryonic stem cell culture conditions, which would not normally be expected to support NSC growth in the absence of ectopic reprogramming factors, due to the differentiation factors present in serum (Reynolds *et al.*, 1992). The $Ptch1^{LacZ/+};Trp53^{-/-}$ MBNS demonstrated

plasticity and maintained growth and self-renewal in ES culture conditions. Furthermore, given the crucial function *Klf4* plays in somatic reprogramming (Yang *et al.*, 2010b) and mouse ES cell self-renewal (Zhang *et al.*, 2010), we examined the role of *Klf4* in maintaining the plasticity and self-renewal of the *Ptch1*$^{LacZ/+}$*;Trp53*$^{-/-}$ MBNS. We observed that *Klf4* is critical in maintaining both the plasticity of the *Ptch1*$^{LacZ/+}$*;Trp53*$^{-/-}$ MBNS in ES culture conditions and clonogenic growth as self-renewing neurospheres. In addition, *Klf4*, a known Stat3-target, was regulated in a Stat3-independent manner during clonogenic growth.

Results

Neurosphere culture-enriched *Ptch1*$^{LacZ/+}$*;Trp53*$^{-/-}$ medulloblastoma line exhibits characteristics of self-renewal and tumor-propagation

CSC are functionally defined as a cell within a tumor with the capability for indefinite self-renewal and tumor initiation and recapitulation of the primary tumor upon secondary transplantation (Clarke *et al.*, 2006). We first sought to functionally assess if stem-like cells cultured from a primary *Ptch1*$^{LacZ/+}$*;Trp53*$^{-/-}$ mouse medulloblastoma exhibit properties of CSC. Self-renewing cells were enriched from primary tumors using neurosphere cultures in serum-free media containing bFGF and EGF (Reynolds and Weiss, 1996), as this approach has been previously utilized for culturing human brain tumor stem cells (Hemmati *et al.*, 2003; Galli *et al.*, 2004; Singh *et al.*, 2003) and has been shown to preserve the genotype, gene expression and histopathology of tumor-propagating cells from human brain tumors (Lee *et al.*, 2006). In addition, traditional serum-based cell cultures of *Ptch1*$^{LacZ/+}$*;Trp53*$^{-/-}$ mouse medulloblastomas have been reported to alter the properties of the original tumor and suppress the Shh pathway activity (Sasai *et al.*, 2006) and serum leads to the terminal differentiation of NSC (Reynolds *et*

al., 1992; Gage *et al.*, 1995). *Ptch1*$^{LacZ/+}$*;Trp53*$^{-/-}$ mouse medulloblastoma neurosphere lines were maintained by dissociating and serially passaging in bulk cultures for more than 50 passages or clonally expanded as subclones. The long-term cultured *Ptch1*$^{LacZ/+}$*;Trp53*$^{-/-}$ MBNS were enriched for self-renewal activity ten-fold, compared to the primary tumor neurospheres and maintained elevated expression of Shh pathway target genes *Gli1* and *Gli2* (C.Lin thesis). As NSC surface markers CD15 and CD133 have been shown to mark tumor-propagating cells in mouse *Ptch1*$^{LacZ/+}$ tumors (Read *et al.*, 2009) and human medulloblastomas (Singh *et al.*, 2004) respectively, we carried out flow cytometry to assess expression of these markers in a primary tumor and the neurosphere culture-enriched *Ptch1*$^{LacZ/+}$*;Trp53*$^{-/-}$ cells. CD15 expression in the MBNS overlapped with the highest expressing cells within the heterogeneous primary tumor, whereas CD133 levels were elevated in the MBNS (Figure 2-1). The *Ptch1*$^{LacZ/+}$*;Trp53*$^{-/-}$ MBNS were also enriched in the expression of NSC markers nestin and *Sox2*, as shown by immunostaining of neurospheres (C. Lin thesis).

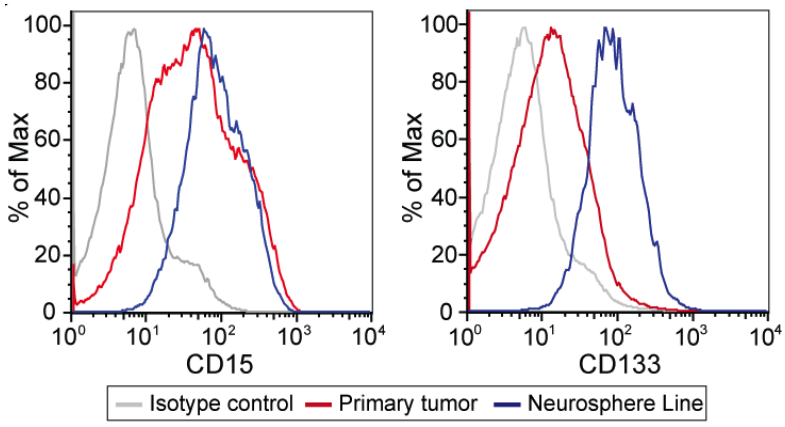

Figure 2-1 A *Ptch1*$^{LacZ/+}$*;Trp53*$^{-/-}$ medulloblastoma-derived neurosphere line is enriched for NSC cell marker expression in comparison to the primary tumor

FACS analyses of cell surface markers CD15 and CD133 in primary tumors and a *Ptch1*$^{LacZ/+}$*;Trp53*$^{-/-}$ medulloblastoma neurosphere (MBNS) line show an enrichment of the expression of these markers in the culture-enriched line.

To determine if these self-renewing MBNS were capable of tumor-initiation *in vivo*, intracerebellar injections were carried out using 10^4, 3 x10^4 and 10^5 cells (n= 2, 3, 3 respectively). Injected animals were sacrificed upon manifestation of neurological symptoms such as hydrocephaly, ataxia, or motor dysfunction and tumors that caused morbidity were observed within six weeks in all animals. X-Gal staining to detect *Ptch1*^{LacZ} expression in a primary tumor (Figure 2-2a) and the allograft tumors (Figure 2-2d) confirmed tumor engraftment in the cerebella. Upon cerebellar transplantation of the MBNS, dissemination to the olfactory bulb was also observed 60% of the time (C. Lin thesis). A comparative histological analyses of a primary *Ptch1*$^{LacZ/+}$*;Trp53*$^{-/-}$ medulloblastoma (Figure 2-2b, c) and a secondary tumor initiated with the injection of 10,000 MBNS cells (Figure 2-2e, f) demonstrated consistent architecture in the primary and secondary tumors, which were typified by dense cells with angulated nuclei and little cytoplasm. The secondary tumors, however, appeared to have a higher mitotic rate and were marked by less differentiated cells with prominent nucleoli and minimal cytoplasm. Furthermore, our lab has observed that when the same number of primary *Ptch1*$^{LacZ/+}$*;Trp53*$^{-/-}$ medulloblastoma cells and culture-enriched MBNS were injected, the MBNS-injected animals display accelerated tumor formation (C. Lin thesis). Together, these results show that *Ptch1*$^{LacZ/+}$*;Trp53*$^{-/-}$ MBNS exhibit properties of self-renewal and secondary tumor propagation.

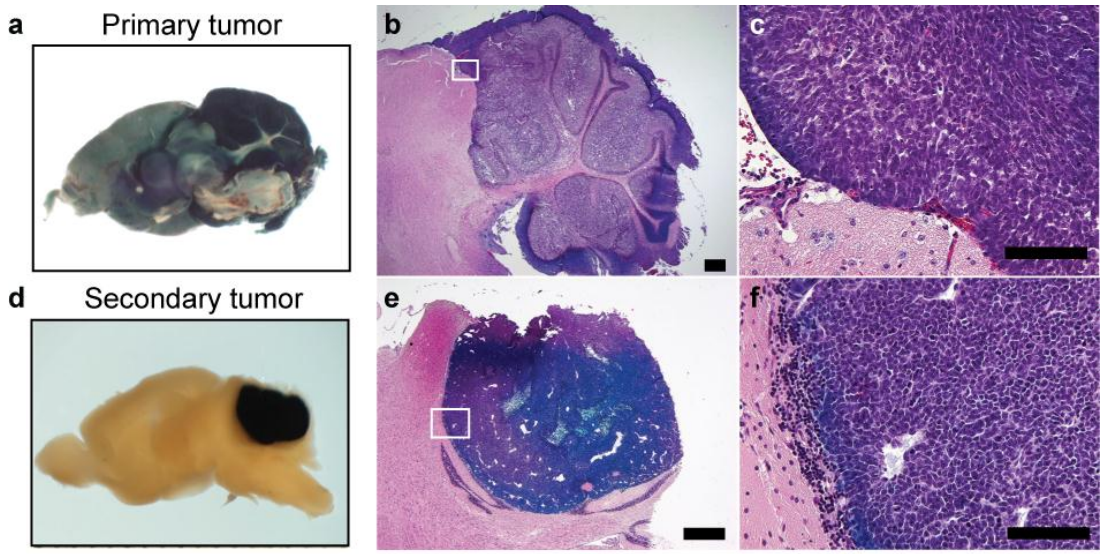

Figure 2-2 A neurosphere line derived from a primary *Ptch1$^{LacZ/+}$;Trp53$^{-/-}$* medulloblastoma is able to propagate secondary tumors recapitulating the primary tumor

(a) X-gal stained sagittal section of a primary *Ptch1$^{LacZ/+}$;Trp53$^{-/-}$* medulloblastoma. (b-c) Hematoxylin and eosin (H&E) stained section of the primary tumor. (d) X-gal stained sagittal section of a secondary tumor formed 4 weeks after intracranially injecting 10,000 *Ptch1$^{LacZ/+}$;Trp53$^{-/-}$* MBNS into nude mice. (e-f) H&E stained sections of the secondary tumor show that the *Ptch1$^{LacZ/+}$;Trp53$^{-/-}$* MBNS can propagate a tumor recapitulating the histology of the primary tumor. Scale bars in (b) and (e) are 500um; (c) and (f) are 100um. The white boxes in (b) and (e) indicate the sections enlarged in (c) and (f), respectively.

Phenotypic conversion of *Ptch1$^{LacZ/+}$;Trp53$^{-/-}$* MBNS grown in ES cell culture conditions

We established an *in vitro* reprogramming assay that would test the responsiveness of MBNS to fetal bovine serum (FBS) by growth under clonal culture conditions established for ES cells. NSC differentiate upon exposure to FBS (Reynolds *et al.*, 1992; Gage *et al.*, 1995), whereas embryonic stem (ES) cells maintain pluripotency in media containing FBS and leukemia inhibitory factor (LIF). To examine reprogramming activity in *Ptch1$^{LacZ/+}$;Trp53$^{-/-}$* MBNS, we plated the MBNS in ES culture conditions and monitored ES-like colony formation morphologically and quantified colonies expressing the ES cell marker alkaline phosphatase (AP) (Figure 2-3a).

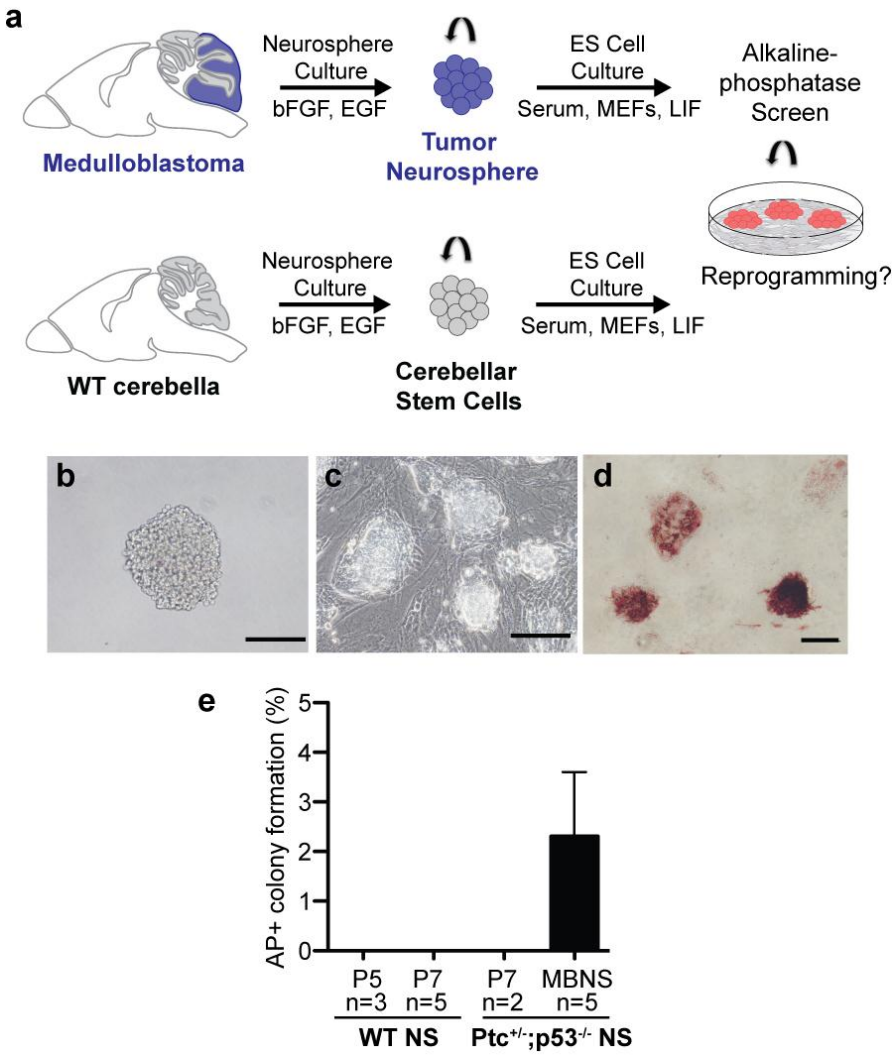

Figure 2-3 MBNS exhibit growth as alkaline phosphatase-positive colonies in ES cell culture conditions.

(a) Schematic of the *in vitro* assay for plasticity, in which *Ptch1*$^{LacZ/+}$*;Trp53*$^{-/-}$ MBNS cells were plated in low density (1500 cell/ml) in ES cell culture conditions containing serum, mouse embryonic fibroblast (MEF) feeders, and leukemia inhibitory factor (LIF). Control conversion experiments were carried out with primary cerebellar neurospheres (NS) enriched from postnatal day 5 (P5) and day 7 (P7) wild-type (WT) and P5 *Ptch1*$^{LacZ/+}$*;Trp53*$^{-/-}$ (Ptc$^{+/-}$; p53$^{-/-}$) cerebella. (b) Phase-contrast image of a *Ptch1*$^{LacZ/+}$*;Trp53*$^{-/-}$ MBNS grown in suspension culture. (c) Phase-contrast image of adherent MBNS colony formation in ES culture conditions, 6 days post-plating. (d) Adherent MBNS colonies in ES culture conditions stained for ES cell marker, alkaline phosphatase (AP). (e) Homogenously AP-positive clones were identified and quantitated from five independent conversion experiments with the *Ptch1*$^{LacZ/+}$*;Trp53*$^{-/-}$ MBNS line. There was no observable colony formation with the cerebellar neurospheres.

The *Ptch1*$^{LacZ/+}$*;Trp53*$^{-/-}$ MBNS, which are maintained in media containing bFGF and EGF (Figure 2-3b) were dissociated and plated at low-density (1500 cells/ml) in ES cell culture conditions. Within 6 days, colonies with an ES cell-like morphology were observed and AP-positive staining was observed at a frequency of 2.3±3.2% (Figure 2-3c, d). By contrast, control CbSC also enriched by NS culture from wild-type (WT) postnatal day 5 and day 7 mice or postnatal day 7 *Ptch1*$^{LacZ/+}$*;Trp53*$^{-/-}$ mice yielded no colonies in this assay (Figure 2-3e), suggesting a tumor-specific plasticity and resistance to differentiation allowing for the growth and maintenance of self-renewal in ES conditions.

The MBNS colonies from this conversion assay were clonally expanded and generated subclones that retained ES colony morphology and maintained stable AP expression for more than 15 passages (passage 7 subclone is shown in Figure 2-4a). The AP^{+} MBNS also showed strong X-Gal staining from the *Ptch1*^{LacZ} allele (Figure 2-4a), likely due to the loss of heterozygosity of the WT *Ptch1* allele (C. Lin thesis). To further determine if the phenotypic plasticity of the *Ptch1*$^{LacZ/+}$*;Trp53*$^{-/-}$ MBNS, as exhibited by the conversion of MBNS into AP^{+} colonies in ES culture conditions *in vitro*, expanded the developmental potency of these cells, we examined the gene expression of pluripotency and reprogramming genes *Oct4* and *Nanog*. Stochastic expression of *Oct4* was observed in one AP^{+} MBNS subclone and *Nanog* expression was present in the parental MBNS and maintained in the AP^{+} MBNS (Figure 2-4b). In contrast, the *Ptch1*$^{LacZ/+}$*;Trp53*$^{-/-}$ tumors had undetectable or relatively lower levels of *Oct4* and *Nanog*, respectively.

To test if the phenotypic conversion in ES conditions and stochastic *Oct4* expression led to an expanded developmental potency of the MBNS *in vivo*, teratoma assays were carried out by

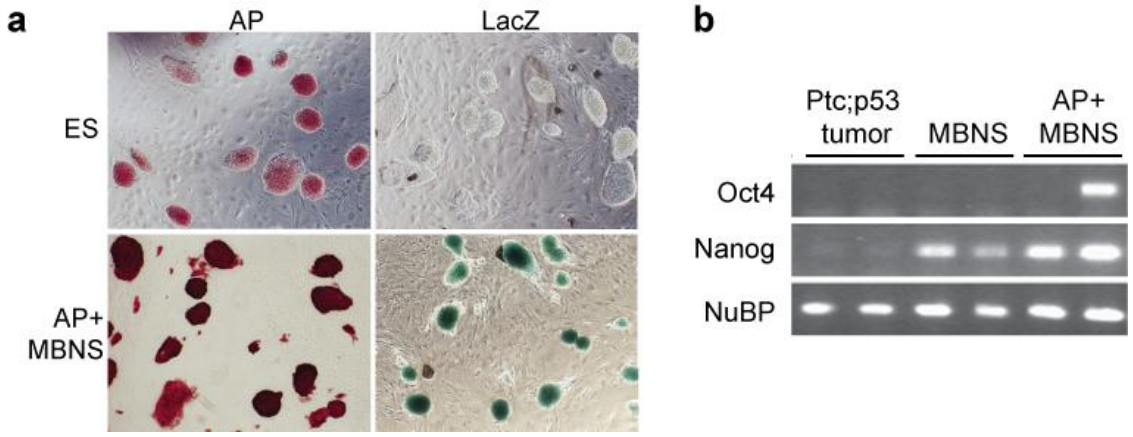

Figure 2-4 AP$^+$ MBNS subclones maintain ES-like morphology and exhibit stochastic expression of pluripotency genes

(a) AP and X-Gal stain of *Ptch1$^{LacZ/+}$;Trp53$^{-/-}$* ES cells and AP$^+$ MBNS subclone (passage 7). (b) RT-PCR of bulk *Ptch1$^{LacZ/+}$;Trp53$^{-/-}$* tumors, MBNS, and AP$^+$ MBNS shows sporadic expression of pluripotency factor *Oct4* in the AP$^+$ MBNS. *Nanog* expression is present in the parental MBNS line and maintained in the AP+ MBNS. *NuBP* (Nucleotide binding protein) is shown as a loading control.

the injection of 10^6 *Ptch1$^{LacZ/+}$;Trp53$^{-/-}$* MBNS and AP$^+$ MBNS cells into the flanks of nude mice and monitored for tumor formation, using *Ptch1$^{LacZ/+}$;Trp53$^{-/-}$* ES cells as a control. While intracerebellar injections of 10^4 *Ptch1$^{LacZ/+}$;Trp53$^{-/-}$* MBNS led to robust tumor formation causing morbidity by six weeks, the subcutaneous injection of 10^6 MBNS and AP$^+$ MBNS cells resulted in small tumors, all of which were significantly smaller than the ES-derived teratomas (Figure 2-5).

Histological analyses showed that the *Ptch1$^{LacZ/+}$;Trp53$^{-/-}$* ES cell-derived teratomas (n=3) were predominantly composed of immature neuroectodermal cells and marked by neuroblasts, but displayed no evidence for endoderm or mesodermal cell types. Nonetheless, the ES-derived tumors exhibited the greatest cell type-diversity between the three cell types injected (Figure 2-6). Tumors formed by subcutaneous injection of the MBNS (n=5) were also neuroblastic in nature, but was comprised of more mature, intermediate-sized cells with vacuoles

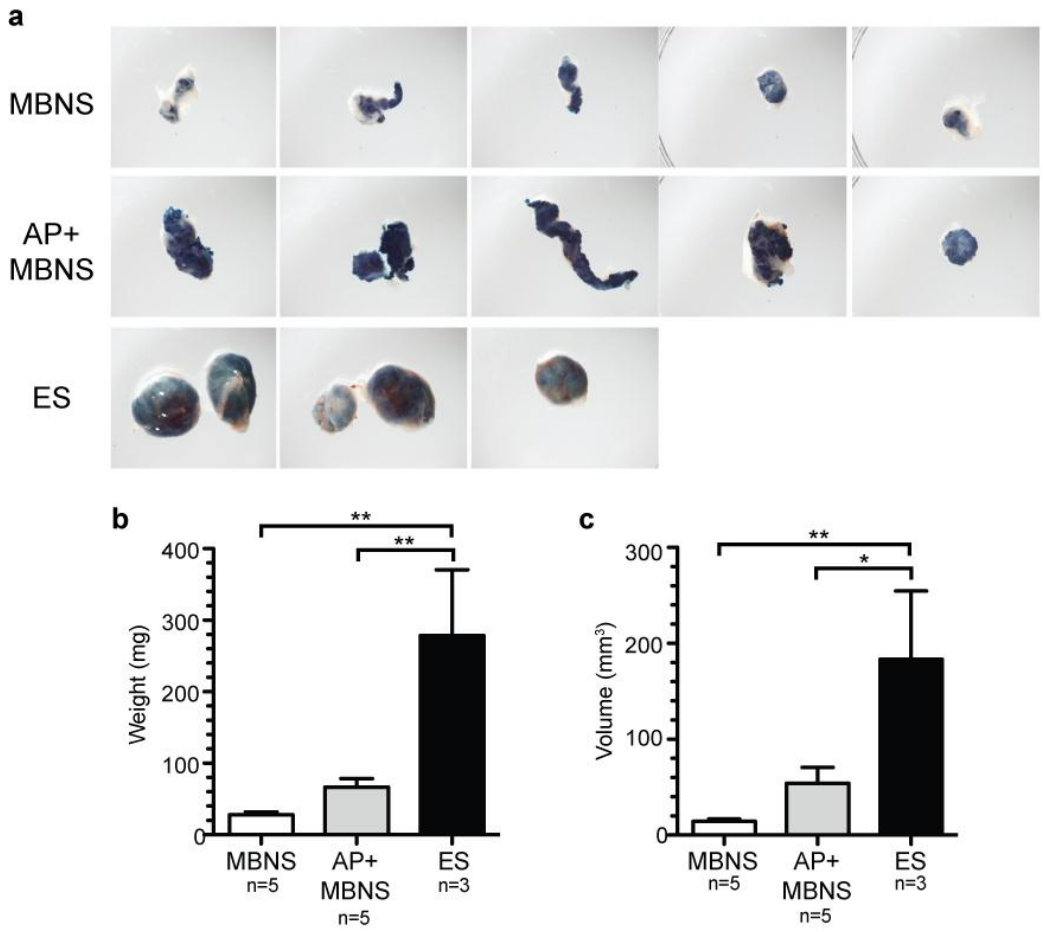

Figure 2-5 AP$^+$ MBNS cells do not form teratomas as robustly as ES cells

(a) X-gal stained tumors dissected from the flanks of nude mice subcutaneously injected with 10^6 MBNS, AP$^+$ MBNS, or *Ptch1*$^{LacZ/+}$;*Trp53*$^{-/-}$ ES cells. Tumors were isolated 3 weeks post-injection. (b) *Ptch1*$^{LacZ/+}$;*Trp53*$^{-/-}$ ES-derived tumors were significantly larger than the MBNS and AP$^+$ MBNS tumors ($p<0.01$ by one-way ANOVA with a Bonferroni post test). (c) After measuring the length (mm) and width (mm) of the tumors, tumor volume (mm^3) was calculated by length x width x width. The volumes of the ES-derived tumors were significantly higher than the MBNS tumors ($p<0.01$) and AP$^+$MBNS tumors ($p<0.05$ by one-way ANOVA with a Bonferroni post test). Average weight and volume of isolated tumors are represented as mean±sem.

(Figure 2-6). Interestingly, the AP$^+$ MBNS-derived tumors (n=5) displayed an intermediate histology, with a predominance of immature hyperchromatic, nucleolated cells with scant cytoplasm that form sheets and rests. Interspersed between this major cell population, however, were more mature regions resembling the cells predominantly present in the MBNS-derived

tumors. While there is no evidence of acquired pluripotency in the AP^+ MBNS, which display a phenotypic adaptation in the ES culture conditions, these results suggest that the AP^+ MBNS are able to exhibit a cellular plasticity to initiate distinct tumors less differentiated than the MBNS-derived tumors.

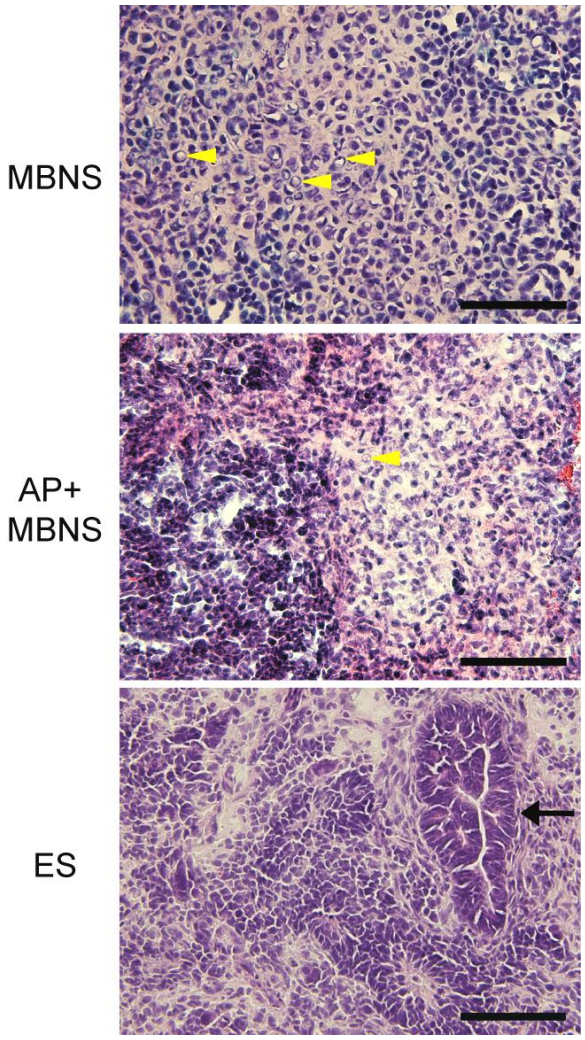

Figure 2-6 AP^+ MBNS-derived teratomas are histologically distinct from the parental MBNS-derived tumors

Representative images of H&E stained sections of tumors isolated from the teratoma assay, carried out by injecting 10^6 MBNS (n=5), AP^+ MBNS (n=5) or *Ptch1*$^{LacZ/+}$;*Trp53*$^{-/-}$ ES cells (n=3) into the flanks of nude mice and monitored for tumor formation for 3 weeks, are shown. Mature, intermediate sized cells with cytoplasmic vacuoles are indicated with the yellow arrowheads in both the MBNS and AP^+ MBNS teratomas. The major cell type in the AP^+ MBNS teratomas, which are the hyperchromatic cells with scant cytoplasm are observed in the left half of the represented AP^+ MBNS image and cells in the right half are more histologically similar to the MBNS-derived tumors. A neuroectodermal structure is indicated with the black arrow in the ES teratoma. Scale bars are 100um.

Klf4 mediates MBNS plasticity during conversion into ES culture conditions

Since the MBNS were converted in ES culture conditions without the induction of exogenous genes, we wanted to determine if epigenetic changes were involved in mediating the MBNS plasticity. We analyzed DNA methylation in the promoters and 5' regulatory regions of pluripotency genes *Oct4, Nanog, Klf4, Sox2, c-myc* and *Stat3* with a quantitative, bisulfite-based mass spectrometry methylation assay. In cancers, methylation alternations have been reported to occur specifically in CpG island shores, located up to 2kb upstream of the promoter CpG islands and are associated with aberrant gene expression (Irizarry *et al.*, 2009). The average methylation frequency across the CpGs in the regions assayed was significantly different between the MBNS and AP^+ MBNS in the *Klf4* and *Sox2* CpG island shores. The most significant differential methylation was observed in the *Klf4* CpG island shore, with 70.7% methylation in the MBNS and a reduction to 34.2% in the AP^+ MBNS (Figure 2-7). Reduced methylation was observed in each individual CpG in this *Klf4* regulatory region in the AP^+ MBNS (Figure 2-8). CpG methylation in the *Sox2* CpG island shore was also reduced in the AP^+ MBNS compared to the MBNS, to a lesser degree (40.9% in the MBNS vs. 30.7% in the AP^+ MBNS). The CpG islands directly upstream of the transcriptional start site (TSS) in the *Klf4* and *Sox2* promoters were not analyzed by the methylation assay. The average methylation remained unchanged in the other pluripotency genes, as the promoters of *c-myc* and *Stat3* remained hypomethylated and *Nanog* remained hypermethylated. The levels of CpG methylation in the *Oct4* promoter also remained similar between the MBNS and the AP^+ MBNS. These results suggest a plasticity in the epigenetic regulation of the CpG island shores of the pluripotency genes *Klf4* and *Sox2* during the conversion of MBNS into ES culture conditions.

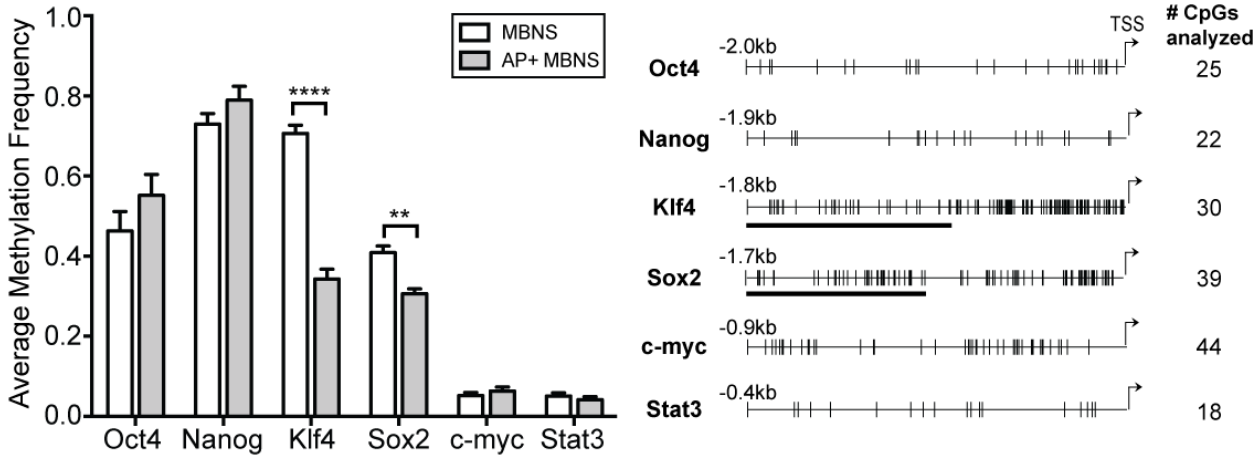

Figure 2-7 CpGs in the 5' regulatory regions of *Klf4* and *Sox2* are differentially methylated between the MBNS and AP+ MBNS

(a) Methylation analyses of the CpGs in the promoters and 5' regulatory regions of pluripotency genes were carried out by quantitative mass spectrometry, in the parental MBNS line and three AP^+ MBNS subclones. Average methylation frequencies across the regions analyzed are plotted as mean+sem. Differential methylation is observed in the 5' regulatory regions between the MBNS and the AP^+ MBNS in *Klf4* ($p<0.0001$) and *Sox2* ($p<0.01$), as determined by two-way ANOVA with a Bonferroni multiple comparisons test. In the right panel, a schematic of the promoter and upstream regions of the pluripotency genes indicating the locations of the CpGs analyzed (vertical hash marks) is represented. The methylation analyses for *Klf4* and *Sox2* only included the CpGs in the 5' regulatory regions (CpG island shores), as indicated by the black bars.

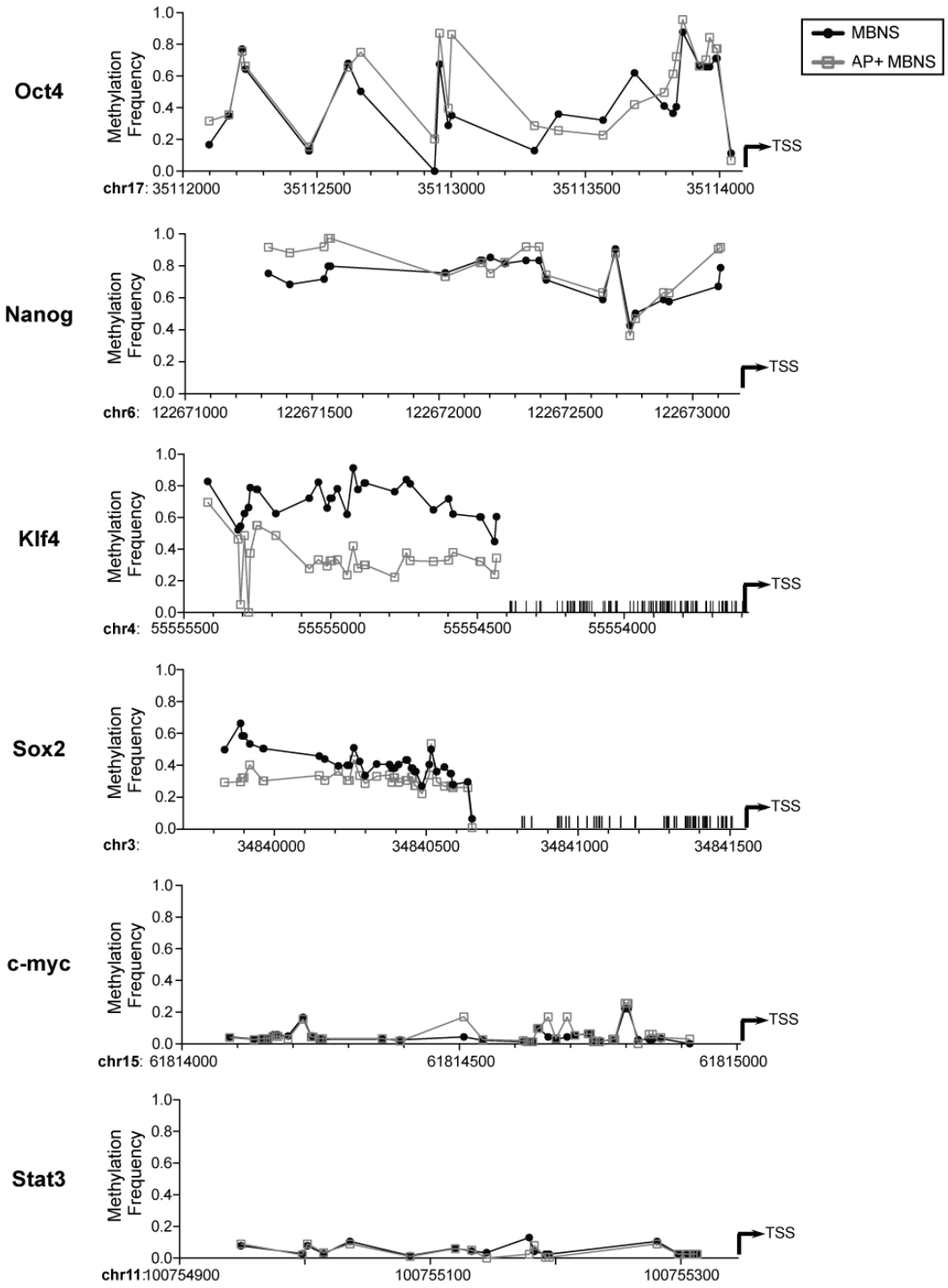

Figure 2-8 Quantitative methylation analyses of individual CpGs in the 5' regulatory regions and promoters of pluripotency genes in MBNS and AP$^+$ MBNS show differential methylation in *Klf4* and *Sox2*

The frequency of methylation at each CpG analyzed is denoted by circles (MBNS) or open squares (AP$^+$ MBNS). Genomic coordinates are indicated on the x-axis. Vertical hashes in the *Klf4* and *Sox2* promoters indicate CpGs that were not analyzed in the methylation array.

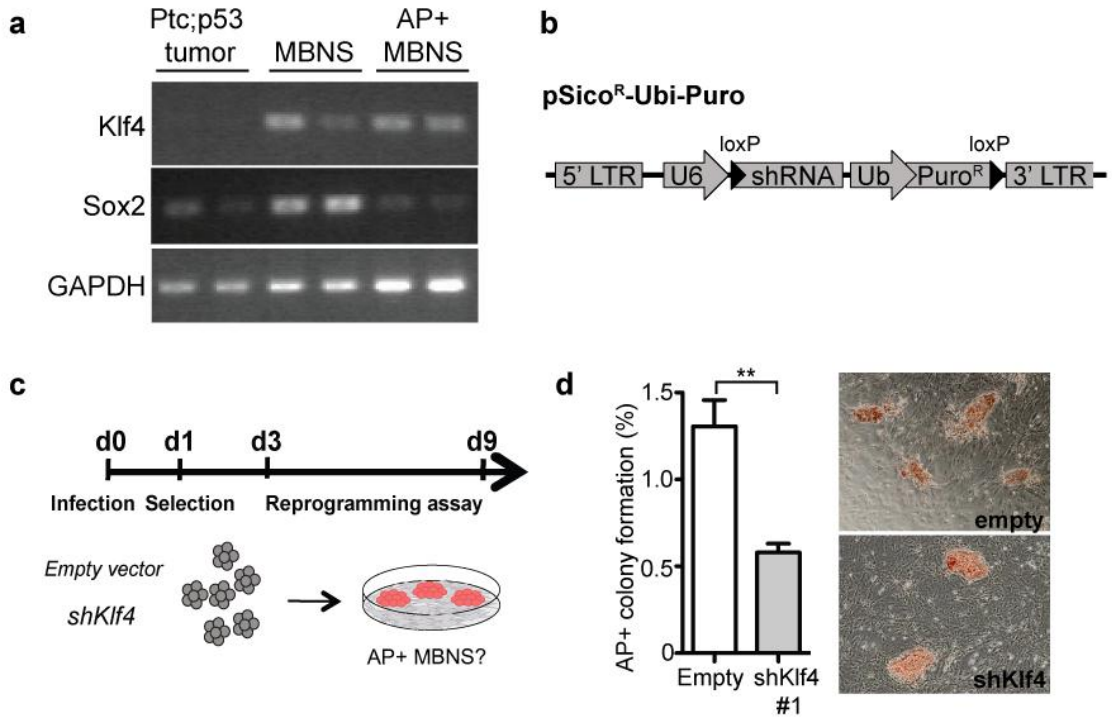

Figure 2-9 *Klf4* mediates MBNS plasticity for conversion into ES culture conditions

(a) Expression analyses of *Klf4* and *Sox2* by gel-based RT-PCR. (b) Schematic of the lentiviral vector pSicoR (Ventura *et al.*, 2004), which was modified for puromycin selection (Puro^R) and shRNA expression driven by a ubiquitin (Ub) promoter. (c) *Klf4* knockdown (kd) MBNS were converted into ES cell culture conditions and monitored for AP$^+$ colony formation, as described in Figure 2-3a. (d) Significant reduction in AP$^+$ colony formation is observed in the sh*Klf4* MBNS (p=0.018 by unpaired t-test). Representative images of AP$^+$ colonies formed are shown.

Klf4 expression is reported to abrogate the requirement for LIF to maintain mouse ES cells in an undifferentiated state (Zhang *et al.*, 2010) and gel-based RT-PCR confirmed the expression of *Klf4* transcript in the AP$^+$ MBNS, as well as the parental MBNS (Figure 2-9a). Although not quantitative, *Klf4* was also further examined because *Sox2* expression appeared to be reduced in the AP$^+$ MBNS (Figure 2-9a). Therefore, we next asked if exogenous LIF in the ES media was required for the initiation and the maintenance of the AP$^+$ MBNS colony formation. To determine if exogenous LIF was required for the initiation of the conversion in the ES culture condition, we carried out the *in vitro* reprogramming assay in the presence and

absence of LIF with an AP^+ MBNS subclone and observed no significant difference in the AP^+ colony formation (Figure 2-10a, b). However, in the absence of MEFs, which is known to provide soluble factors including LIF, while clusters of cells were present, no AP^+ colony formation was observed. To test if exogenous LIF was necessary for the maintenance of self-renewal and colony formation, a clonogenic plating efficiency assay was carried out in the presence and absence of exogenous LIF. AP^+ colony formation was not affected by the removal of exogenous LIF (Figure 2-10c,d). When we further eliminate a potential source of LIF by

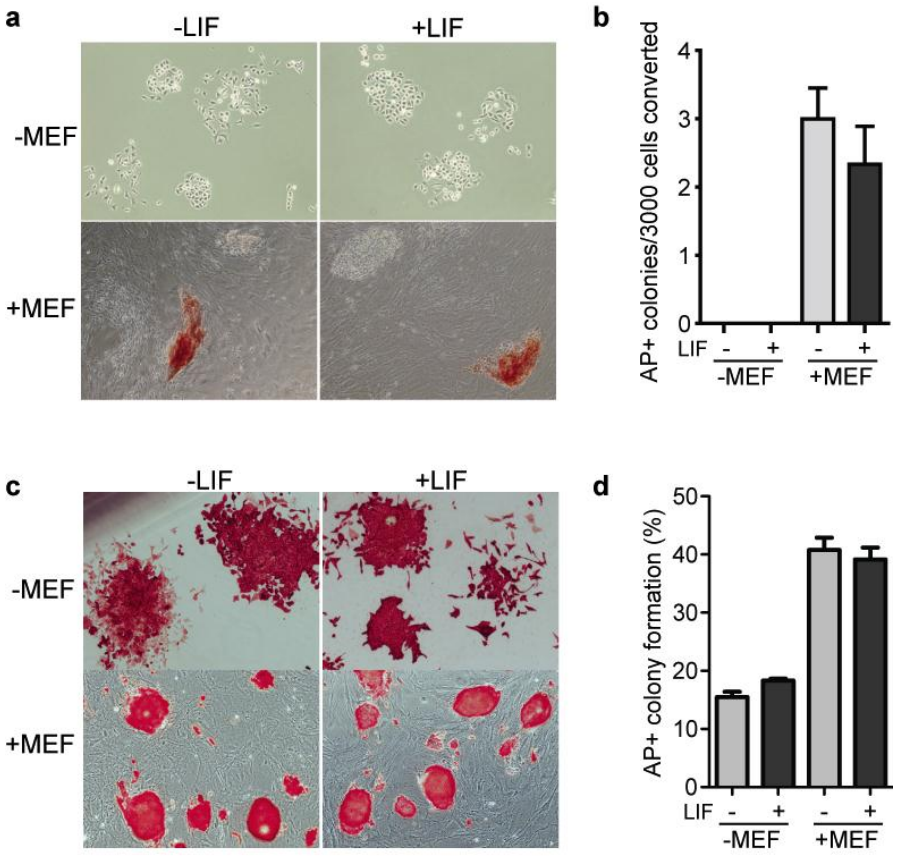

Figure 2-10 Exogenous LIF is not required for the conversion or maintenance of MBNS in ES cell conditions

(a) The conversion of MBNS into ES cell culture conditions was carried out in the presence and absence of both LIF and MEFs. (b) Quantification of AP^+ colony formation shows no observable colony formation in the absence of MEFs. With MEFs, no significant difference is observed in the AP^+ colony formation with or without LIF. (c) A stable AP^+ MBNS subclone line was assayed for clonogenic plating efficiency in the absence and presence LIF and/or MEFs. (d) AP-positive colonies were quantitated by ImageJ analyses, which show no significant difference in colony formation in the absence of LIF.

carrying out the plating efficiency assay in the absence of MEFs, although the overall frequency of colony formation was reduced, no significant difference was observed in the frequency of colony formation in the absence of LIF (Figure 2-10c, d).

To test if the expression of *Klf4* (Figure 2-9a) was functionally involved in the plasticity of the MBNS during the conversion into ES culture conditions, we knocked down *Klf4* with a lentivirally-encoded shRNA against *Klf4* (Figure 2-9b; Table 1) and 3 days post-infection, the *in vitro* reprogramming assay was carried out (Figure 2-9c). AP^+ MBNS colony formation was significantly reduced with the *Klf4* knockdown (kd) (Figure 2-9d), suggesting that *Klf4* was functionally important in mediating MBNS plasticity and colony formation in ES culture conditions.

Table 1. Hairpin sequences of sh*Klf4*

	Position	Sequence	DSIR score	Oligomaker Score
sh*Klf4* #1	839	GCAGCTTGCAGCAGTAACA	NA	7
sh*Klf4* #2	2797	GGTTTCAGATGTGCAATAA	100.3	7

Position indicates the first nucleotide position site where the shRNA binds in the target sequence. Scores as determined by two rule-based design algorithms, DSIR (http://biodev.extra.cea.fr/DSIR/) and pSicoOligomaker 1.5 (http://web.mit.edu/jacks-lab/protocols/pSico.html). The predicated efficacy threshold value is set at 90 in DSIR. A Oligomaker score of greater than 6 is reported to have ~90% chance of silencing the target (Reynolds *et al.*, 2004).

Klf4 is important for the self-renewal of MBNS

As *Klf4* expression is also observed in the parental MBNS prior to conversion into ES conditions (Figure 2-9a), we next examined the role of *Klf4* directly in the MBNS. Quantitative RT-PCR shows that *Klf4* expression is significantly increased in the MBNS compared to WT cerebellum (Cb), *Ptch1*$^{LacZ/+}$, *and Ptch1*$^{LacZ/+}$*;Trp53*$^{-/-}$ tumors, with a 2.3 fold enrichment compared to the WT Cb (Figure 2-11a). To directly test the functional role of *Klf4* in the MBNS, we knocked down *Klf4* with two independent hairpins (Table 1), to levels 20-40% of the control levels (Figure 2-11b) and carried out a clonal density NS formation assay, in which sh*Klf4*

Figure 2-11 *Klf4* kd leads to a reduction in MBNS self-renewal

(a) Expression of *Klf4* mRNA is significantly upregulated in the MBNS compared to wild-type cerebellum (WT Cb), *Ptch1*$^{LacZ/+}$ tumors (Ptc Tu), and *Ptch1*$^{LacZ/+}$*;Trp53*$^{-/-}$ (Ptc;p53 Tu), as measured by quantitative RT-PCR ($p<0.05$ by one-way ANOVA with a Bonferroni post test). (b) Expression analyses of *Klf4*, *Stat3* in the d3 post-infection sh*Klf4* MBNS by quantitative RT-PCR confirm kd of *Klf4* with two independent hairpins (n=3; $p<0.001$ by one-way ANOVA with a Dunnett post test). sh*Klf4*#1 does not affect the expression of *Stat3* but sh*Klf4*#2 reduces *Stat3* expression by about 25% ($p<0.01$ by two-way ANOVA with a Dunnett post test). (c) *Klf4* kd resulted in the significant reduction of self-renewal in the clonal density (100 cell/ml) 6-well NS formation assay. The efficiency of NS formation was expressed relative to the vector control. (n=3; 6 wells quantified per shRNA per experiment; $p<0.001$ by one-way ANOVA with a Dunnett post test). Representative images of wells from the NS formation assay quantitated by ImageJ are shown. (d) Clonogenic limiting dilution assays (Tropepe *et al.*, 1999) were carried out and self-renewal indexes of the sh*Klf4* MBNS were determined by extreme limiting dilution analysis (ELDA) (Hu and Smyth, 2009). 95% confidence intervals (CI) are indicated by the dotted lines. P-values are determined by tests for pair-wise differences between the vector control and each of the shRNAs by ELDA. All values are represented as mean±s.e.m.

Figure 2-11 (Continued)

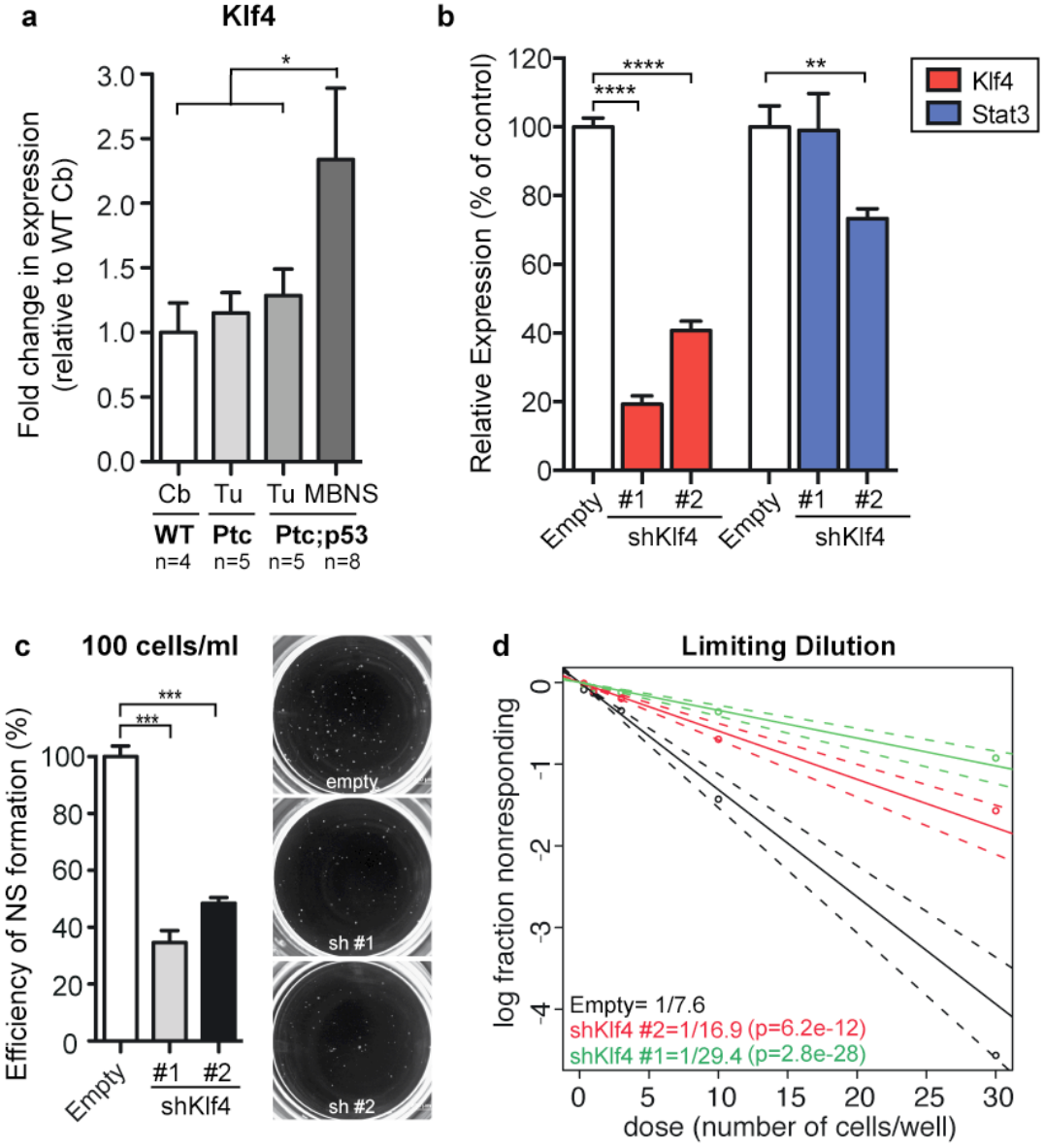

MBNS were plated at a cell density of 100cells/ml, a density ten-fold lower than what is required to ensure a clonal event (Coles-Takabe *et al.*, 2008). When NS formation was quantified 5 days later, *Klf4* kd resulted in a 50-65% reduction in the efficiency of NS formation in the MBNS (Figure 2-11c). The role of *Klf4* in MBNS self-renewal was further confirmed with a limiting dilution assay, where 0.3, 1, 3, 10, and 30 cells were plated per well and assayed for NS formation to determine the frequency of self-renewing cells in the sh*Klf4* MBNS (Tropepe *et al.*, 1999). Extreme limiting dilution analyses (ELDA) (Hu and Smyth, 2009), determined that the self-renewal index was significantly decreased, from 1 in 7.6 cells in the control vector to 1 in 29.4 cells with sh*Klf4* #1 and 1 in 16.9 cells with sh*Klf4* #2 (Figure 2-11d; Table 1). Together, these results support the crucial role of *Klf4* in the mediating MBNS plasticity during conversion into ES culture conditions and in the maintenance of clonogenic self-renewal as neurospheres.

Stat3 signaling is endogenously activated in MBNS

To further gain an understanding of the upstream pathways activating *Klf4* expression in the MBNS, we asked if the Stat3 pathway was involved, as *Klf4* is a known downstream target of Stat3 (Niwa *et al.*, 2009; Bourillot *et al.*, 2009; Hall *et al.*, 2009). Furthermore, given that exogenous LIF was not required for the initiation and maintenance of the AP^+ MBNS (Figure 2-10), we also hypothesized that downstream Stat3 signaling may be endogenously activated or deregulated in the MBNS and subsequently mediating the expression of *Klf4* downstream. Stat3 pathway activation is also known to maintain the self-renewal of ES cells (Niwa *et al.*, 1998) and the survival of NSC (Androutsellis-Theotokis *et al.*, 2006; Yoshimatsu *et al.*, 2006).

Since *Stat3* expression is modulated by an autoregulatory loop (Ichiba *et al.*, 1998) and increased levels of *Stat3* mRNA reflect Stat3 pathway activity, we first compared *Stat3* mRNA

expression among tissues and stem cells from WT or *Ptch1*$^{LacZ/+}$*;Trp53*$^{-/-}$ mice using quantitative RT-PCR. *Stat3* expression in the MBNS was greater than 20-fold higher than the WT Cb and significantly higher compared to *Ptch1*$^{LacZ/+}$*;Trp53*$^{-/-}$ ES cells and tumors (Figure 2-12a). *Stat3* mRNA levels also showed a 15-fold increase in WT P7 CbSC compared to the WT P7 cerebella, consistent with the known developmental role of *Stat3* in NSC. The expression levels between the WT P7 CbSC and MBNS, however, were not significantly different, suggesting that *Stat3* upregulation alone is not sufficient for AP^{+} colony formation in ES conditions.

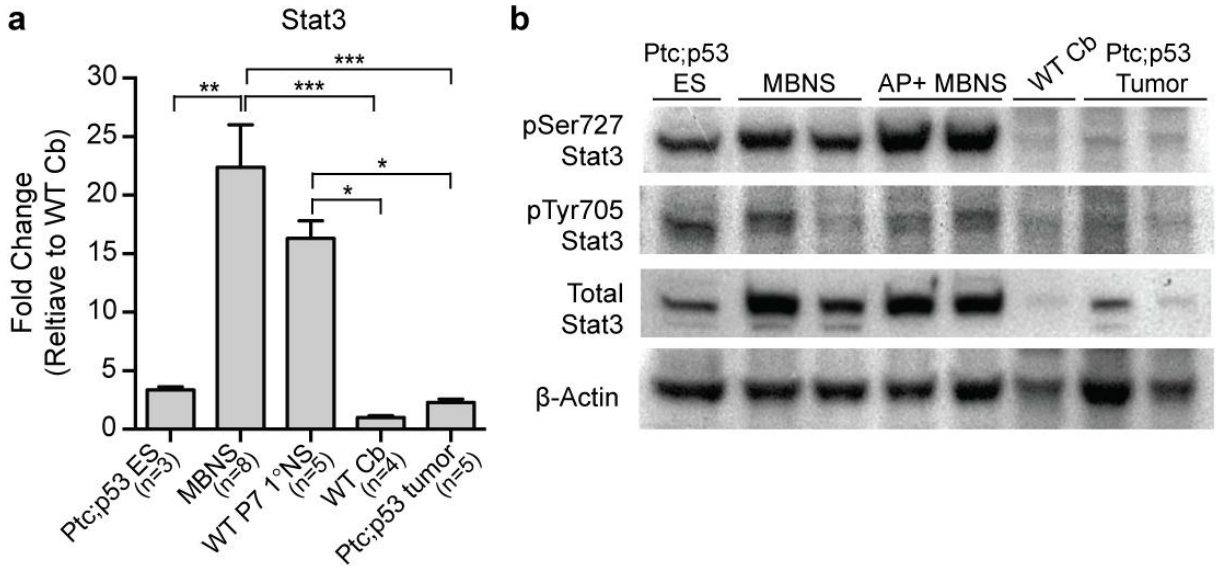

Figure 2-12 Stat3 is endogenously activated in MBNS

(a) Expression of *Stat3* mRNA in *Ptch1*$^{LacZ/+}$*;Trp53*$^{-/-}$ (Ptc;p53) ES (n=3) cells, MBNS (n=8), WT P7 cerebellar stem cells (WT P7 1°NS) (n=5), and *Ptch1*$^{LacZ/+}$*;Trp53*$^{-/-}$ (Ptc;p53) tumors (n=5) compared to wild-type cerebellum (WT Cb) (n=4), as measured by quantitative RT-PCR. All samples are represented as fold change in expression relative to the WT Cb, which is normalized to 1. Significant upregulation of *Stat3* is observed in the MBNS compared to *Ptch1*$^{LacZ/+}$*;Trp53*$^{-/-}$ ES cells ($p<0.01$), WT Cb ($p<0.001$), *Ptch1*$^{LacZ/+}$*;Trp53*$^{-/-}$ tumor ($p<0.001$). *Stat3* is upregulated in the WT P7 1°NS compared to the WT cerebellum ($p<0.05$), *Ptch1*$^{LacZ/+}$*;Trp53*$^{-/-}$ tumor ($p<0.05$). Statistical significance was determined by one-way ANOVA with a Bonferroni post test. (b) Western blot of protein lysates from MBNS in NS media, AP^{+} MBNS in ES culture conditions, tissues from WT Cb, and Ptc;p53 tumors with pSer727, pTyr705, and total Stat3-specific antibodies. ES cells were used as a positive control for Stat3 activation.

Stat3 pathway activation is directly governed by phosphorylation states, such as in NSC, where pSer727 is essential for survival and pTyr705 leads to differentiation (Androutsellis-Theotokis *et al.*, 2006). To address whether alterations in Stat3 phosphorylation might account for the relative contribution of these mechanisms in MBNS, we performed western blotting with phospho-specific Stat3 antibodies. The results showed activation of both phosphorylated forms of Stat3 in the MBNS cultured in NS media and ES conditions, with robust activation of pSer727 Stat3 (Figure 2-12b). WT Cb and *Ptch1*$^{LacZ/+}$*;Trp53*$^{-/-}$ tumors, however, showed relatively lower levels of pSer727 and total Stat3. These results show that the Stat3 signaling pathway is constitutively activated in the MBNS, as indicated by both transcriptional upregulation and activation of Stat3 by phosphorylation, especially at pSer727.

To assess the signaling pathways involved in the constitutive Stat3 pathway activation, we treated MBNS with kinase inhibitors with targets implicated in medulloblastoma stem cells (Hambardzumyan *et al.*, 2008), the activation of Stat3 signaling in cortical NSC (Androutsellis-Theotokis *et al.*, 2006), as well as Stat3 phosphorylation in other cellular contexts (Stephens *et al.*, 1998; Yokogami *et al.*, 2000; Wierenga *et al.*, 2003) (Figure 2-13). Activation of PI3K/Akt/mTOR signaling confers radioresistance and survival to medulloblastoma cells in the perivascular niche (Hambardzumyan *et al.*, 2008). In cortical NSC, Notch signaling also converges on Akt/mTOR pathway activation for subsequent phosphorylation of Ser727 Stat3 and NSC survival (Androutsellis-Theotokis *et al.*, 2006). Human medulloblastomas have constitutive activation of Stat3 signaling (Schaefer *et al.*, 2002), as well as autocrine production of LIF, a major activator of the Jak/Stat signaling pathway (Liu *et al.*, 1999). While Mek1/2 inhibition has been observed to inhibit the migration of a medulloblastoma cell line *in vitro* (MacDonald *et al.*, 2001), the involvement of Stat3 has not been examined.

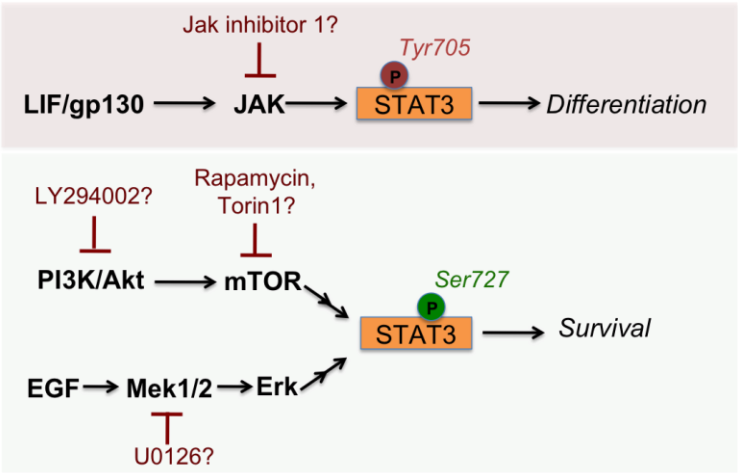

Figure 2-13 Pathways of Stat3 activation and kinase inhibitors used for the treatment of MBNS

Schematic showing the differential roles of phospho-Ser727 Stat3 in survival and phospho-Tyr705 Stat3 in the differentiation of NSC, adapted from *Androutsellis-Theotokis, Leker et al. (2006).* MBNS were treated with small molecule inhibitors of kinases implicated in the activation of pStat3.

Consistent with canonical Stat3 activation, Jak inhibition robustly reduced pTyr705 Stat3 activation without affecting pSer727 Stat3 levels (Figure 2-14a, b). By contrast, Mek1/2 inhibition, validated by monitoring pErk1/2 levels (Figure 2-14a), caused a modest but significant and reproducible 30% decrease in pSer727 Stat3 levels (Figure 2-14a, b). Inhibitors of PI3K or mTOR did not significantly alter either pSer727 or pTyr705 levels. Analysis of Stat3 target gene expression confirmed these results, with Jak inhibition showing reduced *Socs3* and *Stat3* levels within 20 hours (Figure 2-14c). *Socs3*, a direct target of Stat3, is a key response gene in Stat3 signaling (Auernhammer et al., 1999) and Stat3 regulates its own expression (Ichiba et al., 1998). At 20 hours, however, expression levels of the downstream target *Klf4* (Hall et al., 2009; Bourillot et al., 2009) were not affected. These results suggest distinct roles for Jak and Mek signaling pathways during Stat3 activation in MBNS.

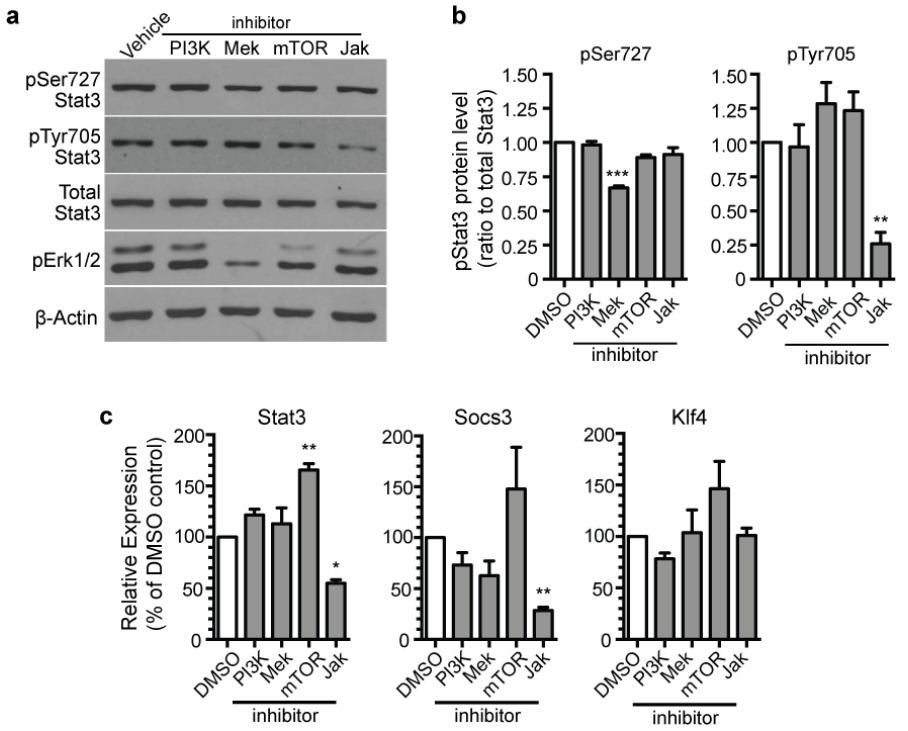

Figure 2-14 pTyr705 and pSer727 Stat3 are differentially regulated by Jak and Mek signaling in the MBNS

(a) Western blot of protein lysates from MBNS treated with inhibitors of PI3K (10uM LY294002), Mek1/2 (10uM U0126), mTOR (50nM Rapamycin) and Jak (1uM Jak inhibitor 1) for 3 hours. A representative western blot from three experiments is shown. (b) Quantification of three independent western blots by densitometry analyses with ImageJ shows significant reduction of pSer727 Stat3 with Mek inhibition ($p<0.0001$) and pTyr705 Stat3 with Jak inhibition ($p<0.01$). (c) Expression analyses of *Stat3* and downstream targets *Socs3* and *Klf4,* by quantitative RT-PCR, 20 hours post-inhibitor treatment show that *Stat3* expression is significantly increased with mTOR inhibition ($p<0.01$) and decreased with Jak inhibition ($p<0.05$). *Socs3 e*xpression is significantly decreased with Jak inhibition ($p<0.01$). *Klf4* expression is not significantly altered with the treatment of any inhibitors. Statistical significance was determined by one-way ANOVA with a Dunnett post test

Combination Jak and Mek inhibition leads to the reduction of MBNS survival

To further inhibit both phosphorylated forms of Stat3, we treated the MBNS with both the Jak inhibitor and Mek inhibitor (U0126), which we have shown to modulate Tyr705 and pSer727 Stat3 phosphorylation, respectively. Combination Mek and Jak inhibitor treatment for 20 hours resulted in the downregulation of both phosphorylated forms of Stat3 (Figure 2-15a). When the functional impact of the inhibition of the Mek and Jak pathways was assessed with the clonal neurosphere formation assay, we observed that individually, Mek or Jak pathway

inhibition did not affect neurosphere formation of the MBNS (Figure 2-15b, c). However, the combinatory inhibition of Mek and Jak inhibitors significantly reduced neurosphere formation and the size of neurospheres formed (Figure 2-15c, d). Together these data reveal that modulation of both phosphorylated forms of Stat3 using a combinatoric treatment of Mek and Jak inhibitors inhibits MBNS formation.

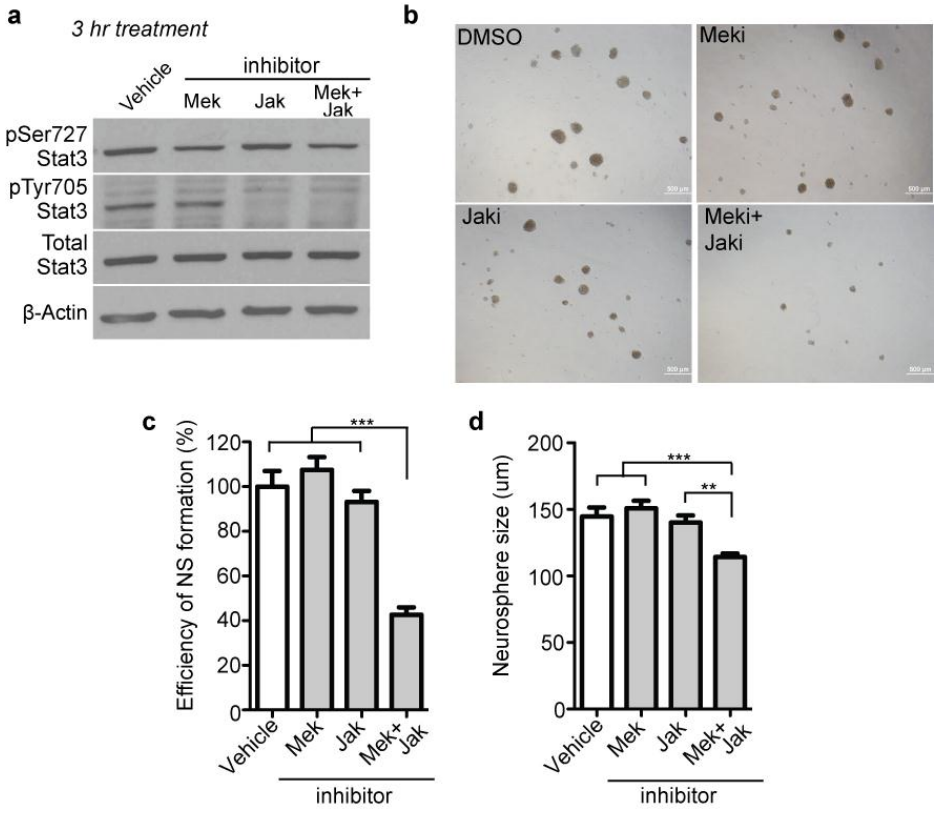

Figure 2-15 Combinatory treatment of Jak and Mek inhibitors leads to a synergistic reduction in MBNS self-renewal and size

(a) Western blot of MBNS protein lysates after Mek, Jak, and Mek+Jak inhibitor treatment for 3 hours. (b) Clonal neurosphere formation assays were carried out in the presence of inhibitors of Mek (10uM U0126), Jak (1uM Jak inhibitor 1), or both Mek and Jak (10uM U0126 and 1uM Jak inhibitor 1) for 7 days, with drug supplementation on day 3. (c) Significant reduction of NS formation is observed with the combination treatment of Mek and Jak inhibitors ($p<0.001$ by one-way ANOVA with a Bonferroni post test). (d) Combination drug treatment also resulted in smaller NS. NS diameters were measured from 60 NS per treatment condition.

MBNS self-renewal is, in part, mediated by *Stat3*, but less significant than the role of *Klf4*

As the kinase inhibitors are not specific to Stat3 and likely affecting many other pathways, to examine the functional role of *Stat3* upregulation in MBNS in a more specific manner, we constructed lentiviral vectors encoding two independent shRNAs (Reynolds *et al.*, 2004) against *Stat3* (Table 2). Western blotting validated *Stat3* kd at the protein level by day 8 (d8) post-infection (Figure 2-16a) and time course analysis of *Stat3* mRNA expression also showed a stable kd throughout day 3 (d3) to day 15 (d15) post-infection. Kd was maintained at about 20% of control levels in the *Stat3* kd bulk cultures, which are seeded at a density of 2-3x10^5 cell/ml (Figure 2-16b). The downstream effect on Stat3 target, *Klf4*, was observed by day 8 (d8). However, we also noted that *Klf4* mRNA expression rebounded to WT levels by d15 post-infection. To determine the functional role of *Stat3* in MBNS self-renewal, on d3 following lentiviral infections, MBNS were plated at clonal density (100 cells/ml) *in vitro* and we observed about a 50% reduction in neurosphere formation compared to the vector control (Figure 2-16c). Similar to the sh*Klf4* MBNS, limiting dilution assays were carried out to determine the frequency of self-renewing cells in sh*Stat3* MBNS and extreme limiting dilution analyses (ELDA) showed that self-renewing indexes decreased from 1 in 5.1 cells in the control to 1 in 10.5 and 1 in 7.3 in the sh*Stat3* #1 and #2 MBNS, respectively (Figure 2-16d). However, the effect on *Stat3* kd on MBNS self-renewal was less significant than the *Klf4* kd. These effects are more apparent when the ELDA was carried out by combining the data from limiting dilution assays from both *Stat3* and *Klf4* kd MBNS (Table 3). These results show that MBNS self-renewal depends, in part, on *Stat3*, an upstream activator of *Klf4.*

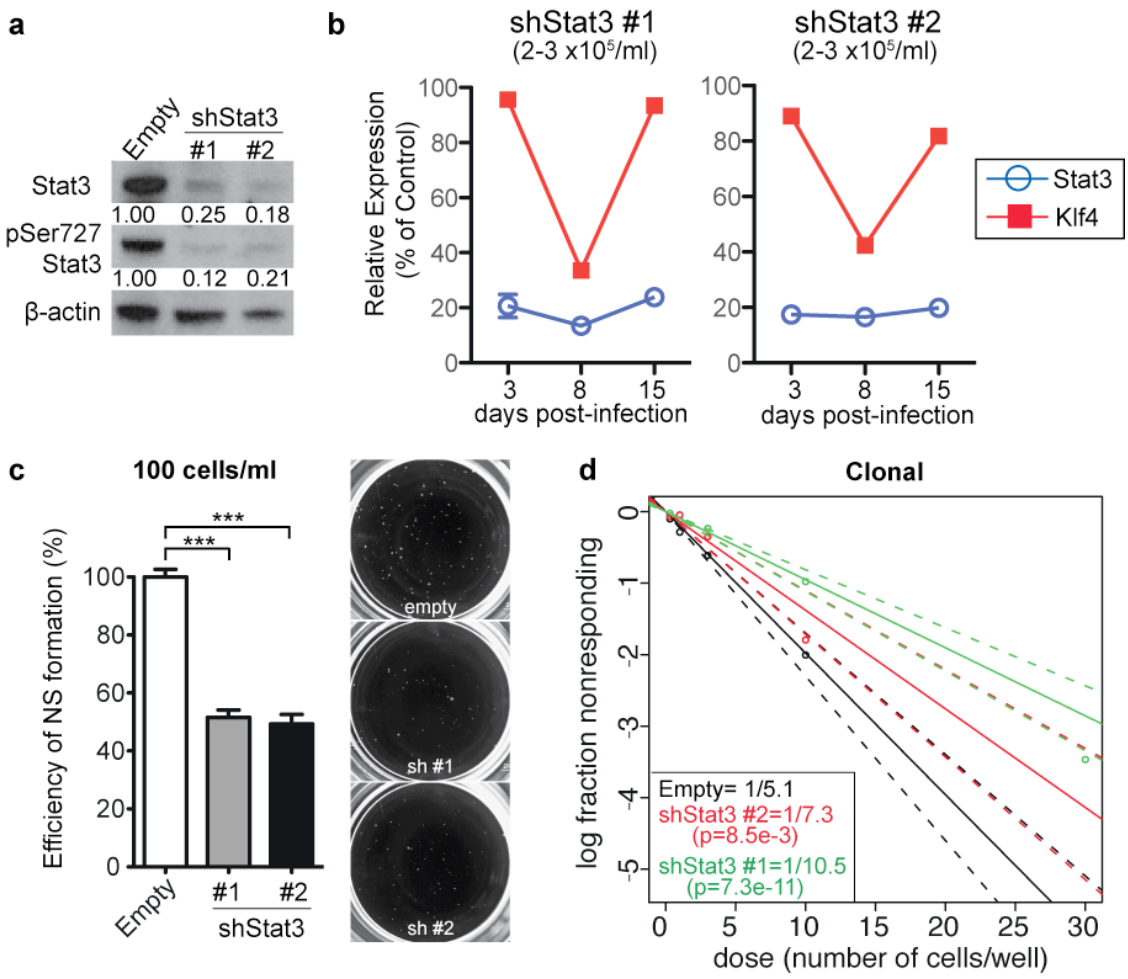

Figure 2-16 *Stat3* kd leads to a reduction in MBNS self-renewal

(a) Western blot of protein lysates from d8 post-infection sh*Stat3* MBNS with total and pSer Stat3 antibodies confirmed *Stat*3 kd with 2 independent shRNA hairpins. (b) A time course-dependent effect on *Stat3* kd and downstream target *Klf4* was measured by quantitative RT-PCR in d3, d8, and d15 post-infection sh*Stat3* bulk cultures. (c) *Stat3* kd resulted in significant reduction of self-renewal in the clonal density (100 cell/ml) 6-well NS formation assay. The efficiency of NS formation was expressed relative the vector control. (n=4 for sh*Stat3* #1, n=3 for sh*Stat3* #2; 6 wells quantified per shRNA per experiment; $p<0.001$ by one-way ANOVA with a Dunnett post test). Representative images of wells from the NS formation assay quantitated by ImageJ are shown. (d) A clonogenic limiting dilution assay (Tropepe *et al*. 1999) was carried out and self-renewal indexes of the sh*Stat3* MBNS were determined by extreme limiting dilution analysis (ELDA) (Hu and Smyth, 2009). P-values are determined by tests for pair-wise differences between the vector control and each of the shRNAs by ELDA. 95% confidence intervals are indicated by the dotted lines. All values are represented as mean±s.e.m.

Table 2. Hairpin sequences of sh*Stat3*

	Position	Sequence	DSIR score	Oligomaker score
sh*Stat3* #1	744	GCAGGATCTAGAACAGAAA	99.4	7
sh*Stat3* #2	1209	GGAGCTGTTCAGAAACTTA	101	7

Position indicates the first nucleotide position site where the shRNA binds in the target sequence. Scores as determined by two rule-based design algorithms, DSIR (http://biodev.extra.cea.fr/DSIR/) and pSicoOligomaker 1.5 (http://web.mit.edu/jacks-lab/protocols/pSico.html). The predicated efficacy threshold value is set at 90 in DSIR. A Oligomaker score of greater than 6 is reported to have ~90% chance of silencing the target (Reynolds *et al.*, 2004).

Table 3. Statistical analyses of extreme limiting dilution analyses (ELDA) of *Stat3* and *Klf4* kd MBNS self-renewal

	Number of	Number of positive well/total wells plated				
	cells/well	**Empty**	**shStat #1**	**shStat3 #2**	**shKlf4 #1**	**shKlf4 #2**
	30	191/192	93/96	48/48	58/96	76/96
	10	156/192	60/96	40/48	29/96	48/96
	3	72/192	20/96	14/48	11/96	17/96
	1	36/192	11/96	2/48	6/96	10/96
	0.3	17/192	2/96	3/48	2/96	1/96
NS formation	Estimate	1/6.25	1/10.51	1/7.25	1/29.38	1/16.86
frequency	(95% CI)	(1/6.97-1/5.60)	(1/12.32-1/8.97)	(1/9.06-1/5.83)	(1/35.7-1/24.2)	(1/19.97-14.26)
Overall test for differences in stem cell frequencies						
		P value	7.66E-58			
Pairwise test for differences in stem cell frequenices						
Empty vs. shStat3 #1		**Pr (>Chisq)**	8.27E-08			
Empty vs. shStat3 #2		**Pr (>Chisq)**	0.241			
Empty vs. shKlf4 #1		**Pr (>Chisq)**	6.84E-53			
Empty vs. shKlf4 #2		**Pr (>Chisq)**	4.54E-25			

Stem cell frequencies, 95% confidence intervals, and statistical tests for significance between stem cell frequencies were determined by the ELDA webtool (http://bioinf.wehi.edu.au/software/elda/).

Klf4 levels rebound in a *Stat3*-independent manner in clonally derived sh*Stat3* MBNS

The partial inhibition of MBNS self-renewal in *Stat3* kd cells suggested the potential for a *Stat3*-independent, compensatory mechanism for the maintenance of self-renewal in clonal cultures. To rule out the possibility that the surviving d8 *Stat3* kd MBNS in the clonal neurosphere formation assay was not due to loss of expression of the *Stat3* hairpins or another RNAi escape mechanism, we examined *Stat3* expression in sh*Stat3* MBNS that emerged from the clonal NS formation assay (Figure 2-17a). *Stat3* kd was maintained at levels significantly lower than the controls in both the clonally derived sh*Stat3* NS and the higher-density bulk cultures at d8 (Figure 2-17b). However, supporting the role for *Klf4* in self-renewal as described above, we observed *Klf4* expression rebounding to levels greater than WT levels in the surviving sh*Stat3* NS derived from the clonal density cultures, but remained decreased as a secondary

effect of *Stat3* kd in the high-density bulk cultures (Figure 2-17b). The clonogenic neurosphere assay assesses the cell-intrinsic ability for self-renewal and survival under stringent, clonogenic conditions. In contrast, higher-density bulk cultures may contain a heterogeneous population of cells, including differentiating cells remaining in NS as a result of cell aggregation that may not require *Klf4* expression for survival. Furthermore, cell-to-cell contact or secretion of other paracrine growth factors by a heterogeneous population of cells may also be involved in supporting the growth or self-renewal of cells in the bulk cultures. In fact, in adult hippocampus NSC, bFGF alone does not support the mitogenic activity in low density cultures; high density cultures are required for the sufficient production of a necessary autocrine/paracrine cofactor (Taupin *et al.*, 2000). These results suggest that a *Stat3*-independent upregulation of *Klf4* is associated with the maintenance of clonogenic MBNS self-renewal.

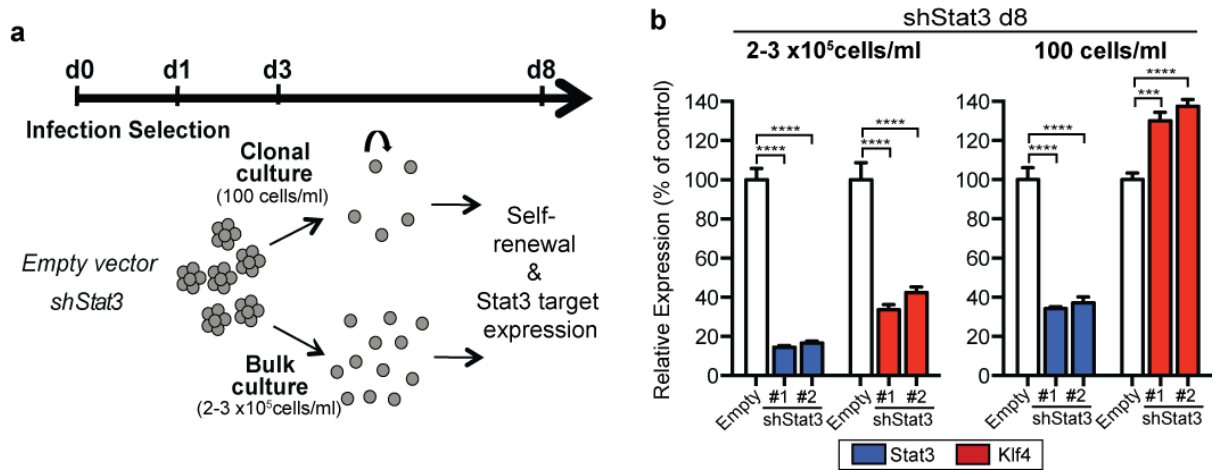

Figure 2-17 *Klf4* expression rebounds in *Stat3*-independent manner in clonal density

(a) Experimental timeline of the *Stat3* kd in the MBNS and the distinct clonal and bulk sh*Stat3* cultures obtained for analyses. Following antibiotic selection of lentivirally infected MBNS, sh*Stat3* MBNS were assayed for *Stat3* knockdown, self-renewal in clonal density (100 cells/ml) cultures, or passaged for maintenance in bulk culture (2-3 x 10^5 cells/ml) on d3 post-infection. (b) Expression analyses of *Stat3* and *Klf4* in self-renewing NS derived from the d8 post-infection sh*Stat3* bulk (2-3 x 10^5 cells/ml) and clonal density (100 cells/ml) cultures show a significant upregulation of *Klf4* in the low-density cultures ($p<0.001$ for sh*Stat3* #1; $p<0.0001$ for sh*Stat3* #2), while *Stat3* kd is maintained at significant low levels ($p<0.0001$). Statistical significance was determined by a one-way ANOVA with a Dunnett post test.

Stat3 and *Klf4* independently regulate the expression of Stat3-target survival genes

As a survival mechanism for cancer cells, *Klf4* has been reported to suppress the apoptotic response of cancer cells following DNA damage (Ghaleb *et al.*, 2007). Stat3 also has known roles in survival by directly regulating the expression of anti-apoptotic target genes including survivin (Gritsko *et al.*, 2006), *Bcl-x* (Catlett-Falcone *et al.*, 1999), *Mcl1* (Epling-Burnette *et al.*, 2001), all of which have been reported to be aberrantly expressed or activated and involved in conferring resistance to apoptosis in various tumor types (Ambrosini *et al.*, 1997; Hazan-Halevy *et al.*, 2010). When we examined the promoter regions of the Stat3-target survival genes, as expected, Genomatix promoter analyses identified Stat3-binding motifs (Figure 2-18a, b, c) within the promoter regions of survivin, *Bcl-x* and *Mcl1* (Figure 2-18c, 19, 20). Interestingly, we also observed predicted Klf4-binding sites (Figure 2-18b) in close proximity to the Stat3-binding sites, further validated by analyzing ChIP-Seq datasets from published studies (Figure 2-18c).

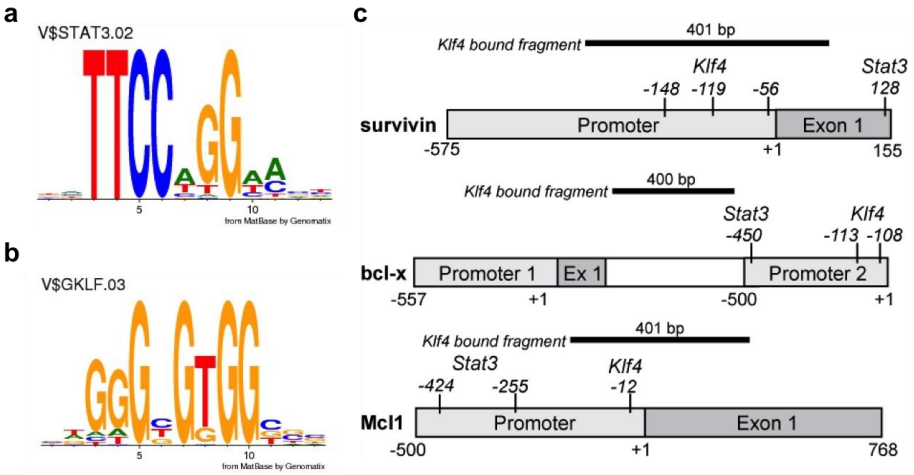

Figure 2-18 Binding site motifs of Stat3 and Klf4 and overview of binding sites in the Stat3-target survival gene promoters as determined by Genomatix

(a-b) The binding motifs have been identified by Genomatix by weight matrices containing 375 binding sites for Stat3 and 355 binding sites for Klf4 from ChIP-Seq data from *Chen et al. 2008.* (c) Schematic of the survivin, *Bcl-x*, and *Mcl1* promoters with locations of predicted Stat3 and Klf4-binding sites. The binding positions indicate the position of anchor sequence (center position) of the predicted binding sites in relation to the transcriptional start site (+1). Analyses of ChIP-Seq data by TRANSFAC showed Klf4 binding to the survival gene promoters in ES cells.

Figure 2-19 *Mcl1* and survivin promoter analyses identify predicted Klf4 binding sites in close proximity to predicted Stat3-binding sites.

Genomic sequence of promoters of Stat3-target survival genes survivin and *Mcl1* and predicted Stat3 (blue) and Klf4 (red)-binding sites by MatInspector (Genomatix Software Suite). Analyses of ChIP-Seq data (from Chen *et al.* 2008) by TRANSFAC showed Klf4 binding to the survival gene promoters in ES cells. Binding fragments are indicated by the pink blocks.

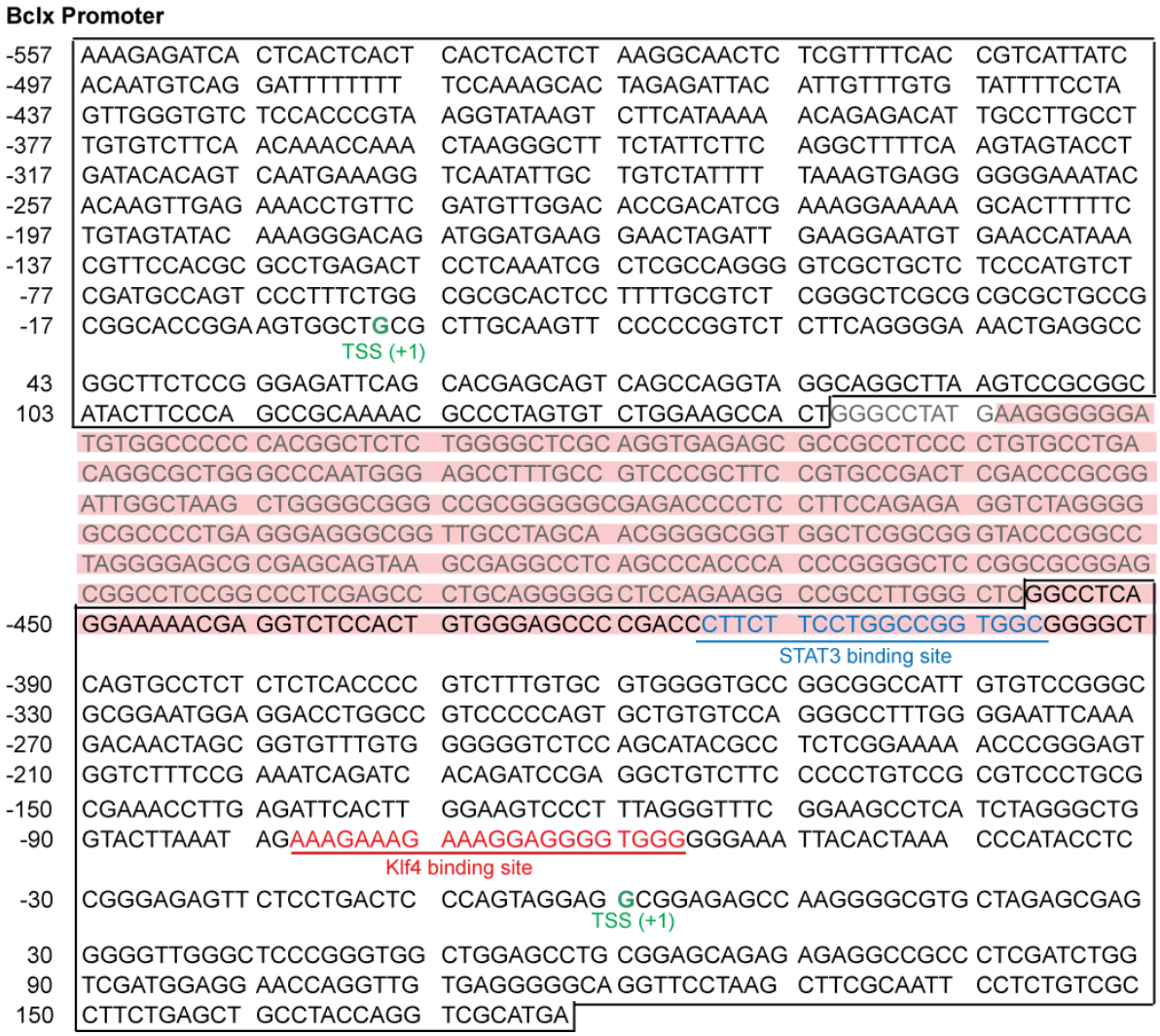

Figure 2-20 *Bcl-x* promoter analysis identifies predicted Klf4-binding sites in close proximity to predicted Stat3 binding sites.

Genomic sequence of promoters of Stat3-target survival gene *Bcl-x* and Stat3 (blue) and Klf4 (red) binding sites predicted by MatInspector (Genomatix Software Suite). Two promoter regions are identified for *Bcl-x*, as indicated by the boxed regions. Analyses of ChIP-Seq data (from Chen *et al*. 2008) by TRANSFAC showed Klf4 binding to the *Bcl-x* gene promoters in ES cells. Binding fragments are indicated by the pink blocks.

Therefore, we next asked if *Stat3* and *Klf4* kd affected expression of the survival genes in the MBNS. When *Stat3* or *Klf4* were individually knocked down at d3 post-infection, the expression of *Bcl-x* and *Mcl1* remained at levels unchanged relative to the control, although survivin expression was reduced in the *Klf4* kd (Figure 2-21a). By d8 post-infection in sh*Stat3* bulk cultures, when *Stat3* and *Klf4* levels were both reduced to 20% and 40% of control levels,

respectively (Figure 2-17b), coordinate downregulation of *Bcl-x* and *Mcl1* expression was observed (Figure 2-21b). However, in the d8 sh*Stat3* clonal cultures, when *Klf4* levels rebounded (Figure 2-17b), survival gene expression was maintained at WT levels, suggesting that *Stat3* and *Klf4* can compensate for each other in maintaining the expression of the target survival genes. The observations in the bulk culture may also reflect the heterogeneity in this high cell-density culture, as suggested by the cells present in the bulk culture with both *Stat3* and *Klf4* levels reduced, which may be representing non-stem cells that do not require *Klf4* and target survival genes for their self-renewal or are dependent on other mechanisms or pathways for survival.

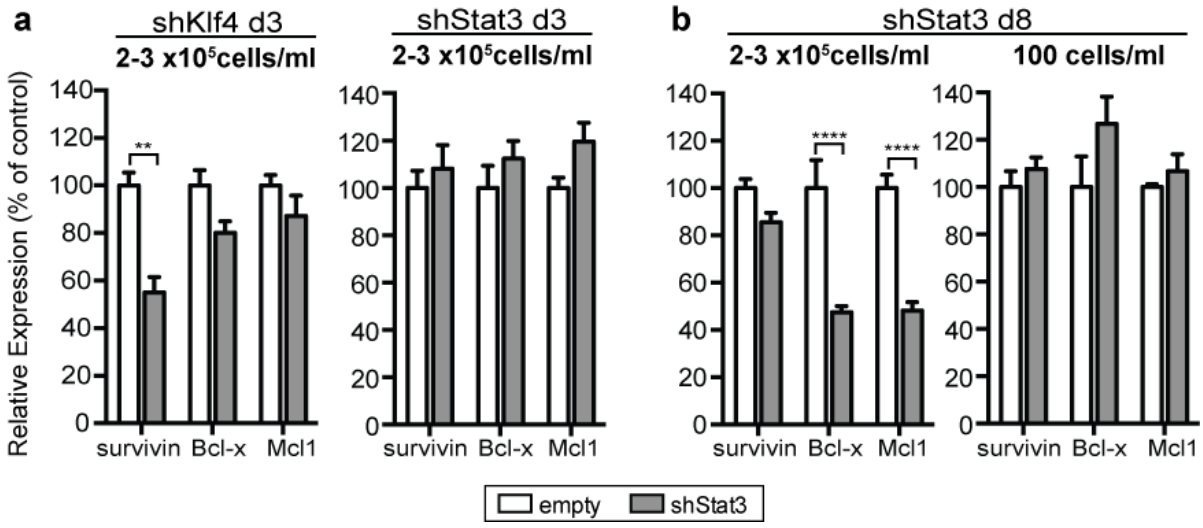

Figure 2-21 *Stat3* or *Klf4* expression is sufficient for the maintenance of Stat3-target survival gene expression

(a) Independent *Stat3* and *Klf4* kd does not affect survival gene expression in MBNS, as measured by quantitative RT-PCR in the d3 post-infection sh*Klf4* and sh*Stat3* MBNS bulk cultures. The expression of *Bcl-x*, and *Mcl1* are not affected by the kd of *Klf4* or *Stat3*. Survivin expression is reduced in the *Klf4* kd MBNS ($P<0.01$). (b) In d8 post-infection sh*Stat3* MBNS, a compensatory upregulation of *Klf4* in the clonal cultures is associated with the maintenance of survival gene expression. In the d8 sh*Stat3* bulk cultures, when both *Stat3* and *Klf4* levels are reduced, there is a significant reduction in the expression of *Bcl-x* and *Mcl1* ($p<0.0001$). Statistical analyses were carried out by one-way ANOVA with a Dunnett post test. Expression values are normalized to the vector control and represented as mean±sem.

BCL-X and CD133 expression in human medulloblastoma is associated with poor survival

When the expression of the STAT3 and KLF4 target survival genes was further analyzed in a human medulloblastoma expression dataset (Kool *et al*., 2012), significant upregulation of *BCL-X*, but not *MCL1* and *BIRC5* (Survivin) was observed in the Group 3 tumors, which have the worst overall survival probability (Northcott *et al.*, 2011b) (Figure 2-22, 23). Furthermore, expression of PROM1 (CD133), a NSC marker enriched in the MBNS (Figure 2-1) was also elevated in Group 3 tumors (Figure 2-23), which have modeled by the *ex vivo* transformation of CD133-enriched CbSC (Pei *et al.*, 2012), suggesting the potential utility for NSC and survival gene markers as prognostic indicators. In conclusion, by asking about plasticity mechanisms within the *Ptch1*$^{LacZ/+}$*;Trp53*$^{-/-}$ MBNS, this led us to the identification of *Klf4*, a reprogramming factor, as a gene also crucial for the clonogenic self-renewal of the MBNS. During the clonogenic self-renewal of MBNS, *Klf4* was upregulated in a Stat3-independent manner and this was further associated with the expression of survival genes.

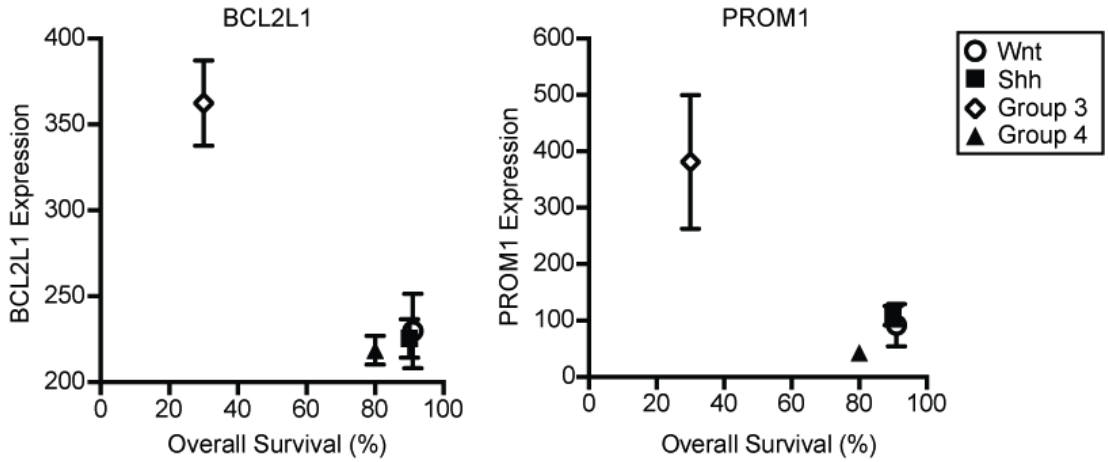

Figure 2-22 *BCL-X* and *PROM1* expression is associated with human medulloblastomas with the poorest prognosis

Expression analyses of *BCL-X* (*BCL2L1*) and *PROM1* (*CD133*) in the human medulloblastomas from the Northcott *et al*. (2011) dataset indicate significant upregulation of these genes in Group 3, the class with the worst overall median survival. All values are represented as mean±s.e.m.

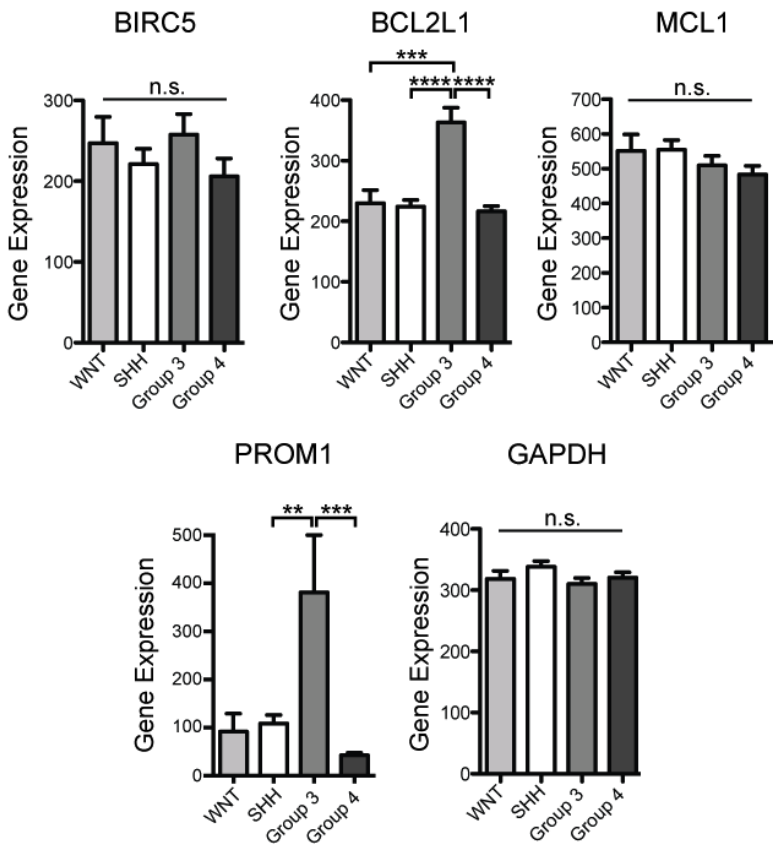

Figure 2-23 *BCL-X* and *CD133* are elevated in Group 3 human tumors

BCL2L1 (*BCL-X*) expression is significantly higher in Group 3 tumors compared to WNT ($p<0.001$), SHH ($p<0.0001$) and Group 4 ($p<0.0001$). *PROM1* (*CD133*) is also elevated in Group 3 compared to SHH ($p<0.01$) and Group 4 ($p<0.001$) tumors. The expression of *BIRC5* (*Survivin*), *MCL1* and *GAPDH*, however, are not significantly (n.s.) different between the tumor classes. Expression values are plotted as mean±s.e.m and statistical analyses was carried out by one-way ANOVA with a Bonferroni post test. The number of human tumors analyzed are as follows WNT=8, SHH=33, Group 3=27; Group 4=35.

Discussion

While efforts to model different subtypes of human medulloblastoma have led to several targeted therapies (Lau *et al.*, 2012), the molecular and genetic pathways involved in relapsing tumors or tumor stem cells are not well understood. In particular, *Ptch1*$^{LacZ/+}$*;Trp53*$^{-/-}$ mouse medulloblastomas provide a tractable model for studying the potential role of self-renewing, stem-like cells in these tumors. *Ptch1*$^{LacZ/+}$tumors have been characterized as granule neuron progenitor (GCP)-driven tumors, which develop as a focal mass and do not exhibit properties of self-renewal in neurosphere culture conditions (C. Lin thesis). In contrast, *Ptch1*$^{LacZ/+}$*;Trp53*$^{-/-}$ tumors are more diffuse and exhibit stem cells characteristics, including high expression of NSC markers such as CD15 and CD184, in comparison to the *Ptch1*$^{LacZ/+}$ tumors, and exhibit self-renewing neurosphere formation. These *Ptch1*$^{LacZ/+}$*;Trp53*$^{-/-}$ MBNS are enriched in stem cell marker expression and are able to initiate tumors upon transplantation *in vivo*. As shown in this chapter, we also observed that these MBNS also displayed plasticity and growth in ES cell culture conditions as self-renewing, AP^{+} colonies, despite the presence of differentiating factors in serum. We further discovered that *Klf4*, a reprogramming factor, was crucial for *Ptch1*$^{LacZ/+}$*;Trp53*$^{-/-}$ MBNS plasticity and self-renewal and *Klf4* expression was upregulated in a LIF/Stat3-independent manner during clonogenic growth. Our work suggests that the *Ptch1*$^{LacZ/+}$*;Trp53*$^{-/-}$ MBNS are able to utilize endogenously activated components of the pluripotency transcription factor network to sustain expression of genes important for growth in clonal conditions in both ES culture conditions in the *in vitro* reprogramming assay and in neurosphere culture conditions.

Tumor-initiating, self-renewing Ptch1$^{LacZ/+}$;Trp53$^{-/-}$ medulloblastoma cells

Ptch1$^{LacZ/+}$;Trp53$^{-/-}$ tumors are able to be propagated as self-renewing neurospheres, display enriched expression of stem cell markers including CD15, CD133 (Figure 1-1), nestin, Sox2 (C. Lin thesis) and are capable of secondary tumor initiation when transplanted into the cerebella of immunocompromised mice. Serum-free neurosphere culture with growth factors EGF and bFGF was initially developed for the isolation of multipotent NSC (Reynolds *et al.*, 1992), but has been extensively utilized for the enrichment of human brain tumor stem cells *in vitro* (Singh *et al.*, 2003; Hemmati *et al.*, 2003; Galli *et al.*, 2004; Dirks, 2008). Neurosphere cultures have been shown to select for cells with tumor-initiating ability that reliably maintain the characteristics of the primary tumor (Lee *et al.*, 2006), whereas non-sphere-forming cells were unable to initiate tumor-formation *in vivo* (Yuan *et al.*, 2004). Postnatal CbSC have also been isolated and characterized as a *Math1*-negative, bFGF-responsive, CD133-positive population, which grow as self-renewing, Sox2 and nestin-positive neurospheres *in vitro* and exhibit multipotent differentiation *in vitro* and *in vivo* (Lee *et al.*, 2005). This is in contrast to Math1-positive GCP of the cerebellum, which cannot proliferate in response to bFGF (Lee *et al.*, 2005), consistent with the observation that bFGF inhibits GCP proliferation and induces differentiation in *Ptch1$^{LacZ/+}$*tumor cells (Fogarty *et al.*, 2007). The presence of bFGF-responsive *Ptch1$^{LacZ/+}$;Trp53$^{-/-}$* cerebellar stem-like cells in the tumors and in 3 week old animals (C. Lin thesis), suggests an aberrantly persistent population of CbSC. Alternatively, the possibility of GCPs to develop a resistance to bFGF-induced differentiation or acquire a more dedifferentiated state cannot be excluded. To differentiate between these two possibilities, lineage-tracing studies following the prospectively labeled CbSC and GCP populations would be necessary.

Although the aforementioned characteristics of the *Ptch1*$^{LacZ/+}$*;Trp53*$^{-/-}$ MBNS is suggestive of the enrichment of a tumor-propagating cell from the primary tumors with neurosphere culture, the possibility of clonal selection of cells or tissue culture-induced changes promoting increased proliferation and survival must be considered. To ascertain the role of *bona fide* cancer stem cells in these tumors, prospective isolation of an endogenous cell population with a stem cell marker that can isolate the self-renewal and tumor-initiating activity is necessary and will be further addressed in Chapter 3. In the absence of a validated prospective marker, in acute myeloid leukemia (AML), for example, where CSC were first identified, injections of ten-fold limiting dilution series of unfractionated AML cells were carried out for the quantification of AML-initiating cells (Bonnet and Dick, 1997). To further bolster the role of stem cells in the *Ptch1*$^{LacZ/+}$*;Trp53*$^{-/-}$ medulloblastomas, neurosphere differentiation assays to determine multipotency and quantitative serial transplantation assays will also need to be carried out. Nonetheless, it is important to understand the role of these *Ptch1*$^{LacZ/+}$*;Trp53*$^{-/-}$ MBNS, as they are responsive to culture conditions validated for the enrichment of NSC and other brain tumor stem cells (Dirks, 2008) and demonstrate robust self-renewal and tumor-initiating capability.

Phenotypic conversion of MBNS

Phenotypic conversion of MBNS in an *in vitro* reprogramming assay suggests that pathways shared with the pluripotency network of ES cells can be utilized as a plasticity mechanism by MBNS. The reprogramming of somatic cells to pluripotency involves directed dedifferentiation through ectopic expression of the transcription factors, *Oct4, Sox2, c-myc,* and *Klf4* (Takahashi and Yamanaka, 2006). These same reprogramming genes are normally expressed in CD133-enriched WT cerebellar cells and neurospheres (Po *et al.*, 2010), suggesting

that the pluripotency networks are mostly conserved in NSC. However, our control experiments with developmental CbSC did not provide evidence for colony formation in the *in vitro* reprogramming assay when dissociated neurosphere cells were plated in ES culture conditions. While cortical NSC require exogenous *Oct4* expression for reprogramming (Kim *et al.*, 2009), the MBNS showed endogenous activity and AP^+ colony formation and growth without added factors. Our data suggest that the requirement for exogenous factors may be relieved by tumorigenesis. In human cancers, a c-myc centered transcriptional network contributes to the ES-like signatures observed in cancer, rather than the core ES module defining ES cells (Kim *et al.*, 2010), challenging the notion of the dedifferentiation of cancer cells to an ES-like state. Nonetheless, the molecular underpinnings of the MBNS with ES-like gene signatures led us to predict that these cells may exhibit characteristics of plasticity and respond in ES culture conditions. In fact, histological analyses of the AP^+ MBNS-derived teratomas suggest an increased diversity in the cell types generated in comparison to the parental MBNS-derived tumors which are characterized by a more differentiated cell type, although further marker analysis is required to definitively determine the distinct neural cell types present. It should be also noted that the control $Ptch1^{LacZ/+};Trp53^{-/-}$ ES cell-derived teratomas only consisted of neuroectodermal cells and did not exhibit the formation of all three germ layers, which may be due to the mutant $Ptch1^{LacZ/+}$genotype biasing the differentiation into neural lineages in the teratoma assay. The role of Shh signaling in neural development is well established and neural tube defects and overgrowth in the hindbrain, spinal cord and headfold are observed in *Ptch1* null embryos (Goodrich *et al.*, 1997).

Cancer genomes have previously been reported to be epigenetically reprogrammed to pluripotency by nuclear transplantation (Li *et al.*, 2003; Hochedlinger *et al.*, 2004) and through

induction of ectopic pluripotency factors (Lang *et al.*, 2012). The *in vitro* reprogramming assay may be selecting for those MBNS with tumor-associated epigenetic changes that allow the cells to modulate pluripotency transcription factors and respond to ES culture conditions. Methylation analyses of the regulatory regions of pluripotency genes showed that *Oct4* and *Nanog* remained methylated in the AP^+ MBNS and *c-myc* and *Stat3* remained hypomethylated. However, a significant reduction in DNA methylation was observed at the 5' regulatory regions of *Klf4* (and *Sox2* to a lesser degree) between the MBNS and AP^+ MBNS, which led us to ask if *Klf4* may be involved modulating the phenotypic plasticity. We have not, however, quantitatively examined if the differential CpG methylation at the 5' regulatory regions directly reflects a modulation of gene expression. Nonetheless, *Klf4* has a known role for preventing the differentiation of ES cells in the absence of LIF (Zhang *et al.*, 2010) and *Klf4* expression is required for epiblast stem cells (EpiSC) with restricted potency to attain the ground state pluripotency of ES cells (Guo *et al.*, 2009). Consistent with this, *Klf4* kd resulted in reduction of AP^+ colony formation in ES culture conditions. Furthermore, *Klf4* was also functionally important in the clonal self-renewal of MBNS. It is unknown, however, if the conversion of MBNS in the reprogramming assay is occurring due to a culture-induced epigenetic adaptation or through the selection of a pre-existing population of cells in the primary tumor. For example, the MBNS culture may contain a more primitive NSC, which has been shown to be present as a LIF-dependent population of cells in the neuroectoderm before the formation of the neural tube (Hitoshi *et al.*, 2004).

The role of the *Trp53* mutation during the phenotypic conversion of the MBNS must also be considered and may be exhibiting a two-fold effect. *Trp53* is a potent barrier to reprogramming, as *Trp53* inhibition accelerates the generation of dedifferentiated stem cells (Utikal *et al.*, 2009; Marión *et al.*, 2009; Hong *et al.*, 2009; Kawamura *et al.*, 2009; Li *et al.*,

2009). In addition, p53 loss also increases the adult stem cell pool in various tissue systems including the CNS (Meletis *et al.*, 2006). Therefore, the acquisition of developmental plasticity and an increase in the stem cell pool by the inactivation of *Trp53* may render the *Ptch1*$^{LacZ/+}$*;Trp53*$^{-/-}$ tumor cells more susceptible to tumor-associated reprogramming (Spike and Wahl, 2011).

Oncogenic role of Klf4 in MBNS

Klf4 is a zinc finger transcription factor, which has known roles in a wide range of functions including the regulation of cell proliferation, differentiation and apoptosis. *Klf4* is highly expressed in the intestine, where it was first identified, and in skin epithelial cells (Shields *et al.*, 1996). *Klf4* has been shown to function as both an inhibitor of cell proliferation and inducer of differentiation. In a colon cancer cell line, *Klf4* negatively regulates cell proliferation by inhibition of cell cycle progression at G1/S (Chen *et al.*, 2001). The crucial role of *Klf4* in the induction of differentiation is highlighted in the *Klf4* knockout mice, which die perinatally due to a defective skin barrier function and dehydration caused by aberrant differentiation of the skin (Segre *et al.*, 1999) and colon epithelia (Katz *et al.*, 2002). In human tumors, *Klf4* has been reported to display opposing functions, as either a tumor suppressor or an oncogene depending on the context and tumor type. While *Klf4* is a tumor suppressor gene in colon and gastric cancer, it has oncogenic roles in other cancer cancers such as squamous cell carcinoma and breast cancers (Rowland and Peeper, 2006).

The role of *Klf4* in medulloblastomas has not been studied extensively, but it has been reported that *Klf4* expression is silenced by genetic events such as chromosomal deletions and promoter methylation in human medulloblastomas (Nakahara *et al.*, 2010). This study also

showed that overexpression of *Klf4* in medulloblastoma cells lines led to growth suppression both *in vitro* and *in vivo*, suggesting the role of *Klf4* as a tumor suppressor. Although, one must consider that serum-cultured cell medulloblastoma lines were utilized. However, other studies show an association between tumorigenesis and upregulation of *Klf4* expression. In $Ptch1^{+/-}$ tumors, *Klf4* expression was observed to be elevated in comparison to the pre-neoplastic lesions and GCPs (Oliver *et al.*, 2005). And as a STAT3-target, high KLF4 expression has also been observed as part of the genetic signature of human tumors with activated Stat3 signaling (Alvarez *et al.*, 2005). Our results with RNAi and small molecule inhibitors show that in the $Ptch1^{LacZ/+};Trp53^{-/-}$ MBNS, *Klf4* expression is also, in part, regulated by Stat3 and *Klf4* expression is specifically upregulated in the self-renewing MBNS. Recently, *Klf4* has been shown to be functionally important in the self-renewal of ES cells and the reprogramming of somatic cells to iPS cells, as one of the original four reprogramming factors (Takahashi and Yamanaka, 2006). As a reprogramming factor, *Klf4* was characterized to function as a key component of the transcriptional network of pluripotency in ES cells, as an upstream regulator of *Oct4*, *Sox2*, *Nanog*, and *c-myc* (Kim *et al.*, 2008a). Specifically, in the absence of LIF, *Klf4* expression prevents ES cell differentiation by regulating *Nanog* (Li *et al.*, 2005; Zhang *et al.*, 2010). *Klf4* is also expressed in normal NSC and CbSC (Po *et al.*, 2010; Kim *et al.*, 2009), although the function has not been directly addressed. In a study that examined the role of *Klf4* in cortical NSC, high levels of *Klf4* expression was observed in the NSC but was decreased in differentiated neurons and astrocytes (Qin *et al.*, 2011), suggesting its potential role in the maintenance of stem cells. However, overexpression of *Klf4* resulted in the reduction of proliferation and self-renewal and led to impairment in neural differentiation (Qin *et al.*, 2011). While this shows that precise levels of *Klf4* are critical for the regulation of normal neurogenesis,

the role of endogenously expressed *Klf4* in NSC still remains unclear. The functional role of *Klf4* in the cerebella or cerebellar stem cells, specifically, has also not yet been described.

In *Ptch1*$^{LacZ/+}$*;Trp53*$^{-/-}$ MBNS, our results suggest that *Klf4* functions to maintain self-renewal through both Stat3-dependent and independent mechanisms. The compensatory Stat3-independent expression of *Klf4* during clonogenic neurosphere formation supports an oncogenic function with its involvement in the maintenance of MBNS self-renewal. In the context of CSC, a study in breast cancers has shown that *Klf4* kd results in a reduction in the frequency, self-renewal, and *in vivo* tumorigenicity of the breast CSC population (Yu *et al.*, 2011). Also in breast cancer, the upregulation of *Klf4* via miR-29 repression contributes to the expansion of $CD44^{+}/CK5^{+}$ stem-like tumor-initiating cells and knockdown of *Klf4* leads to the reduction of the frequency of these cells (Cittelly *et al.*, 2013), further providing evidence for an oncogenic role of *Klf4* in certain tumor stem cells.

Role of constitutive activation of Stat3 in MBNS self-renewal

Several lines of evidence show aberrantly activated STAT3 signaling to be important in human tumors including medulloblastomas (Yu and Jove, 2004). Tumor-specific activation of pSer727 STAT3 is observed in primary human medulloblastomas (Yang *et al.*, 2008a) and the MBNS also showed elevated *Stat3* expression that was associated with robust pSer727 activation. The elevated expression of *Stat3*, which was also seen in WT CbSC, suggests that overexpression of *Stat3* in MBNS may be reflective of a developmental origin of these tumors. Abundant expression of *Stat3* has, in fact, been observed in cerebellar white matter at P3 and P10 in the postnatal rat brain (Gautron *et al.*, 2006). Recent studies have demonstrated that small molecule drugs can inhibit the proliferation of the Daoy medulloblastoma cell line *via* inhibition

of Stat3 and Akt pathways (Yang *et al.*, 2008a; 2010b). Although it must be noted that Daoy cells are also propagated as adherent serum-adapted cultures, which have been described to alter the characteristics of the original tumors (Lee *et al.*, 2006; Sasai *et al.*, 2006), while we have specifically examined the function of Stat3 activation in the self-renewing MBNS.

The effect of Stat3 pathway inhibitors on MBNS shed some light on the differential function of the two post-translational modifications of Stat3; pTyr705 Stat3 is robustly inhibited by Jak inhibition and Mek inhibition led to a partial, but consistent decrease in pSer727 Stat3. Mek inhibition may be reducing pSer Stat3 by blocking the activity of ERK2, a downstream kinase shown to phosphorylate Stat3 at Ser727 in different contexts (Chung *et al.*, 1997; Turkson *et al.*, 1999). However, pSer727 Stat3 was only partially inhibited and this is likely due to the contribution of other tumor-related MAPK pathway kinases such as JNK, p38, and PKC (Roberts and Der, 2007). The treatment of MBNS with Jak and Mek inhibitors suggest that these pathways independently are not crucial for the maintenance of MBNS self-renewal. The lack of an effect on the clonal self-renewal with the Jak inhibitor despite the robust inhibition of pTyr705 Stat3, the main transcriptional activation signal, suggests that the activation of Stat3 signaling is not crucial for the maintenance of MBNS self-renewal. The inhibition of Mek signaling, which is involved a multitude of functions including transcriptional regulation, proliferation, differentiation limits the use of the Mek inhibitor to query a Stat3-specific effect. However, the robust inhibition of Mek signaling, as measured by the reduction of MAPK phosphorylation shows that Mek inhibition alone also does not significantly affect MBNS self-renewal.

The combination treatment of Jak and Mek inhibitors results in a significant reduction of neurosphere formation, suggesting that the concurrent inhibition of both pathways is important

for the effective reduction in MBNS self-renewal. Similarly, a synergistic effect of Stat3 and Mek pathway reduction has been observed to inhibit the growth of multiple myeloma cells (Nelson *et al.*, 2008). However, the limitations of utilizing kinase inhibitors must be taken into consideration when interpreting the specific roles of *Stat3* and *Klf4* in the MBNS. While the activation of pStat3 is a major role of Jak kinases, they are also involved in a variety of other functions such as the phosphorylation and activation of other growth factor and cytokine receptors, including the granulocyte macrophage colony-stimulating factor (GM-CSF) and type I interferon receptor (Rane and Reddy, 2000) that may lead to a Stat3-independent effect. Furthermore, as mentioned above Mek signaling is involved in a variety of cellular processes. Nonetheless, further examination of the mechanism involved in the inhibition of MBNS self-renewal by the combination Jak and Mek inhibitors may reveal novel effectors of survival signaling in the MBNS.

While *Stat3* expression may not be necessary for the maintenance of MBNS self-renewal and survival, sustained Stat3 signaling may be aiding the stabilization of the transcriptional circuitry for pluripotency and survival in the MBNS. Stat3 functions in cooperation with the pluripotency factor *Oct4* to sustain ES cell self-renewal by inducing *Klf4* expression (Hall *et al.*, 2009). Furthermore, *Stat3* synergizes with *Klf4* and *Nanog* to reset the transcriptional program to overcome the barrier for reprogramming epiblast stem cells (EpiSC) to pluripotency (Yang *et al.*, 2010b). The role of pTyr705 Stat3 in direct transcriptional regulation of target genes, including *Klf4* and *c-myc*, is well established. In the MBNS, pTyr705 Stat3 inhibition by Jak kinase inhibition reduces the expression of *Socs3*, *Stat3* and secondarily, the expression of *Klf4*. While pSer727 Stat3 in mice has been reported to be required for maximal transcriptional activity, its role in DNA binding and gene regulation is not well established (Decker and Kovarik, 2000).

However, the human homolog pSer STAT3 has been shown to directly bind DNA and activate the transcription of antiapoptotic genes such as *survivin, Mcl1, Bcl-x* in CLL in a pTyr705 STAT3-independent manner (Hazan-Halevy *et al.*, 2010). This may reflect a conserved mechanism for regulating survival genes in MBNS, through the collaborative involvement with *Klf4*.

Role of Stat3-independent regulation of Klf4 during clonogenic self-renewal

Despite the MBNS exhibiting significantly elevated levels of *Stat3* mRNA expression and phospho-Stat3 activation, *Stat3* kd by RNAi and kinase inhibitors led to a moderate decrease in the formation of self-renewing neurospheres and the *Stat3* kd was not as functionally significant as the role of *Klf4*, especially apparent in the limiting dilution neurosphere formation assay. We have observed two discreet phenomena of *Klf4* regulation that occur in a cell density-dependent manner. The upregulation of *Klf4* expression in MBNS with sustained *Stat3* kd suggests that MBNS can, in part, escape and self-renew if *Klf4* expression is selectively upregulated during clonogenic growth. At higher cell densities, the compensatory mechanism of *Klf4* expression does not take effect, suggesting that there may be cell non-autonomous signals at higher cell densities, which relieve the necessity for *Klf4* expression. This leads us to hypothesize that gene expression networks may be relaxed if not necessary, but under environmental challenges such as clonal growth, the consolidation of gene expression necessary for MBNS survival occurs, either by the selection of cells expressing *Klf4* or by inducing cells to rapidly upregulate *Klf4*. Additionally, this suggests that the major mode of *Klf4* regulation during MBNS clonogenic growth can occur through a mechanism independent of the canonical LIF/STAT3 pathway, for which *Klf4* is direct downstream target.

While the partial effect of the *Stat3* kd on MBNS self-renewal may be attributable to the downregulation of *Klf4* downstream of Stat3, the inhibition of Stat3 signaling alone is not sufficient because Stat3-independent activators of *Klf4* can compensate. These activating signals of *Klf4* remain to be determined, but Shh signaling may be involved in a Stat3-independent mechanism for *Klf4* activation *via* the network of pluripotency factors, as Shh has been reported to be upstream of transcriptional activation of *Klf4* (Sengupta *et al.*, 2007; Moon *et al.*, 2011). Furthermore, the MBNS we describe are driven by loss of the *Ptch1* tumor suppressor that governs Shh signaling. Overexpression of *Gli1*, a downstream activator of Shh signaling, has also been shown to enhance clonogenic NSC, which was associated with the concurrent upregulation of pluripotency genes including *Nanog, Sox2, Klf4,* and *CD133* (Stecca and Ruiz i Altaba, 2009), of which *Nanog* and *Sox2* have been shown to be directly regulated by Gli1/2 binding (Po *et al.*, 2010; Takanaga *et al.*, 2009). It will be important to further elucidate the multiple modes of activation of *Klf4* expression for the effective inhibition of MBNS survival and self-renewal for therapeutic applications. In conclusion, our work suggests that *Ptch1*$^{LacZ/+}$*;Trp53*$^{-/-}$ MBNS are able to utilize the endogenously active components of the pluripotency transcription factor network, specifically *Klf4*, which is functioning partially via the Stat3 signaling pathway, as a factor critical for both MBNS plasticity and clonal self-renewal.

Methods

Neurosphere culture of MBNS line

A primary *Ptch1*$^{LacZ/+}$*;Trp53*$^{-/-}$ medulloblastoma was isolated, minced with razor blades and homogenized in Accutase (Chemicon) and was maintained in suspension culture as neurospheres in DMEM:F12 containing B27 Supplement (Invitrogen), 20ng/ml bFGF (Invitrogen), 20ng/ml

EGF (Invitrogen), and 100U/ml penicillin/streptomycin (Invitrogen) by weekly serial passaging. Neurosphere cultures were passaged by dissociation and trituration with Accutase, centrifugation, and followed by resuspension of the cells in fresh NS media. For isolation of CbSC, postnatal d5 or d7 cerebella were dissected, mechanically dissociated and homogenized with Accutase (Chemicon) and cultured in neurosphere media. After 7 days of culture, primary neurospheres were dissociated and plated in the *in vitro* reprogramming assay.

Flow cytometry for cell surface marker expression analyses

A primary *Ptch1*$^{LacZ/+}$*;Trp53*$^{-/-}$ medulloblastoma and neurosphere culture-enriched MBNS line was isolated and dissociated as described above and resuspended in Phosphate-buffered saline (PBS) with 2mM ETDA and 0.5% BSA. The samples were incubated with PE-conjugated CD15 (R&D Systems), PE-conjugated CD133/Prominin (Miltenyi), or anti-mouse isotype control antibodies for 30 minutes, washed with PBS, then analyzed on the BD LSRII (BD Biosciences). Analyses for PE staining were carried out on FlowJo software (Tree Star).

Intracerebellar transplantation assays

4-6 week old NCr nude (*CrTac:NCr-Foxn1*^{nu}) mice were anesthetized with ketamine/xylazine and placed into a stereotaxic frame (Stoelting). A 1 cm incision was made in the scalp and a hole was drilled approximately 1mm lateral and 3mm posterior to lambda. 10000, 30000 or 100,000 cells in 2ul of PBS were drawn into a glass needle and injected into the cerebellum 3mm below the surface using a PicoPump (World Precision Instruments). Animals were monitored for the development disease symptoms on a daily basis. Mice were maintained in pathogen-free

conditions at Boston Children's Hospital and procedures were performed following approval by the Institutional Animal Care and Use Committee (IACUC).

In vitro assay for reprogramming

For the *in vitro* reprogramming experiments, 3000 MBNS or CbSC were plated per well of a 6-well plate on irradiated mouse embryonic fibroblasts (MEF) in Dulbecco's Modified Eagle Medium (DMEM) (Invitrogen) containing 15% FCS (Millipore), 2mM L-Glutamine (Invitrogen), 100U/ml penicillin/streptomycin, 100uM non-essential amino acids (Invitrogen) and 1000U/ml leukemia inhibitory factor (Millipore). Six days post-plating, cells were fixed with 2% paraformaldehyde (Electron Microscopy Sciences) and stained for alkaline phosphatase (Vector Laboratories). The frequency of AP-positive ES-like colony formation was determined by counting the homogenously AP-positive colonies. Stable AP^+ MBNS subclones were maintained in standard ES cell culture conditions. Plating efficiency assays to determine LIF-dependency were performed by plating 3000 AP^+ MBNS per well of a 6-well plate in technical triplicates, on gelatin or MEF in ES media with or without LIF. Six days post-plating, colonies were fixed, stained for AP, and quantified by ImageJ. Briefly, images of wells were photographed, converted to a grayscale image and thresholded to highlight the colonies, which were counted by the "measure nuclei" macro under the analyze particles function menu.

Teratoma assays

The flanks of 4-6 week of NCr nude (*CrTac:NCr-Foxn1*^{nu}) mice were subcutaneously injected with 10^6 *Ptch1*$^{LacZ/+}$*;Trp53*$^{-/-}$ ES cells (n=3), MBNS (n=5), and AP^+ MBNS (n=5) resuspended in 100ul of PBS. Animals were monitored daily for the development disease symptoms, sacrificed

3 week post-injection and tumors were dissected and embedded in OCT (Tissue-Tek) for cryosectioning for H&E staining for histological analyses.

Bisulfite-based mass spectrometry methylation analyses

Genomic DNA (gDNA) from the parental MBNS and three AP^+ MBNS subclone lines were isolated with the AllPrep DNA/RNA kit (Qiagen). The MassArray EpiTYPER platform (Sequenom, San Diego, CA, USA) was utilized for quantitative analyses of CpG methylation at promoter regions and 5' regulatory regions ~2kb upstream of the TSS for pluripotency genes *Oct4, Nanog, Klf4, Sox2* and *Stat3*. Briefly, sodium bisulfite-treated gDNA is PCR-amplified with gene-specific primers and followed by *in vitro* RNA transcription and base-specific cleavage. Cleavage products are subsequently analyzed by MALDI-TOF mass spectrometry to distinguish between the methylated and unmethylated gDNA.

Gel-based and Quantitative RT-PCR

Total RNA (1ug) isolated from WT adult cerebella, *Ptch1*$^{LacZ/+}$*;Trp53*$^{-/-}$ primary tumors, WT and *Ptch1*$^{LacZ/+}$*;Trp53*$^{-/-}$ ES cells, WT P7 CbSC, and *Ptch1*$^{LacZ/+}$*;Trp53*$^{-/-}$ MBNS lines with the RNeasy Kit (Qiagen) was used for cDNA synthesis with the High-Capacity cDNA Reverse Transcription Kit (Applied Biosystems). Gel-based RT-PCR was carried out by amplifying *Oct4* and *Nanog* for 31 cycles, *Sox2* and *Klf*4 for 28 cycles, *NuBP* for 26 cycles and *Gapdh* for 23 cycles. Quantitative RT-PCR was carried out in technical triplicates using the SYBR Green PCR Master Mix (Applied Biosystems) using cDNA dilutions determined by prior primer optimization experiments. *Stat3, Socs3, Klf4,* survivin, *Bcl-x* and *Mcl1* expression was normalized to GAPDH and changes in gene expression were determined by the ddCT method

and represented as expression levels relative to the WT cerebella control, vehicle-treated or vector control.

Primers:

Gapdh: 5' GTTGTCTCCTGCGACTTCA 3'; 5' TGGTCCAGGGTTTCTTACTC 3'

STAT3: 5' TGAGAGTCAAGACTGGGCATA 3'; 5' ACTCTTGCAGGAATCGGCTA 3'

Socs3: 5' GTTCCTGGATCAGTATGATGC 3'; 5' CGCTTGTCAAAGGTATTGTCC 3'

Klf4: 5' CCCGGCGGGAAGGGAGAAGA 3'; 5' GGCCGGGAAGTGGGGGAAGT 3'

survivin: 5' CTACCGAGAACGAGCCTGAT 3'; 5' GGGAGTGCTTTCTATGCTCCT 3'

Bcl-x: 5' GGTGAGTCGGATTCAAGTT 3'; 5' TGTTCCCGTAGAGATCCACA 3'

Mcl1: 5' GTAAGGACGAAACGGGACTG 3'; 5' CGCCTTCTAGGTCCTGTACG 3'

Western Blot Analyses

MBNS grown in suspension culture were harvested and centrifuged for protein isolation. For isolation of protein lysates from adherent ES cells or AP^+ MBNS grown in ES conditions, MEFs were removed by spot-plating on gelatin-coated plates. Cell pellets were lysed in RIPA buffer (Upstate) containing phosphatase and protease inhibitors (Pierce) on ice for 30 minutes, with vortexing every 10 minutes. After determination of protein concentration by the Dc-Protein Assay (Bio-Rad), 30ug of protein was fractionated on a 8% polyacrylamide gel, transferred to nitrocellulose membranes and probed with rabbit anti-pSer727 Stat3 (1:10,000, gift from D.Frank (Kim *et al.*, 2008a)), rabbit anti-pTyr705 Stat3 (1:10,000, Cell Signaling), rabbit anti-Stat3 (1:10,000, Santa Cruz), rabbit anti-pErk1/2 (1:10,000, Cell Signaling), mouse anti-actin (1:5000, Abcam). Anti-mouse and rabbit HRP-conjugated secondary antibodies (1:10,000,

Jackson ImmunoResearch) were incubated on the blots and detected with the Western Lightning ECL Reagent (Perkin Elmer).

Pathway inhibitor treatment of MBNS

Dissociated MBNS were treated with 10uM PI3K inhibitor LY294002 (Cell Signaling), 10uM Mek1/2 inhibitor U0126 (Cell Signaling), 250nM mTOR inhibitor Rapamycin (Gift from D. Sabatini), and 1uM Jak inhibitor (Calbiochem), or combination Mek and Jak inhibitor. Treated MBNS were harvested for protein and RNA isolation or plated in the neurosphere self-renewal assay (see below) with additional inhibitor media supplementation 4 days post-plating. Neurosphere formation and size was quantified 7 days post-plating.

Generation of shRNA and lentiviral vectors

shRNA against *Stat3* and *Klf4* were generated with two rule-based shRNA design software, DSIR (http://biodev.extra.cea.fr/DSIR/) and pSicoOligomaker 1.5 (http://web.mit.edu/jacks-lab/protocols/pSico.html). Oligos were ligated into a pSicoR vector modified from the original vector (Ventura *et al.*, 2004) to express the puromycin resistance cassette under the control of the Ubiquitin promoter. Transformed bacterial colonies were picked for colony PCR to screen for shRNA insertion and further validated by sequencing.

Lentiviral infection of the MBNS lines

Viral supernatant was produced by transient calcium chloride transfection of human embryonic kidney cells (HEK293) cells with 10ug PAX lentiviral packaging vector and 5ug VSV envelope vectors and 15ug pSicoR-puro-shRNA vectors. Sixteen hours following transfection, the media

was changed to fresh media. Viral supernatant was collected 48 hours after transfection, supplemented with Polybrene (8ug/ml) and passed through a 0.45um filter. Dissociated MBNS (~10^6) were resuspended with the filtered viral supernatant and centrifuged for 45 minutes at 2500 rpm for lentiviral transduction. Puromycin selection (2ug/ml) was applied 1d post-infection for 48 hours and on d3 post-infection, the lentivirally-infected MBNS were collected for RNA isolation, plated in self-renewal assays, or passaged for maintenance as bulk cultures.

In vitro neurosphere self-renewal assay and limiting dilution assay

At d3 post-infection, sh*Stat3*, sh*Klf4*, and vector control MBNS were dissociated and plated at 200 cells per well of 6-well plate in neurosphere media. Neurosphere formation was quantified 5 days post-plating by ImageJ. The neurospheres that emerged from these clonal density assays were collected for RNA isolation for gene expression analyses of d8 clonal cultures.

For the limiting dilution assays, d3 post-infection sh*Stat3* and sh*Klf4*, vector control MBNS were dissociated and plated at 0.3, 1, 3, 10 cells per well of a 96 microwell plate in neurosphere media with 48 wells for each cell concentration. Five days post-plating, each well was scored for positive or negative neurosphere formation. The self-renewal index, which is the number of cells required for the formation of one neurosphere, was determined with the extreme limiting dilution assay (ELDA) webtool (http://bioinf.wehi.edu.au/software/elda/).

Analyses of human medulloblastoma gene expression datasets

Human medulloblastoma gene expression datasets from Northcott et al. (2011) were accessed from the Gene Expression Omnibus (GEO) database and the 103 tumor samples were sorted based on the annotated subclasses (Shh=33 tumors, Wnt=8 tumors, Class 3=27 tumors, Class

4=35 tumors). Expression values were obtained from corresponding gene probes for STAT3 (3757840), KLF4 (3219215), MYC (311504), BIRC5 (3736290), BCL2L (3902489), MCL1 (2434438).

In silico promoter analyses

Promoters of *survivin, Mcl1, Bcl-x* were retrieved from the Genomatix ElDorado genome database. Promoters in Genomatix are defined as regions 500bp upstream and 100bp downstream of the transcriptional start site (TSS). Binding site identification was carried out for promoters defined by "gold" transcripts, which are those verified by mapping of 5' full length cDNAs or at least 4 CAGE (cap analyses gene expression) by Genomatix MatInspector and further analyzed for transcription factor binding sites for STAT3 and GKLF (Klf4).

Chapter 3 : Mechanisms of aberrant persistence of cerebellar stem cells during medulloblastoma development

ChieYu Lin[1,2,4], Ronnie Yoo[1,2,4], Juliana Brown[1,2], Abby Sarkar[3], Katrin Arnold[3], Christopher Kanner[2], Konrad Hochedlinger[3], and Laurie Jackson-Grusby[1,2]

[1]Pathology Department and Kirby Center for Neuroscience, Children's Hospital Boston, [2]Harvard Stem Cell Institute, Harvard Medical School, Boston, MA, [3]Massachusetts General Hospital Boston, MA, Department of Stem Cell and Regenerative Medicine, Harvard University Cambridge, MA

[4]These authors contributed equally

Author Contributions

CYL contributed to the conception and design of experiments, acquired and analyzed results, prepared figures. RY acquired and analyzed results, wrote the manuscript and prepared figures. JB acquired results. AS, KA, KH contributed to the development of the methodology and reagents. LJG contributed to the conception and design of experiments, analyzed results and supervised the study.

Introduction

The cell of origin of the SHH subtype of medulloblastomas has been established and well-characterized to be a granule cell progenitor (Yang *et al.*, 2008b; Schüller *et al.*, 2008). Following the identification of self-renewing, tumor-initiating cells in human primary medulloblastomas (Singh *et al.*, 2004), recent studies have examined the potential roles of non-GCP stem cell populations as the cell of origin in medulloblastoma tumorigenesis. As such, it has been shown that a cerebellar stem cell population (Lee *et al.*, 2005), upon transformation with an oncogene, can lead to the formation of malignant medulloblastomas (Sutter *et al.*, 2010; Pei *et al.*, 2012). Furthermore, $Ptch1^{LacZ/+};Trp53^{-/-}$ medulloblastomas have been characterized to contain a population of self-renewing cells expressing NSC markers with the ability for potent tumor-initiation upon secondary transplantation (C. Lin thesis).

The stem cell population of particular interest in the $Ptch1^{LacZ/+};Trp53^{-/-}$ model is the aberrantly self-renewing, premalignant cells in the 3 week cerebella. In WT animals, self-renewal activity is decreased by 3 weeks of age (C. Lin thesis). The persistence of self-renewing cells beyond the normal developmental window may be expanding the pool of potential targets for malignant transformation, leading to the establishment of a tumor-initiating stem cell population. This may be analogous to the abnormal proliferative rests of granule cell progenitors in the $Ptch1^{LacZ/+}$ model, which are predisposed for progression to tumor formation upon the acquisition of additional oncogenic mutations (Kim *et al.*, 2003). A comprehensive comparison of the gene expression profiles between the $Ptch1^{LacZ/+};Trp53^{-/-}$ aberrant tissue stem cells and developmental stem cells in both P7 WT and $Ptch1^{LacZ/+};Trp53^{-/-}$ animals will allow for the

elucidation of mechanisms and pathways that are allowing the stem cells to persist developmentally and contribute to tumorigenesis in the *Ptch1*$^{LacZ/+}$*;Trp53*$^{-/-}$ model.

The strategy described in the previous chapter for studying the self-renewing, tumor-initiating cell population in *Ptch1*$^{LacZ/+}$*;Trp53*$^{-/-}$ tumors relied on the enrichment of these cells by *in vitro* neurosphere culture and the use of heterogeneously expressed markers. *Ptch1*$^{LacZ/+}$*;Trp53*$^{-/-}$ tumor cells have been reported to undergo changes during adherent, serum-enriched *in vitro* tissue culture, such as downregulation of Shh signaling, highlighting concerns that *in vitro* cell lines may not be representative of the original tumor (Sasai *et al.*, 2006). While the serum-free neurosphere culture conditions employed may better preserve the *in vivo* characteristics of the *Ptch1*$^{LacZ/+}$*;Trp53*$^{-/-}$ medulloblastoma cells, we cannot exclude the possibility of the medulloblastoma neurospheres (MBNS) undergoing genetic and/or epigenetic changes or clonal selection during the long term passaging of NS cultures. Furthremore, an alteration of cell character due to the absence of the normal developmental environment and niche signals may inaccurately represent what is occurring *in vivo*. Therefore, a validated prospective marker, allowing for the enrichment directly from the brain would greatly facilitate the investigation of these endogenous cell populations.

CD133 (also known as prominin 1) is widely accepted as a cell surface marker for the isolation of NSC and tumor-initiating cells in brain cancers (Lee *et al.*, 2005; Singh *et al.*, 2004), as well as a variety of different solid tumors (Visvader and Lindeman, 2008). While CD133 has been extensively used as an established marker for NSC, it has been shown to be heterogeneously expressed in NSC and in addition, CD133-negative fractions also contain self-renewing, multipotent stem cells (Sun *et al.*, 2009). As a CSC marker, the validity of CD133 as a definitive marker for fractionating cells with cancer-initiating ability has also been challenged in

multiple studies (Beier *et al.*, 2007; Joo *et al.*, 2008; Wang *et al.*, 2006; Chen *et al.*, 2010). This must be considered when using CD133 for the isolation of either NSC or CSC and necessitates the identification and characterization of other definitive markers. Furthermore, in the MBNS lines derived from the *Ptch1*$^{LacZ/+}$*;Trp53*$^{-/-}$ tumors, CD133 expression occurs in an exceedingly heterogeneous fashion, as clonal lines derived from a highly self-renewing MBNS line showed considerable variability in the cell surface expression of CD133, as well as CD15 and CD184, other commonly used markers of NSC (C. Lin thesis).

While markers such as CD133 have been crucial in advancing our understanding of CSC in various tumors types, there are limitations of using such cell surface markers. Cell surface markers do not necessarily encompass functional significance and, as such, are not reflective of the underlying biology of the tissue stem cell that regulates the development of the organ (Clevers, 2011). For the same reason, while cancer stem cells hold promise as a potential target for therapeutic intervention, the currently employed markers are not functional drug targets that will affect CSC survival.

Sox2, a SRY family transcription factor, is important for the maintenance of pluripotency and self-renewal in various stem cells including ES cells (Avilion *et al.*, 2003, Takahashi and Yamanaka, 2006), embryonic and adult NSC (Ellis *et al.*, 2004; Suh *et al.*, 2007), and other tissue stem cells of the stomach, testes, lens, and teeth (Arnold *et al.*, 2011; Juuri *et al.*, 2012). In the brain, *Sox2* expression is restricted to neural progenitors (neuroepithelial cells of the neural plate and early neural tube) in the mouse embryo and maintained in the neurogenic regions such as the dentate gyrus of the hippocampus and the subventricular zone surrounding the lateral ventricles in adults (Ellis *et al.*, 2004). Subsequent fate mapping studies have shown that *Sox2*-expressing cells are, in fact, multipotent NSC that can differentiate into multiple lineages *in vivo*

(Suh *et al.*, 2007). Functionally, hypomorphic *Sox2* alleles and *Sox2* knockout studies in the brain have further confirmed the crucial role of *Sox2*-expressing cells in the neural stem and progenitor cell population during neurogenesis (Cavallaro *et al.*, 2008; Ferri *et al.*, 2004; Favaro *et al.*, 2009). In the cerebellum, *Sox2* expression has been observed in the white matter at P7 (Sutter *et al.*, 2010), consistent with the presence of prominin^{+} CbSC in the white matter. In addition, *Sox2* is also observed in the Bergmann glia, both at P7 (Sutter *et al.*, 2010) and in adult mice and humans (Sottile *et al.*, 2006; Alcock *et al.*, 2009). It has been suggested that these *Sox2*-expressing Bergmann glia may also represent a novel population of multipotent stem cells, but this has not been directly examined.

The observation of high *Sox2* expression in the 3 week *Ptch1*$^{LacZ/+}$*;Trp53*$^{-/-}$ cells cultured in neurosphere conditions (C. Lin thesis) and the known role of *Sox2* in NSC prompted us to examine *Sox2* as a potential prospective marker in our medulloblastoma model. Preliminary results from our lab characterized *Sox*2 as a marker for the prospective isolation of CbSC in WT P7 animals using a *Sox2-GFP* reporter allele (C. Lin thesis). Isolation of *Sox2*-expressing cells at P7 leads to the fractionation of self-renewal activity and these cells exhibit enriched expression of the stem cell gene *Hes1* and downregulation of the granule progenitor marker *Math1*. As cerebellar development progresses, the frequency of *Sox2*-expressing cells diminishes, consistent with the reduction of self-renewal activity by 3 weeks of age. Here, I expand and confirm these observations and further examine the role of the *Sox2*-expressing cells in the *Ptch1*$^{LacZ/+}$*;Trp53*$^{-/-}$ animals and show that *Sox2* also marks the aberrantly self-renewing stem cells in 3 week old *Ptch1*$^{LacZ/+}$*;Trp53*$^{-/-}$ animals. The establishment of *Sox2* as a marker for the prospective isolation of CbSC and the aberrant tissue stem cells during medulloblastoma tumorigenesis will be

valuable for examining the endogenous mechanisms and pathways that go awry during medulloblastoma tumorigenesis.

Results

Sox2-expression marks the self-renewing stem cells in the postnatal day 7 cerebella

To examine if *Sox2* can be used as a prospective marker of CbSC, we first analyzed the cerebella of WT *Sox2-GFP* reporter mice. The reporter allele utilized is designed to target the endogenous *Sox2*-locus and replace the *Sox2* open reading frame with an *EGFP-loxP-neo^R-loxP* cassette, while maintaining the upstream regulatory domains (Ellis *et al.*, 2004). This allele has been demonstrated to recapitulate the WT *Sox2* expression during embryonic and postnatal neural development (Ellis *et al.*, 2004). To determine the frequency of *Sox2*-expressing cells during cerebellar development, we dissociated the cerebella from WT animals at P7 and 3 weeks and analyzed the *Sox2-GFP* expressing cells by FACS. At P7, there was a clearly separable population of GFP-expressing cells comprising approximately 11% of total cells (Figure 3-1). In contrast, there was a greater than 100-fold reduction of GFP-expressing cells by 3 weeks age (Figure 3-1), the time-point when cerebellar development has been completed and self-renewal activity is undetectable (C. Lin thesis).

Functionally, to determine if the *Sox2*-expressing cells can isolate the normal self-renewing CbSC at P7, we sorted WT *Sox2-GFP* negative and positive cells into a clonal density neurosphere formation assay. Neurosphere formation was only observed in the GFP-positive sorted wells, at a frequency of about 4%, and all neurospheres formed expressed GFP (C. Lin

thesis, Figure 3-2). These data show that *Sox2* can be utilized as a functional marker for the prospective isolation of self-renewing stem cells in the P7 cerebella.

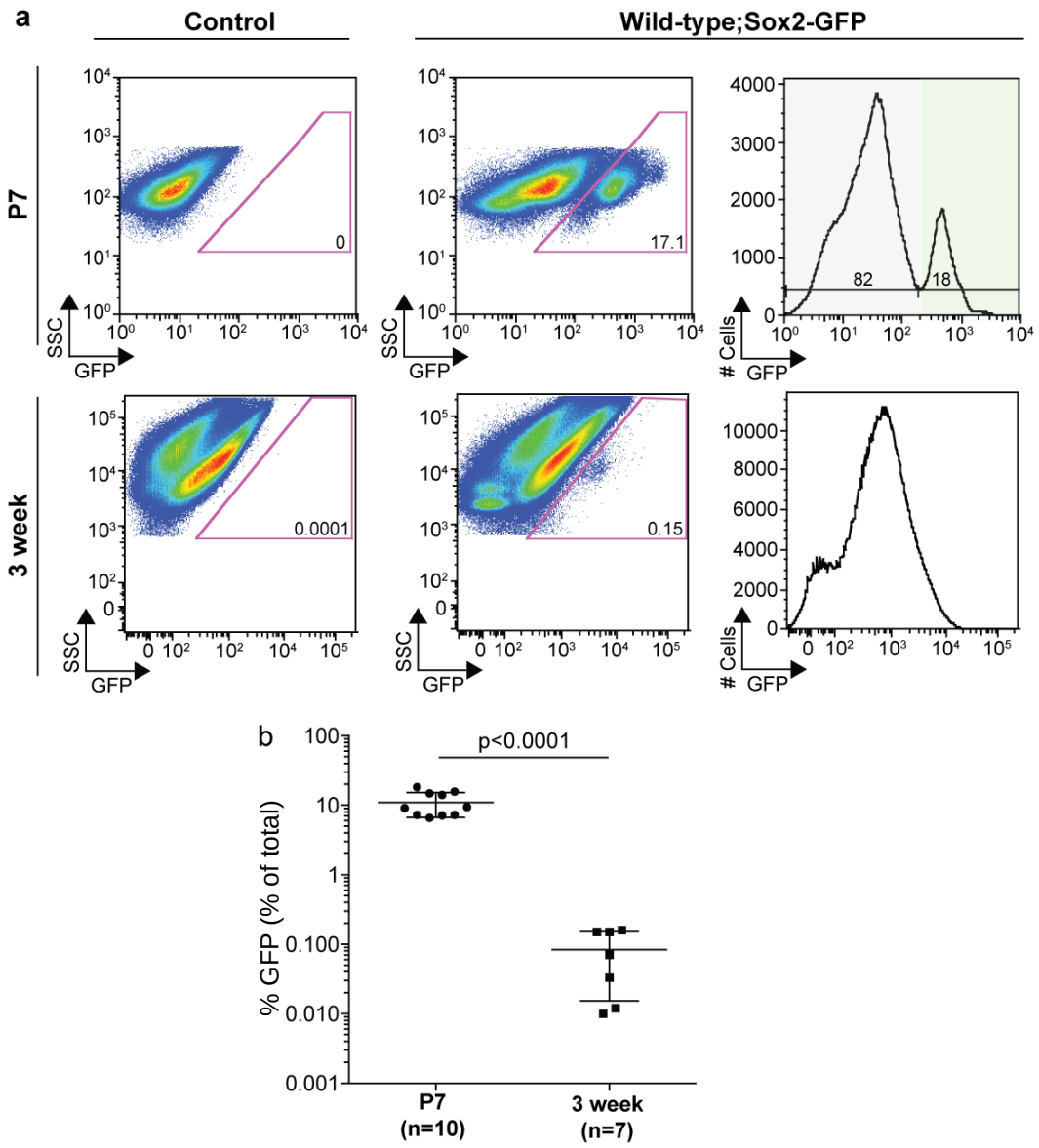

Figure 3-1 The frequency of *Sox2-GFP* positive cells is significantly reduced during cerebellar development in wild-type animals

(a) Representative FACS analyses of *Sox2-GFP*-positive cells in the cerebella of postnatal day 7 and 3 week old, control and *Sox2-GFP* knock-in reporter colony mice. (b) The frequency of *Sox2-GFP*-positive cells is significantly decreased during development from P7 to 3 weeks (data shown as mean±s.d; p=0.0008 by an unpaired t-test). The results represent a compilation of experiments performed by C. Lin and R.Yoo.

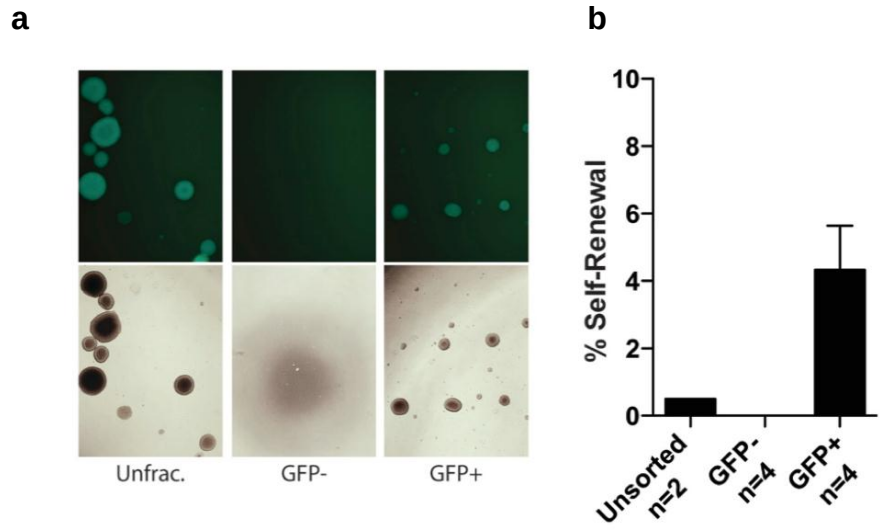

Figure 3-2 *Sox2* expression fractionates the self-renewal activity of CbSC in wild-type P7 animals

(a) Unfractionated, *Sox2-GFP*-negative, and *Sox2-GFP*-positive cells were sorted into a low-density neurosphere formation assay (2000 cells per well of a 6-well plate). As observed in the fluorescent and bright field images, NS were only observed in the *Sox2-GFP*-positive wells and all NS are GFP-positive. (b) Quantification of self-renewal was carried out by counting the number of neurospheres by ImageJ analyses. C. Lin carried out these experiments and published figures in Ph.D thesis.

Enrichment of stem cell gene expression in *Sox2-GFP* positive CbSC

The isolation of the self-renewing cells by *Sox2*-expression led us to ask if other commonly used NSC markers were co-expressed with *Sox2*. The *Sox2-GFP* positive fraction had a higher frequency of cells expressing CD133 and CD15 compared to the GFP-negative cells (C. Lin thesis, Figure 3-3a). High levels of *Stat3* expression in the MBNS and CbSC (Chapter 2), suggest that MBNS self-renewal and survival mechanisms utilize conserved pathways present in developmental NSC and CbSC. Indeed, expression of *Stat3* and target genes *Klf4* and *c-myc* were highly upregulated in the *Sox2-GFP* positive cells (Figure 3-3b). The enrichment of NSC markers and genes functionally important in MBNS self-renewal, in particular *Klf4*, in the *Sox2*-positive fraction further supports the validation of *Sox2* as a marker for self-renewing CbSC.

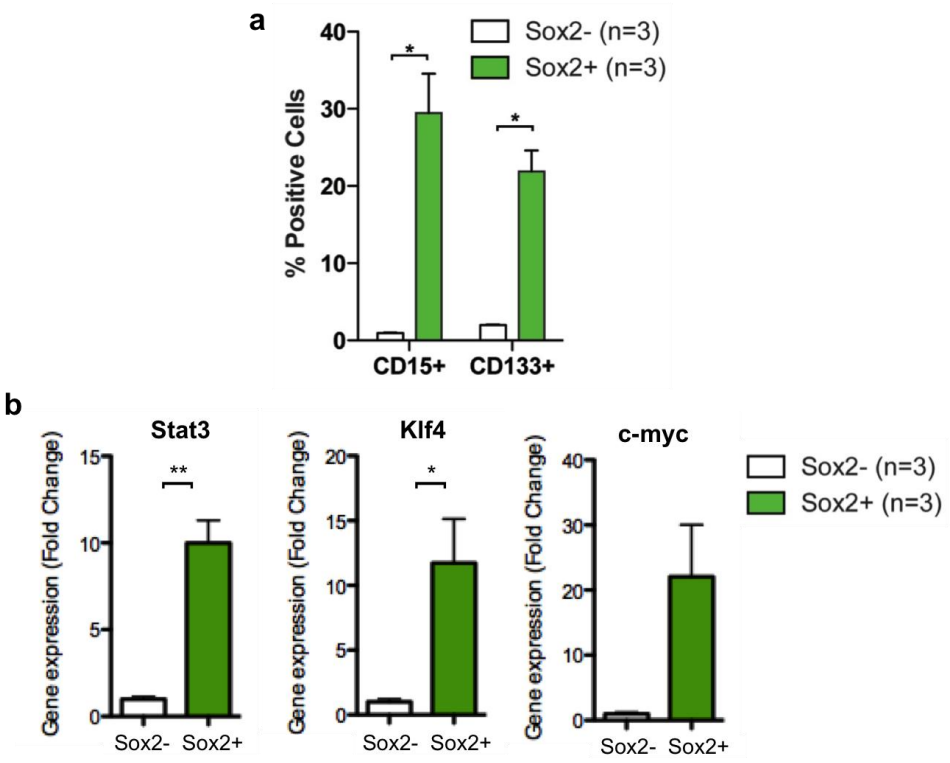

Figure 3-3 Expression of stem cell genes are enriched in WT P7 *Sox2-GFP* positive cells

(a) Cell surface marker CD15 and CD133 expression measured by FACS in *Sox2-GFP*-negative and positive fractions. C. Lin carried out these experiments and published figures in Ph.D thesis. (b) Quantitative RT-PCR analyses of *Sox2-GFP*-negative and positive fractions from wild-type postnatal day 7 cerebella (n=3) show elevated levels of genes functionally involved MBNS self-renewal in the GFP positive fractions (*Stat3*, p=0.0024; *Klf4*, p=0.0342; c-*myc*, p=0.0578 by unpaired t-test).

Characterization of *Sox2-GFP* positive cells in *Ptch1$^{LacZ/+}$;Trp53$^{-/-}$* chimeras

Following the validation of the preliminary observations in the lab, we next wanted to analyze the role of the Sox2-expressing cells in the *Ptch1$^{LacZ/+}$;Trp53$^{-/-}$* animals during medulloblastoma progression. The Sox2-GFP reporter (Ellis et al., 2004) was knocked into the endogenous Sox2 locus in *Ptch1$^{LacZ/+}$;Trp53$^{-/-}$* ES cells for the generation of chimeric animals. Analyses of *Ptch1$^{LacZ/+}$;Trp53$^{-/-}$* chimeras have shown that the *Ptch1$^{LacZ/+}$;Trp53$^{-/-}$* ES cells preferentially colonize the cerebella and these chimeras develop medulloblastomas which recapitulate the tumor characteristics and kinetics of colony (germline-mutant) mice (C. Lin thesis). Quantitative

analyses by qPCR have indicated that following blastocyst injection, Ptch1 mutant ES cells have a competitive growth advantage over the host cells in the developing cerebellum, leading to increased ES cell contribution in the cerebellum observed as early P7 in these chimeric mice. Therefore, we used this system to generate larger cohorts of *Ptch1*$^{LacZ/+}$*;Trp53*$^{-/-}$*;Sox2-GFP* compound mutant animals, genotypes which are obtained at low frequency by breeding, as both Ptch1 null (Goodrich et al., 1997) and Sox2 null (Avilion et al., 2003) mutations are embryonic lethal. We carried out the analyses in the P7 and 3 week *Ptch1*$^{LacZ/+}$*;Trp53*$^{-/-}$*;Sox2-GFP* chimeras, while concurrently breeding the Sox2-GFP allele into the *Ptch1*$^{LacZ/+}$*;Trp53*$^{-/-}$ mouse colony for analyses of non-mosaic animals.

In the *Ptch1*$^{LacZ/+}$*;Trp53*$^{-/-}$ P7 chimeras, the Sox2-GFP positive cells compose a distinguishable population and were consistently present at a higher frequency than WT P7 mice, with 26% in the *Ptch1*$^{LacZ/+}$*;Trp53*$^{-/-}$ vs. 11% in the WT (Figure 3-4b, Figure 3-1b). In addition, the population of Sox2-GFP positive cells remains present in the 3 week old *Ptch1*$^{LacZ/+}$*;Trp53*$^{-/-}$ animals at a frequency of about 5%, 50-fold higher than in the WT 3 week animals (Figure 3-4b). The GFP-expressing cells in the P7 WT and *Ptch1*$^{LacZ/+}$*;Trp53*$^{-/-}$ cerebella are present as a distinct cluster of cells based on forward and side scatter analyses by FACS, as shown by backgating analyses of the GFP-positive populations (Figure 3-5a). The GFP-positive cells observed in the 3 week *Ptch1*$^{LacZ/+}$*;Trp53*$^{-/-}$ chimeras also appear to reside in the same distinct cluster of cells, a population of cells which is largely diminished by 3 weeks in the WT animals Figure 3-5b). These observations suggest that the Sox2-expressing cells in the *Ptch1*$^{LacZ/+}$*;Trp53*$^{-/-}$ animals are a developmentally persistent cell population, existing beyond the normal developmental window.

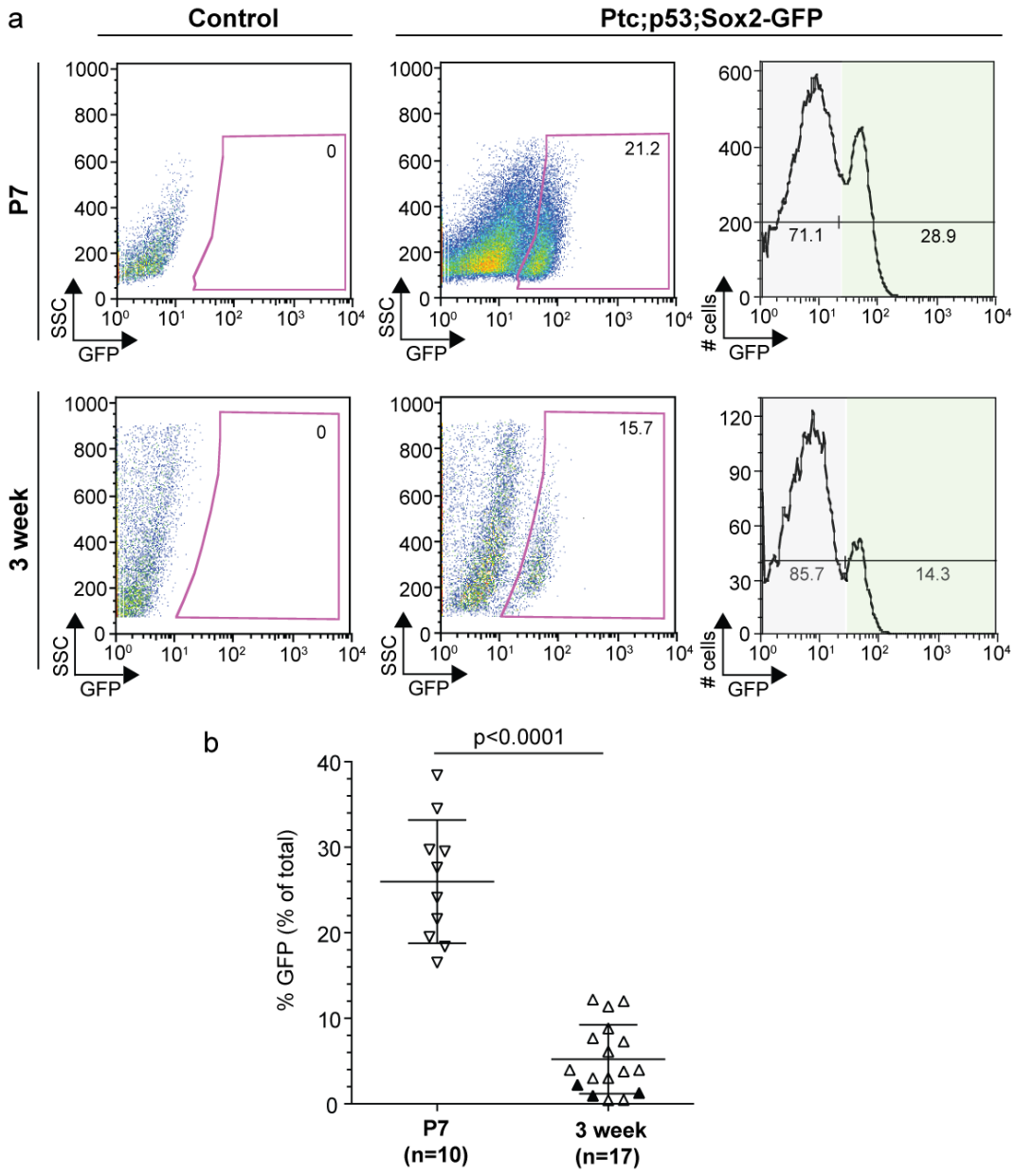

Figure 3-4 An identifiable population of *Sox2-GFP* expressing cells is maintained at 3 weeks in *Ptch1$^{LacZ/+}$;Trp53$^{-/-}$* animals

(a) Representative FACS analyses of *Sox2-GFP*-positive cells in the cerebella of P7 and 3 week old, control and *Ptch1$^{LacZ/+}$;Trp53$^{-/-}$;Sox2-GFP* knock-in reporter chimeric mouse. *Sox2-GFP* positive cells persist at 3 weeks in the *Ptch1$^{LacZ/+}$;Trp53$^{-/-}$* animals. (b) The frequency of *Sox2-GFP* cells is decreased during development from P7 to 3 weeks in *Ptch1$^{LacZ/+}$;Trp53$^{-/-}$* animals (data shown as mean±s.d; p<0.0001 by an unpaired t-test. Open triangles represent chimeras and closed triangles denote colony (germline mutant animals).

Figure 3-5 Backgating analyses of *Sox2-GFP* positive cells in WT and *Ptch1*$^{LacZ/+}$;*Trp53*$^{-/-}$ P7 and 3 week animals suggest that the *Sox2*-positive cell population in the 3 week *Ptch1*$^{LacZ/+}$;*Trp53*$^{-/-}$ is a developmentally persistent population

(a) Backgating analyses of the GFP-positive population show that the *Sox2*-expressing cells comprise a cell population that is distinguishable by the FSC and SSC profiles in the WT and *Ptch1*$^{LacZ/+}$;*Trp53*$^{-/-}$ P7 cerebella. (b) *Sox2*-expressing cells in 3 week *Ptch1*$^{LacZ/+}$;*Trp53*$^{-/-}$ animals are also present as a distinct cell population, as recognizable by FSC and SSC profiles. This population is absent in 3 week WT animals.

Figure 3-5 (Continued)

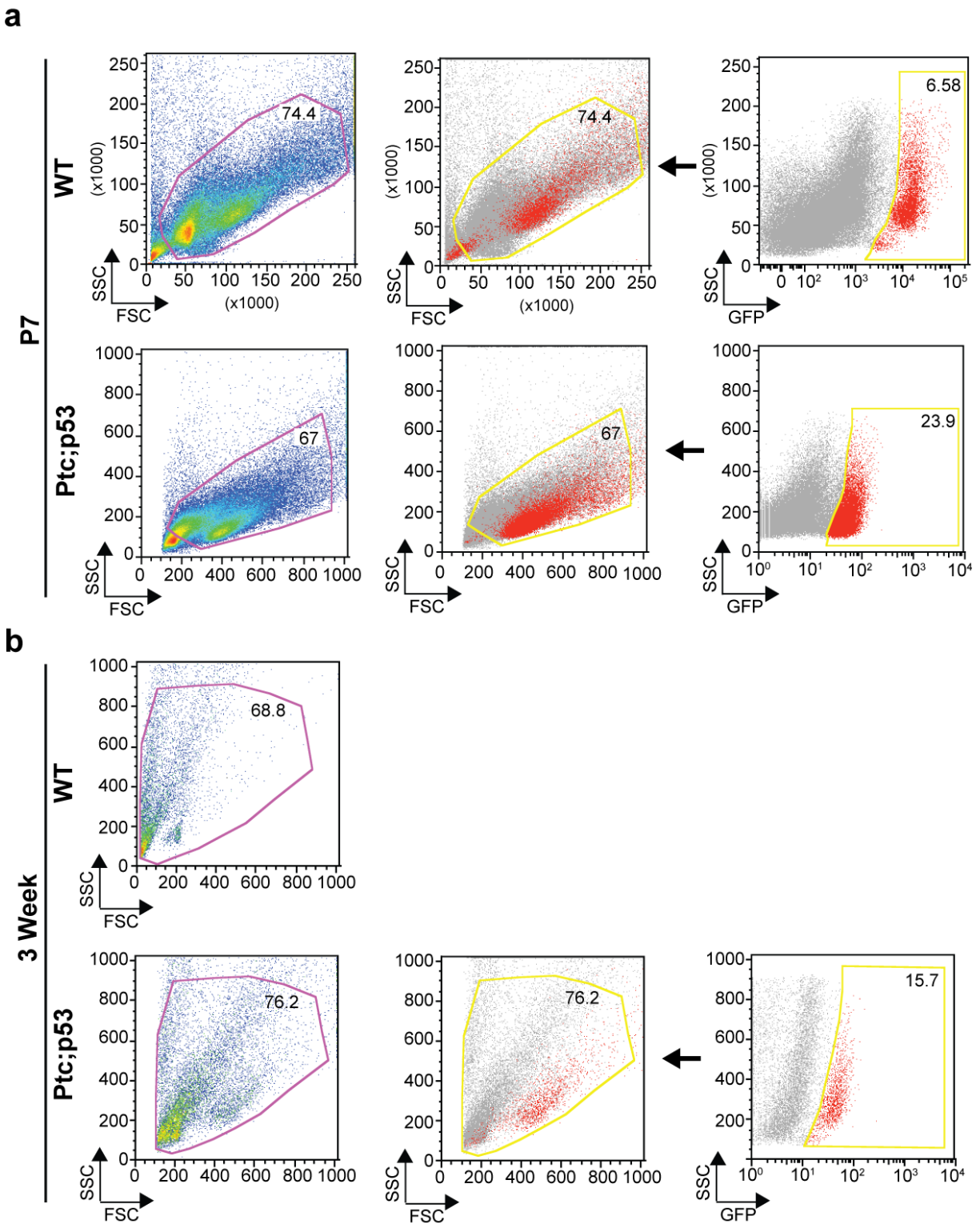

Sox2-expression isolates the self-renewing cells in 3 week *Ptch1*$^{LacZ/+}$;*Trp53*$^{-/-}$ cerebella

We next asked if the *Sox2*-expressing cells persisting at 3 weeks in the *Ptch1*$^{LacZ/+}$;*Trp53*$^{-/-}$ animals are functionally associated with the aberrantly self-renewing population by sorting the GFP-negative and GFP-positive cells from *Ptch1*$^{LacZ/+}$;*Trp53*$^{-/-}$ colony mice directly into the clonal-density, neurosphere formation assay. (As further described in the discussion, *Ptch1*$^{LacZ/+}$;*Trp53*$^{-/-}$ chimeras were not analyzed for self-renewal activity due to confounding factors of host cell contribution). As observed in the WT CbSC, neurosphere formation only occurred in the GFP-positive fraction and all NS formed were GFP-positive (Figure 3-6). While the number of animals analyzed was limited due to low frequency of deriving the *Ptch1*$^{LacZ/+}$;*Trp53*$^{-/-}$;*Sox2-GFP* compound mutants by breeding, the results suggest that *Sox2-GFP* expression also exclusively marks the aberrantly self-renewing cells in the *Ptch1*$^{LacZ/+}$;*Trp53*$^{-/-}$ animals at 3 weeks. Furthermore, the GFP-positive population is significantly higher in the *Ptch1*$^{LacZ/+}$;*Trp53*$^{-/-}$ animals at both P7 and 3 weeks, suggesting that deregulation of the stem cell population may be occurring in early postnatal development.

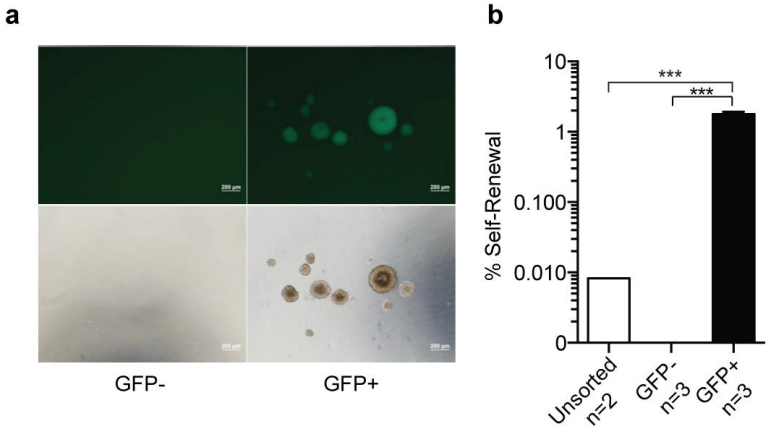

Figure 3-6 *Sox2*-expressing cells mark the self-renewing cells in the 3 week *Ptch1*$^{LacZ/+}$;*Trp53*$^{-/-}$cerebella

(a) *Ptch1*$^{LacZ/+}$;*Trp53*$^{-/-}$; *Sox2-GFP* positive and negative cells were sorted into the clonal-density NS formation assay (2000 cells per well of a 6-well plate). Enrichment of self-renewal activity was observed in the *Sox2-GFP* fraction and all NS are GFP positive. (b) Quantification of self-renewal carried out by ImageJ show an average self-renewal of 1.8%. Statistical analyses were carried out by one-way ANOVA with a Bonferroni post test.

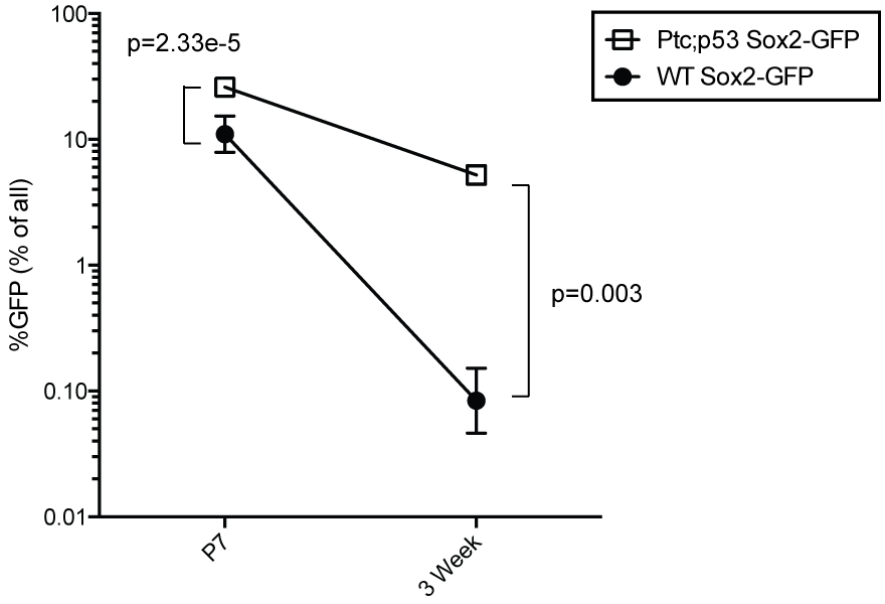

Figure 3-7 Summary of the frequency of GFP-expressing cells in P7 and 3 week WT *Sox2-GFP* and *Ptch1$^{LacZ/+}$;Trp53$^{-/-}$ Sox2-GFP* animals

Comparison of the frequency of GFP-positive cells between the WT and *Ptch1$^{LacZ/+}$;Trp53$^{-/-}$ Sox2-GFP* animals at P7 and 3 weeks shows a significant increase in GFP-positive cells in the *Ptch1$^{LacZ/+}$;Trp53$^{-/-}$* genotype at both timepoints. Statistical significance was determined by individual t-tests between the two different genotypes.

Differential gene expression between P7 WT and 3 week *Ptch1$^{LacZ/+}$;Trp53$^{-/-}$ Sox2-GFP* positive cells

To determine if there are differences in gene expression between the *Sox2*-expressing and non-expressing cells, we sorted the GFP-negative and positive fractions from P7 WT colony mice and 3 week *Ptch1$^{LacZ/+}$;Trp53$^{-/-}$* chimeras and colony mice for the isolation of RNA. Re-sorting the GFP-negative and positive fractions further improved the purity of the FACS fractionation, ensuring expression analyses from cells highly enriched for *Sox2*-expressing and non-expressing cells (Figure 3-8).

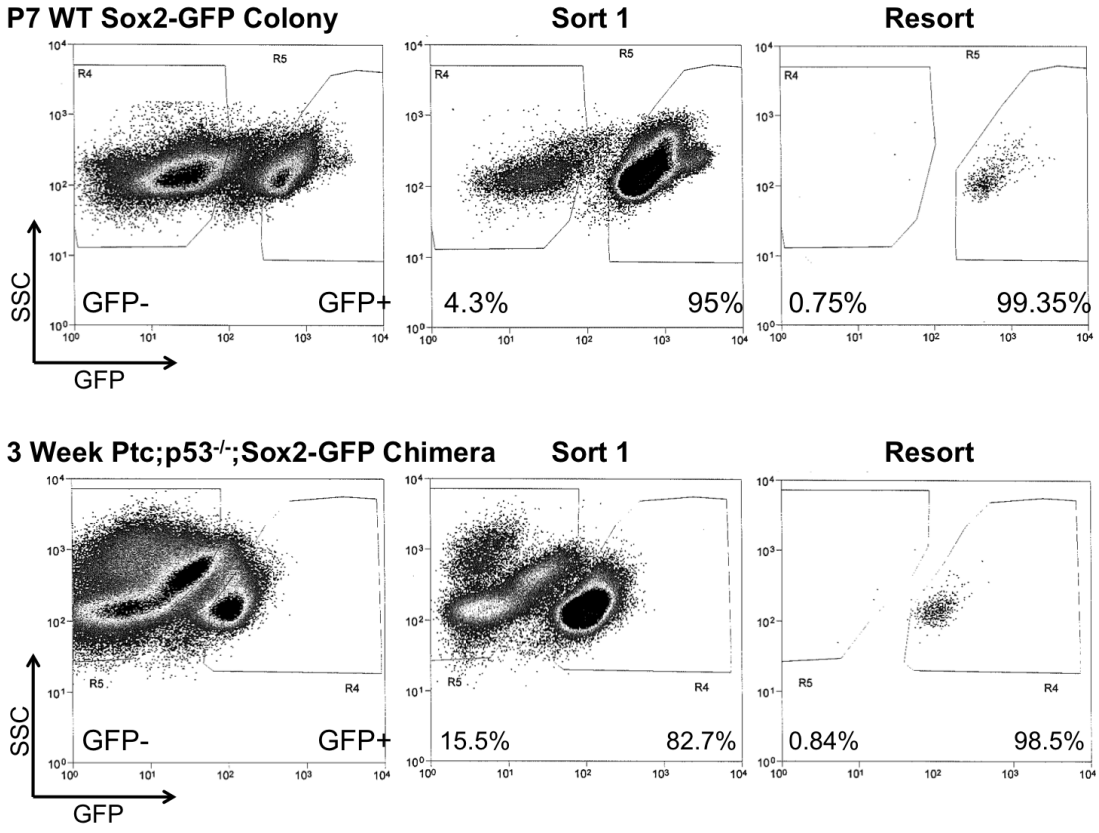

Figure 3-8 *Sox2-GFP* negative and positive cells were re-sorted to increase purity for RNA isolation for gene expression analysis

Representative examples of FACS plots of GFP expression in P7 WT and 3 Week *Ptch1*$^{LacZ/+}$*;Trp53*$^{-/-}$*;Sox2-GFP* cerebella as analyzed by MoFlo. GFP-negative and positive fractions were collected and each fraction was re-sorted to obtain an increased purity in the fractions.

For validation of the FACS sorts, we examined the expression of the *GFP* transgene and observed a 50-fold enrichment in the WT P7 *Sox2-GFP* fractions and about 20-fold enrichment in all of the 3 week *Ptch1*$^{LacZ/+}$*;Trp53*$^{-/-}$ *Sox2-GFP* positive fractions, relative to a P7 WT *Sox2*-negative control. We next examined the gene expression of a small panel of stem cell, granule cell progenitor, and Shh pathway activation genes in the *Sox2*-positive fractions, which were all normalized to a P7 WT *Sox2*-negative sample. In the WT P7 cerebella, enrichment of *Sox2* expression and upregulation of *Hes1,* a gene important in the self-renewal of NSC (Nakamura *et al.*, 2000) was negatively correlated with the expression of *Math*1, a marker for cerebellar

granule neurons (Figure 3-9a). In contrast, in the 3 week *Ptch1*$^{LacZ/+}$*;Trp53*$^{-/-}$ animals, *Sox2* expression was not associated with a depletion of Math1 expression, but showed an increase in *Math1* in comparison to the WT P7 *Sox2*-negative fraction (Figure 3-9b). In addition, *Gli1* and *Gli2* expression was also slightly higher in the 3 week *Ptch1*$^{LacZ/+}$*;Trp53*$^{-/-}$*;Sox2*-positive cells. This suggests that while the 3 week *Ptch1*$^{LacZ/+}$*;Trp53*$^{-/-}$*;Sox2*-positive cells represent a population of aberrantly self-renewing stem cells, they are also responsive to the differentiation signals of the Shh pathways, which are active during cerebellar development, and may be maintaining characteristics of both cerebellar stem cell and granule cell progenitors.

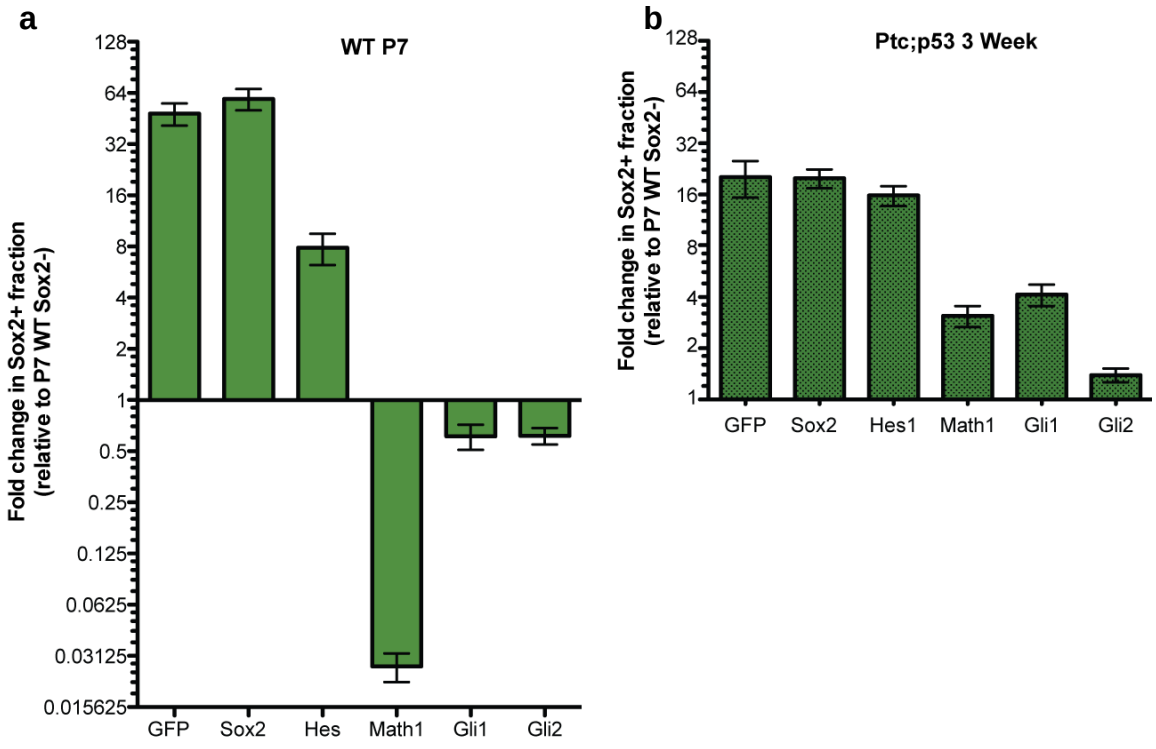

Figure 3-9 Differential gene expression of granule cell progenitor markers in the 3 week *Ptch1*$^{LacZ/+}$*;Trp53*$^{-/-}$*; Sox2-GFP* positive cerebellar cells

qRT-PCR expression analyses of stem cell markers *Sox2* and *Hes1* and granule cell progenitor markers *Math1, Gli1* and *Gli2* in *Sox2*-positive sorted cells from (a) wild-type P7 colony mice (n=8) and (b) *Ptch1*$^{LacZ/+}$*;Trp53*$^{-/-}$ 3 week chimeras (n=4). Fold change in expression is represented relative to P7 WT *Sox2*-negative cell fractions, which is normalized to 1.

Discussion

The *Ptch1*$^{LacZ/+}$*;Trp53*$^{-/-}$ mouse model of medulloblastoma reveals a population of self-renewing cells from the tumor and at 3 weeks, a developmental time-point when normal cerebellar development is complete and self-renewal activity is largely non-existent (C. Lin thesis). While the MBNS have potent tumor-initiating capability, the aberrantly self-renewing cells from 3-week-old mice have not yet undergone loss of heterozygosity of the *Ptch1* allele, the tumor-initiating event in the *Ptch1* model, and do not form tumors (Yang *et al.*, 2008b) (C. Lin thesis). While *in vitro* enrichment of this pre-malignant tissue stem cell population by serial neurosphere culture has been valuable in uncovering the mechanisms for tumor-initiating events, a prospective marker allowing for isolation of an endogenously occurring, *bona fide* self-renewing tissue stem cell circumvents concerns about tissue culture-induced changes or enrichment of heterogeneous cell types. Here we show that *Sox2-GFP* expression fractionates the self-renewal activity in both the P7 WT and 3 week *Ptch1*$^{LacZ/+}$*;Trp53*$^{-/-}$ cerebella, thus validating *Sox2* as a marker for the prospective isolation of the endogenous self-renewing CbSC as well as the aberrant CbSC. This novel marker will have great utility for further examination of stem cell regulation during medulloblastoma tumorigenesis.

Sox2 as a prospective marker for self-renewing normal and aberrantly persistent CbSC

Critical for the validation of CSC markers is the strict correlation between marker expression with *bona fide* self-renewal activity (Clarke *et al.*, 2006). For example, it has been shown that CD133, a widely used cell surface marker, does not strictly isolate stem cell activity, as CD133-negative cells also demonstrated properties of self-renewal (Sun *et al.*, 2009). Variations in FACS isolation with cell surface marker staining have also been reported to be

subject to inconsistencies due to antibody differences and other technical variations (Visvader and Lindeman, 2012). By using an endogenous reporter for *Sox2*-expression, we show that the prospective isolation of *Sox2*-expressing cells fractionated the self-renewing, developmental CbSC at P7. No NS formation was observed in the GFP-negative fraction and all the neurospheres that formed were GFP-positive. By 3 weeks of age, the frequency of *Sox2*-expressing cells is significantly reduced, consistent with the abolished self-renewal activity at 3 weeks in WT animals. In contrast, although at a significantly lower frequency than the P7 $Ptch1^{LacZ/+};Trp53^{-/-}$ animals, GFP-positive cells were reliably sorted from every 3 week $Ptch1^{LacZ/+};Trp53^{-/-}$ animal. However, the functional significance of the wide variability in the frequency of *Sox2*-positive cells in the 3 week $Ptch1^{LacZ/+};Trp53^{-/-}$ cerebella is unknown. Nonetheless, *Sox2*-expression also unambiguously marked the self-renewing cells in the developmentally persistent stem cells in the 3 week $Ptch1^{LacZ/+};Trp53^{-/-}$ cerebella. While the mechanism of developmental persistence is unknown, the absence of GFP-negative NS suggests that the expression of *Sox2* may be functionally important in the self-renewal of CbSC, further supporting *Sox2* as a robust marker. The functional role of *Sox2* in NSC maintenance and neurogenesis is well-established and it's role in CSC self-renewal, specifically, has also been demonstrated in glioblastoma (Gangemi *et al.*, 2009) and breast cancer (Leis *et al.*, 2011). Alternative to the hypothesis of the persistence of *Sox2*-positve CbSC during development, we must also consider the possibility of a *Sox2*-expressing population arising *de novo* during the development of $Ptch1^{LacZ/+};Trp53^{-/-}$ animals, rather than an endogenous *Sox2*-expressing population persisting from early development. To address this, an inducible *Sox2-GFP* allele may be utilized to track the *Sox2*-expression during development. Using the *Sox2*-

CreER;ROSA26-Isl-EYFP mice, tamoxifen-induced recombination can be carried out to activate the expression of the fluorescent marker then tracked during cerebellar development.

Analyses of Ptch1$^{LacZ/+}$;Trp53$^{-/-}$;Sox2-GFP chimeras

It must be noted that the analyses of the *Ptch1$^{LacZ/+}$;Trp53$^{-/-}$;Sox2-GFP* chimeras have caveats. While the complete colonization of the cerebella by *the Ptch1$^{LacZ/+}$;Trp53$^{-/-}$* ES cells in chimeric mice has been carefully validated (C. Lin thesis), the effect of the *Sox2-GFP* reporter allele on this colonization phenotype has not been directly examined. The *Sox2-GFP* reporter allele is knocked into the endogenous *Sox2* promoter and targeting results in the inactivation of one *Sox2* allele. While the *Sox2* heterozygous animals are viable and display no overt abnormalities (Avilion *et al.*, 2003), given the importance of *Sox2* in NSC, the possibility of a haploinsufficient effect of *Sox2* heterozygosity on the colonization phenotype cannot be disregarded. The analyses of P7 *Ptch1$^{LacZ/+}$;Trp53$^{-/-}$;Sox2-GFP* chimeras demonstrate that this in fact, may be the case; the formation of GFP-negative neurospheres was observed in the *Sox2-GFP* negative fractions in the low-density neurosphere formation assay, implying that there may be WT host-derived contamination. To circumvent the confounding factors introduced by the contamination of the host cells WT for *Sox2*, further analyses of *Ptch1$^{LacZ/+}$;Trp53$^{-/-}$;Sox2-GFP* animals were only carried out with colony (germline-mutant) animals.

Differential gene expression between the Sox2-GFP expressing P7 cerebellar stem cells and 3 week aberrant tissue stem cells

Despite the complications that may arise from the chimeric analyses, as the host cells lack the GFP allele, the *Sox2-GFP*-positive fractions from the chimeras are all necessarily

derived from ES cells, and thus have been used for analyses of gene expression. In the case of the GFP-negative cells, although wild-type host cells are not expected to express *Sox2* at 3 weeks, they do retain both copies of the WT *Sox2* allele and may confound the analyses of gene expression in the 3 week *Ptch1*$^{LacZ/+}$*;Trp53*$^{-/-}$ *Sox2*-negative fractions. Therefore, chimera-derived GFP-negative cells from 3 week old mice have not been included in the gene expression analyses; the *Sox2-GFP* negative fractions of the WT *Sox2-GFP* animals derived from the colony were used as controls.

In the WT P7 *Sox2-GFP* positive cells, there was an enrichment for the expression of *Hes1*, a stem cell marker, and *Sox2*-expression was negatively correlated with *Math1*. This pattern of gene expression is consistent with the *Sox2*-positive cells representing CbSC and the *Sox2*-negative cells containing the *Math1* lineage-restricted granule cell progenitors, which are actively proliferating at P7. The maintenance of the *Math1* expression and to a lesser extent *Gli1* and *Gli2* expression in the 3 week *Ptch1*$^{LacZ/+}$*;Trp53*$^{-/-}$ *Sox2*-positive cells suggests that the aberrantly self-renewing cells are responsive to the Shh signaling pathway for granule-lineage determination, but also concurrently exhibit NSC characteristics. Whether this is due to a resistance to differentiation or an ectopic acquisition of stem cell behavior in differentiated granule cell progenitors are both potential mechanisms that may be explored. bFGF, which is present in NS culture conditions, has been shown to abolish Shh-induced proliferation and promote differentiation of the GCP (Fogarty *et al.*, 2007). Neurosphere formation of the *Ptch1*$^{LacZ/+}$*;Trp53*$^{-/-}$ *Sox2*-positive cells from 3 week old animals suggests that these cells are exhibiting a block in differentiation.

Future Studies

Using the *Sox2-GFP* positive and negative sorted fractions, a genome-wide expression analyses will be carried out. There will be great utility for the genome-wide expression profiles and signatures of the specific subsets of cell populations, such as CSC and premalignant stem cells in the *Ptch1*$^{LacZ/+}$*;Trp53*$^{-/-}$ model. Potentially, gene expression profiles specifically identifying the CSC population may have important clinical implications. In fact, in the hematopoietic system, the characterization and comparison of HSC and leukemia stem cell expression profiles have allowed for the accurate prediction of patient outcomes (Eppert *et al.*, 2011). It can be imagined that the identification of a medulloblastoma stem cell-specific expression profile can be used to better predict prognoses and improve risk stratification. Insights into the mechanisms and pathways involved in the persistence of aberrant tissue stem cells will also be important. For example, if the aberrantly persisting stem cells are expanding the pool of targets for oncogenic transformation, reduction or elimination of this population may decrease the frequency of cells acquiring the transforming mutation (Wicha *et al.*, 2006), allowing for earlier therapeutic intervention.

Sox2-positive cells can also be isolated from postnatal day 7 *Ptch1*$^{LacZ/+}$*;Trp53*$^{-/-}$ *Sox2*-positive animals. By comparing this to the WT *Sox2-GFP* cells, this will allow us to determine if the *Ptch1*$^{LacZ/+}$*;Trp53*$^{-/-}$ genotype exhibit aberrant patterns of gene expression early on in cerebellar development.

Methods

ES cell generation

V6.5 wild-type ES cells were electroporated with the *Sox2-GFP* targeting vector (Ellis et al., 2004, generous gift from K. Hochedlinger) and selected in neomycin for 7 days. The *Sox2-GFP*

targeting vector was modified to exchange the neomycin-selection cassette with a puromycin-selection cassette for electroporation into *Ptch1*$^{LacZ/+}$*;Trp53*$^{-/-}$ ES cells. Neomycin- and puromycin-resistant colonies were picked and expanded for genotyping for targeting by a quantitative qPCR for genomic copy number of the *Sox2* allele.

Generation of mouse chimeras and animal husbandry

Blastocyst stage embryos were isolated from CD-1 superovulated females crossed to CD-1 males (Charles River) at 2.5dpc and cultured in KSOM-AA overnight. Expanded blastocysts were injected with 5-10 WT *Sox2-GFP* and *Ptch1*$^{LacZ/+}$*;Trp53*$^{-/-}$ *Sox2-GFP* ES cells and transferred to 2.5dpc pseudopregnant CD-1 females. WT *Sox2-GFP* chimeric males were crossed to Albino/B6 females and germline transmission was confirmed by genotyping F1 pups for the *Sox2-GFP* allele. *Sox2-GFP* mice were bred into the *Ptch1* and *Trp53* mutant background for generation of *Ptch1*$^{LacZ/+}$*;Trp53*$^{-/-}$ animals. *Ptch1*$^{LacZ/+}$*;Trp53*$^{-/-}$ *Sox2-GFP* chimeras were used directly for experiments. Mice were maintained in pathogen-free conditions at Boston Children's Hospital and procedures were performed following approval by the Institutional Animal Care and Use Committee (IACUC).

Flow cytometry

Cerebellar tissues were dissociated into single cell suspension by mincing with a razor blade and followed by trituration in NS media, washed and resuspended in PBS+2mM EDTA+0.5% BSA and run on a BD FACS Aria and Beckman Coulter/Dako MoFlo at the HSCI/Joslin Flow Cytometry Core. Samples were stained with 7-AAD (BD Biosciences) for exclusion of dead cells and gated on the GFP-positive or GFP-negative fractions. For the low-density neurosphere

formation assay, cells were sorted directly into a 6-well plate with neurosphere culture media (DMEM:F12 containing B27 Supplement (Invitrogen), 20ng/ml bFGF (Invitrogen), 20ng/ml EGF (Invitrogen), and 100U/ml penicillin/streptomycin (Invitrogen)).

Expression analyses by quantitative PCR

Sox2-GFP-positive and negative sorted cells were pelleted and resuspended in Trizol Reagent (Invitrogen) for RNA isolation, using RNase-free glycogen (Invitrogen) as a carrier. Isolated RNA was treated with DNaseI (New England Biolabs) and synthesized as cDNA using the High-Capacity cDNA Reverse Transcription Kit (Applied Biosystems). Quantitative RT-PCR was carried with the SYBR Green PCR Master Mix (Applied Biosystems) using cDNA dilutions determined by prior primer optimization experiments. *GFP, Sox2, Gli1, Gli2, Hes1*, and *Math1* expression was normalized to Gapdh and changes in gene expression were determined by the ddCT method and represented as expression levels relative to the P7 WT *Sox2-GFP* negative control.

Primers:

Gapdh: 5' GTTGTCTCCTGCGACTTCA 3'; 5' TGGTCCAGGGTTTCTTACTC 3'

GFP: 5' GAACGGCATCAAGGTGAAC 3' ; 5' CTTGTACAGCTCGTCCATG 3'

Sox2: 5' CCGAGGAGGAGAGCGCCTGT -3'; 5'- GCTCGAGACGGGCGAAGTGC 3'

Gli1: 5' TTCAAGGCCCAATACATGCT 3'; 5' GCGTCTTGAGGTTTTCAAGG 3'

Gli2: 5' GGTCTCTTGGAGGACAGCAG 3'; 5' TCTCATGTCAATCGGCAAAG 3'

Hes1: 5' ATGCCGGGAGCTATCTTTCT 3'; 5' ACACCGGACAAACCAAAGAC 3'

Math1: 5' ACAGGTCCTTCTGTGCCATC 3'; 5' GCTTCCTCTGGGGGTTACTC 3'

Chapter 4 : Conclusions and Future Directions

Prior to the emergence of "medulloblastomics", medulloblastoma has been largely considered and studied as a single-entity disease but it has become evident that it is, in fact, a heterogeneous collection of tumors comprised of distinct molecular subtypes (Northcott *et al.*, 2012). The generation and examination of subtype-matched mouse models have shed light on discrete mechanisms for disease progression and the cell of origin (Kool *et al.*, 2012). Now with the core four groups of medulloblastoma established, studying the heterogeneity within a subgroup for further subcategorization may also be relevant for the investigation of targeted therapies. As such, it has been shown that within the SHH tumors, pediatric and adult tumors are transcriptionally, genetically, and clinically discrete (Northcott *et al.*, 2011a). Work in our lab has also shown that the *Ptch1*$^{LacZ/+}$ and *Ptch1*$^{LacZ/+}$*;Trp53*$^{-/-}$ genotypes also result in functionally distinct tumors in mice. Notably, the *Ptch1*$^{LacZ/+}$*;Trp53*$^{-/-}$ model results in aggressive tumors with a population of self-renewing and tumor-propagating cells (C. Lin thesis). In addition, while the cell of origin in the SHH tumors has been established as the granule cell progenitors (GCP), cerebellar stem cells (CbSC) have been suggested as another potential tumor-initiating cell population (C. Lin thesis). Recent work has also shown that postnatal CbSC transformed with the overexpression of c-myc can lead to tumor-initiation upon transplantation (Kawauchi *et al.*, 2012; Pei *et al.*, 2012). The presence of a self-renewing, tumor-initiating stem cell population in the *Ptch1*$^{LacZ/+}$*;Trp53*$^{-/-}$ tumors and the observation of an aberrantly self-renewing, premalignant population of CbSC further substantiated the examination of stem cell regulation in this medulloblastoma model.

In Chapter 2, we wanted to examine the pathway dependencies and plasticity mechanisms of the self-renewing, tumor-initiating cells in the *Ptch1*$^{LacZ/+}$*;Trp53*$^{-/-}$ medulloblastomas. Specifically, we asked if an endogenously active pluripotency transcription factor network could be utilized for the survival and maintenance of self-renewal of the *Ptch1*$^{LacZ/+}$*;Trp53*$^{-/-}$ MBNS. The observation of phenotypic plasticity and conversion of the tumor-initiating medulloblastoma neurosphere cells in the ES culture conditions in the absence of ectopic factors led us to ask if epigenetic regulation such as DNA methylation alterations could be involved. This subsequently led to the identification of reprogramming factor *Klf4* as a gene important in the mediating both the MBNS plasticity and self-renewal.

The functional role of pluripotency genes in mediating cancer stem-like phenotypes has been described. For example, *Oct4* expression induces the dedifferentiation of melanoma cells and leads to the acquisition of CSC characteristics, such as expression of melanoma stem cell markers and multipotent differentiation (Kumar *et al.*, 2012). Furthermore, the induction of pluripotency gene expression in immortalized breast epithelial cells results in the formation of cancer stem-like cells with tumor-initiating ability and interestingly, an increased resistance to chemotherapeutic agents (Nishi *et al.*, 2013). The similarities between the expression profiles of ES cells and high-grade, malignant tumors (Ben-Porath *et al.*, 2008) further provide a rationale for the "oncogenic reprogramming" model for the generation and maintenance of CSC. However, the examination of the role of *c-myc* in the transcriptional profiles of cancer cells has revealed that the ES gene signature is merely reflective of an activated *c-myc* signature of tumors (Kim *et al.*, 2010). Functionally, the role of *c-myc* has been further shown to globally amplify the output of existing transcriptional programs by increased binding at the promoters and enhancers of genes already activated (Lin *et al.*, 2012), shedding light on the mechanism for the diverse

effects of *c-myc* observed in various tumors. If *c-myc* is functioning in a similar manner in the *Ptch1*$^{LacZ/+}$*;Trp53*$^{-/-}$ medulloblastomas, it can be postulated to be playing a role in promoting stem cell-driven tumorigenesis by amplifying the activated stem cell signatures in the aberrant tissue stem cells. Though the potential mechanism of dedifferentiation of GCP or CbSC during *Ptch1*$^{LacZ/+}$*;Trp53*$^{-/-}$ tumor progression has not been directly addressed in this study, the plasticity of tumor cells to alter cellular states and respond to different environmental variations remains an plausible mechanism for tumor stem cell survival, metastases and treatment evasion.

*Klf4 o*verexpression has been shown to abrogate the necessity for exogenous LIF in ES culture media for the maintenance of ES cells in an undifferentiated state (Zhang *et al.*, 2010). *Klf4* is also a known direct downstream target of the Stat3 pathway, crucial in ES cells (Niwa *et al.*, 1998), NSC (Yoshimatsu *et al.*, 2006; Androutsellis-Theotokis *et al.*, 2006) and observed to be aberrantly activated in various tumors (Yu and Jove, 2004), including brain tumors (Schaefer *et al.*, 2002; Yang *et al.*, 2008a). Based on the observation of LIF independence and *Stat3* overexpression and constitutive activation in the MBNS, we hypothesized that upstream Stat3 signaling may be mediating the function of *Klf4*. However, *Stat3* kd by pharmacological inhibition and RNAi both led to a partial and non-significant effect on the self-renewal of the MBNS, especially in the limiting dilution assay. Furthermore, *Klf4* expression levels rebounded in *Stat3* kd neurospheres, suggesting that the regulation of *Klf4* can occur in a manner independent of the canonical LIF/Stat3 pathway to maintain clonogenic growth. The *Stat3*-independent compensatory mechanism remains to be determined, but highlights the importance of uncovering the multiple modes of *Klf4* regulation for a more extensive understanding of the transcriptional networks regulating the self-renewal and survival pathways in the tumor-initiating cells.

Through the modulation of *Stat3* and *Klf4* levels, we observed that the expression of *Klf4* is crucial for MBNS plasticity and self-renewal and can be regulated in a *Stat3*-independent manner. The novel role of *Klf4* in maintaining the clonogenic growth of self-renewing cells in a medulloblastoma model provides the rationale to further examine the function of *KLF4* in human medulloblastomas, specifically in the class of human tumors with the poorest rates of survival. While *KLF4* expression is not enriched in the Class C human medulloblastomas (data not shown), which have the lowest survival rates, if it is functioning in a small subset of self-renewing cells within the bulk tumor, the expression levels may not be reflected in the gene expression analysis of bulk tumors. The expression levels of *KLF4* specifically in a population of cells enriched for self-renewal, such as prominin 1 positive cells, may be important and interesting to analyze. Further, the therapeutic potential of *KLF4* inhibition can also be considered. A pilot experiment in the MBNS testing the synergy between *Klf4* kd and gamma irradiation, a treatment modality used in human medulloblastoma patients, suggests that the kd of *Klf4* may sensitize the cells to doses of radiation ineffective in cells with WT levels of *Klf4*, as measured by a decrease in NS formation frequency with the combination of *Klf4* kd and irradiation. Further validation of this experiment must be carried out, but these initial observations provide an additional motivation for studying the role of *Klf4* in the survival of the tumor-initiating, self-renewal population in medulloblastomas. In the MBNS, the maintenance of antiapoptotic gene expression was associated with the compensatory upregulation of *Klf4.* While this is suggestive of an antiapoptotic role of *Klf4*, which has been reported (Ghaleb *et al.*, 2007), functional apoptosis following *Klf4* kd must first be addressed and can be measured by a variety of assays such as TUNEL staining, cleaved Caspase-3 staining in the MBNS. During Ras-mediated transformation, Klf4 has been shown to directly repress the transcription of p53,

leading to resistance to DNA-damage mediated apoptosis (Rowland *et al.*, 2005). Since a mechanism for radiation sensitization by *Klf4* inhibition will be a *Trp53*-independent mechanism if demonstrated in *Ptch1*$^{LacZ/+}$;*Trp53*$^{-/-}$, this will be important, considering that human medulloblastoma patients harboring somatic *TP53* mutations exhibit early disease recurrence and lack of long-term survival compared to patients with WT *TP5*3 receiving the same craniospinal irradiation and chemotherapy (Tabori *et al.*, 2010).

The compensatory mechanism of transcription factors in related pathways may be a general mechanism of CSC to exhibit plasticity and survival against the environmental challenges they must overcome, such as irradiation or adaptation to a new niches during metastases. Therefore, it will be important to characterize such mechanisms and determine if multiple pathways must be targeted for effective treatment. In contrast to oncogene addiction, in which tumor cells are dependent on a specific gene for survival, CSC may exhibit flexibility in the regulation of the expression of functionally redundant genes important for its survival and therefore require targeting multiple genes to exert a "synthetic lethality" effect (Luo *et al.*, 2009).

Further expanding on the idea of targeting multiple pathways in CSC, our observations may provide the rationale for the combinatory inhibition of the Shh pathway and pathways important for self-renewal. Since the effect of Stat3 inhibition alone on self-renewal was partial, the inhibition of the Shh pathway in combination with Stat3 inhibition is a potential approach that may be examined. Considerable efforts have been made to target the Stat3 and Shh pathways in medulloblastomas and other tumors, therefore small molecule inhibitors are readily available. Constitutive Stat3 activation is observed in human medulloblastomas (Schaefer *et al.*, 2002; Yang *et al.*, 2008a), with the NSC survival-associated phosphorylation of Ser727 (Androutsellis-Theotokis *et al.*, 2006) occurring as a tumor-specific activation (Schaefer *et al.*, 2002; Yang *et*

al., 2008a). Multikinase inhibitors whose activities are associated with the inhibition of Stat3 phosphorylation (Yang *et al.*, 2008a; 2010a), selective inhibitors of the Jak2/Stat3 pathway (ie. JSI-124) (Lo *et al.*, 2008), and Stat3 DNA binding site inhibitors (Ball *et al.*, 2011) have all been shown to reduce proliferation and induce apoptosis in multiple medulloblastoma cell lines. Interestingly, JSI-124 treatment was shown to sensitize the medulloblastoma cells to an otherwise ineffective chemotherapeutic, BCNU, and displayed synergy with cisplatin in inhibiting medulloblastoma cell survival (Lo *et al.*, 2008). Importantly, both chemotherapeutics are currently used to treat medulloblastoma patients in the clinic. Specifically in brain tumor stem cell populations, small molecule Stat3 inhibitors (Stattic and STA-21) have been demonstrated to inhibit glioblastoma stem cell neurosphere formation and induce apoptosis (Sherry *et al.*, 2009; Villalva *et al.*, 2011). However, the effect of *Stat3* inhibition on the expression of target gene *Klf4* has not been examined in these studies and remains to be determined if the therapeutic function of *Stat3* inhibitors is mediated by a downstream inhibition of *Klf4*, as suggested in our work.

Given the well-established role of the SHH pathway in cerebellar and medulloblastoma development, a number of SHH inhibitors, including Cyclopamine and SMO antagonist, HhAntag have been reported to be effective in slowing the growth of SHH tumors (Berman *et al.*, 2002; Romer *et al.*, 2004). In particular, SMO antagonist GDC-0449 has had partial success in the clinic, whereby rapid tumor regression was observed following GDC-0449 treatment in an adult patient with a SHH pathway-activated tumor (Rudin *et al.*, 2009). However, tumor relapse occurred rapidly and widespread dissemination followed. The mechanism of resistance was subsequently identified to be a somatic mutation in the drug binding site in SMO, which did not exist prior to treatment (Yauch *et al.*, 2009). To overcome resistance mechanisms, new inhibitors

effective against the GDC-0449-resistant mutants were identified in a small molecule inhibitor screen, but additional resistance mechanisms occurring downstream of SMO prompted the targeting of an alternative pathway for overcoming resistance (Dijkgraaf *et al.*, 2011). Importantly, GDC-0449-resistant mutants were sensitive to PI3K/Akt inhibition, suggesting this pathway as a potential target in GDC-044- resistant tumors (Dijkgraaf *et al.*, 2011). These observations are consistent with the idea that a unique population of cells within the tumor may possess the ability to utilize multiple compensatory pathways for survival. Therefore, studying the self-renewing cells that specifically exhibit properties of plasticity and survival in varying growth conditions may also present a novel strategy for examining resistance mechanisms.

In Chapter 3, we sought to validate *Sox2* as a prospective marker for the isolation of postnatal CbSC and further establish it as a marker for the enrichment of the aberrantly self-renewing, premalignant stem cells in the *Ptch1*$^{LacZ/+}$*;Trp53*$^{-/-}$ animals. Culturing glioblastoma cells as neurospheres in serum-free culture in the presence of bFGF and EGF has been described for the isolation of self-renewing, multipotent, tumor-initiating cells expressing NSC markers (Yuan *et al.*, 2004) and maintenance of the characteristics of the primary tumors (Lee *et al.*, 2006). Only the neurosphere cells, but not the non-sphere-forming cells, were able to initiate tumor-formation *in vivo* (Yuan *et al.*, 2004). Similarly, in the absence of appropriate markers for CSC for the *Ptch1*$^{LacZ/+}$*;Trp53* medulloblastomas, we first utilized the neurosphere culture-based system to isolate and characterize pathways important in self-renewal and survival. The *Ptch1*$^{LacZ/+}$*;Trp53* MBNS exhibit self-renewal, as demonstrated by limiting dilution assays and the derivation of clonal lines, high expression of NSC markers CD133, nestin, and possess potent ability for tumor-initiation *in vivo* (C. Lin thesis). We must note, however, that the multipotent

differentiation capability of these medulloblastoma-initiating neurosphere cells has not been directly addressed. Growth factor withdrawal from the *Ptch1*$^{LacZ/+}$*;Trp53* MBNS suggests a block in differentiation as observed by the maintenance of *Sox2* expression following bFGF and EGF removal. The withdrawal of growth factors from the aberrant *Ptch1*$^{LacZ/+}$*;Trp53* tissue stem cells, also enriched by neurospheres cultures, however, exhibited a reduction in *Sox2* expression. The neurosphere culture method has also been utilized to isolate bFGF and EGF-responsive multipotent CbSC from the postnatal d7 cerebella (Lee *et al.*, 2005). The persistence of a bFGF and EGF-responsive population in 3 week old *Ptch1*$^{LacZ/+}$*;Trp53* animals at a time point when cerebellar development is complete, suggests an developmentally persistent population of stem cells. Cerebellar granule progenitor cells proliferate in response to SHH during cerebellar development, but bFGF directly inhibits SHH signaling (Fogarty *et al.*, 2007). The CbSC may have a block in differentiation that allows them to persist as stem cells, however, the possibility of progenitor cells dedifferentiating to stem-like cells with neurosphere-forming capability also cannot be ruled out. To further this question, a marker for the prospective genetic marking of stem cells is necessary, which we have started to address by examining the potential for *Sox2* as a prospective marker for the aberrant CbSC during medulloblastoma progression.

Using an endogenous *Sox2-GFP* reporter allele, we observed that the prospective isolation of *Sox2*-expressing cells was able to fractionate the self-renewing activity in the WT CbSC and the aberrant tissue stem cells. Preliminary expression analyses with a small subset of genes also show that expression of *Math1*, a marker for GCP, is inversely correlated with *Sox2* expression in the WT CbSC. However, in the 3 week *Ptch1*$^{LacZ/+}$*;Trp53*$^{-/-}$*;Sox2-GFP* cells, the expression of *Math1, Gli1* and *Gli2* suggest that the responsiveness to the Shh signaling for granule cell differentiation is intact, but stem cell characteristics are also maintained. Genome-

wide transcriptional profiling of these aberrantly self-renewing stem cells will provide further insight into the mechanisms and pathways of developmental persistence and block in differentiation. In addition, comparison of the 3 week aberrant tissue stem cells and the P7 CbSC will allow us to identify pathways or therapeutic targets specific to the aberrant population, which is especially critical given that medulloblastomas are developmental tumors and nonspecific effects of therapeutics may have dire side effects in young patients. Comparison of the WT and *Ptch1*$^{LacZ/+}$*;Trp53*$^{-/-}$*;Sox2-GFP* CbSC at P7 may also provide insight into the early mechanisms of stem cell deregulation.

For future studies, the *Sox2-GFP* reporter can also be utilized to determine the localization of *Sox2*-expressing cells during cerebellar development and malignant progression. At P7, *Sox2* expression is observed in the white matter, coinciding with the location of the CD133-positive CbSC (Lee *et al.*, 2005). With further maturation of the cerebellum, by P25 and in the adult, *Sox2* expression is restricted to the Purkinje cell layer, specifically marking the Bergmann glia (Sottile *et al.*, 2006). The location of the *Sox2*-expressing population in the 3 week *Ptch1*$^{LacZ/+}$*;Trp53*$^{-/-}$ cerebella is currently unknown. Based on the current knowledge of *Sox2*-expression during normal cerebellar development, it can be postulated that the *Sox2*-positive cells are marking the subset of CbSC present in the white matter, aberrantly persisting due to a deficiency in differentiation. Alternatively, *Sox2*-expression may be marking an expanded *Sox2*-positive Bergman glial cell population, which has been proposed as a potential NSC population that has yet to be characterized (Sottile *et al.*, 2006). Another possibility is the dedifferentiation of lineage-restricted GCP cells of the EGL, due to an acquisition of stem cell character during progenitor expansion. Histological or immunohistochemical analyses of *Sox2* expression in both WT and *Ptch1*$^{LacZ/+}$*;Trp53*$^{-/-}$ tissues will allow for us to determine the location

of the *Sox2*-expressing cells and further our understanding of the possible cell of origin and mechanisms of *Ptch1*$^{LacZ/+}$*;Trp53*$^{-/-}$ medulloblastoma progression. In addition, similar to the recent lineage tracing studies which identified *bona fide* CSC *in vivo*, with an inducible *Sox2-GFP* reporter, lineage tracing can be carried out to examine the individual contribution of the *Sox2*-expressing cells during medulloblastoma progression and if the progeny of the *Sox2-GFP* cells do, in fact, mark the resultant tumor in the *Ptch1*$^{LacZ/+}$*;Trp53*$^{-/-}$ animals.

The *Sox2-GFP* marker may be useful, not only in the developmental context but also as a marker for the MBNS in the endpoint *Ptch1*$^{LacZ/+}$*;Trp53*$^{-/-}$ tumors. The analyses of *Sox2*-expressing cells in the tumors may yield greater insight into the potential role for dedifferentiation or reprogramming-like mechanisms in CSC. The use of long-term passage MBNS lines for the *in vitro* reprogramming assay has made it difficult to address whether or not the cells with the capability for growing in ES culture conditions were a preexisting population in the tumor or a result of long-term culture-induced changes. The direct isolation of the *Sox2*-GFP population into ES culture conditions in the *in vitro* reprogramming assay will allow us to determine more definitively if a pre-existing, endogenous population of stem cells with the ability for reprogramming is preexisting in the tumor.

In a tentative hypothesis for the aberrant persistence of tissue stem cells in the *Ptch1*$^{LacZ/+}$*;Trp53*$^{-/-}$ animals (Figure 4-1), we postulate that a deregulation of stem cell self-renewal and resistance to differentiation may be mediated by collaboration between the loss of *Trp53* function and activated Shh signaling. This is suggested by the increase in basal level of self-renewal in 3 week *Trp53*$^{-/-}$ animals (C. Lin thesis), which is consistent with the role of p53 in the maintenance of NSC populations (Meletis *et al.*, 2006) and dedifferentiation during

somatic reprogramming (Krizhanovsky and Lowe, 2009). Furthermore, a *Gli1* and *Trp53* negative regulatory loop was described to control NSC numbers (Stecca and Ruiz i Altaba, 2009), whereby *Gli1* negatively regulates *Trp53* to increase stem cell activity and *Trp53* in turn inhibits *Gli1* activity, thereby ensuring the control of NSC proliferation. However, in the $Ptch1^{LacZ/+};Trp53^{-/-}$ genotype, it can be hypothesized that both genetic mutations alter the stem cell activity, as the *Ptch1* mutation will lead to an increase in downstream *Gli1* expression and the *Trp53* null genotype to a deregulation in the inhibitory loop. The activation of the HH-GLI pathway has been reported to maintain the self-renewal of glioma stem cells (Clement *et al.*, 2007) and induce an ES stem-like signature in metastatic colon cancers (Varnat *et al.*, 2010). Furthermore, *Gli2* has been reported to bind to the enhancer and activate the transcription of *Sox2* in neuroepithelial cells (Takanaga *et al.*, 2009), providing a potential mechanism for the increased *Sox2* expression in a $Ptch1^{LacZ/+};Trp53^{-/-}$ mutants. Stat3 signaling also converges onto *Sox2*, as the direct regulation of *Sox2* by *Stat3* has been described in neural precursor cells (Foshay and Gallicano, 2008). Furthermore, the upregulation of both *Gli* and *Sox2* transcription factors in the $Ptch1^{LacZ/+};Trp53^{-/-}$ mutant background may lead to an increased co-binding of *Gli1* and *Sox2* to activate the expression of cooperatively regulated target genes, as observed during neural patterning and progenitor specification (Peterson *et al.*, 2012). Transcriptional profiling of the CbSC and aberrant tissue stem cells will allow for us to determine if a gene signature specific for CbSC can be identified and if enhanced activation of a subset of genes in the aberrant tissue stem cell are coregulated by *Gli* and *Sox2*.

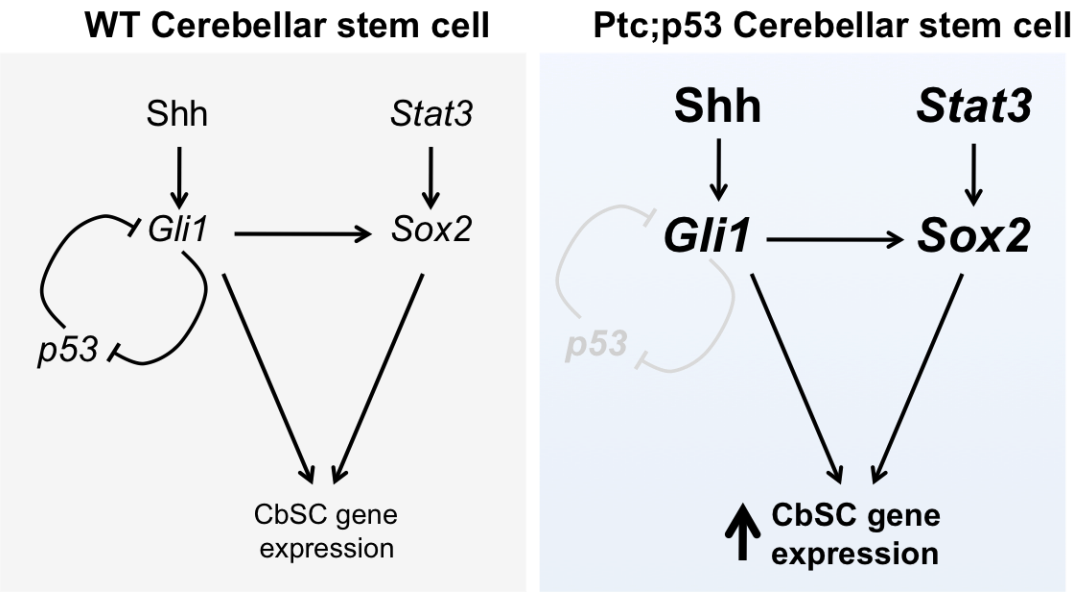

Figure 4-1 Tentative hypothesis for the aberrant persistence of *Sox2*-expressing cerebellar stem cell in the 3 week *Ptch1*$^{LacZ/+}$;*Trp53*$^{-/-}$ animals

In the WT CbSC, the Gli1-p53 negative regulatory loop regulating stem cell numbers is intact and CbSC genes are expressed at normal levels. However, in the *Ptch1*$^{LacZ/+}$;*Trp53*$^{-/-}$ cerebella, loss of *p53* and *Ptch1* inactivation may be leading to enhanced *Gli1* activation, which in cooperation with *Sox2* may be aberrantly maintaining a subset of CbSC genes. Furthermore, high levels of Stat3 expression, which is observed in MBNS, may also be playing a role in maintaining the persistent expression of its target gene *Sox2*.

Chapter 5 : References

Al-Hajj M, Wicha MS, Benito-Hernandez A, Morrison SJ, and Clarke MF. (2003). Prospective identification of tumorigenic breast cancer cells. *Proc Natl Acad Sci USA* **100**: 3983–3988.

Alcock J, Lowe J, England T, Bath P, and Sottile V. (2009). Expression of Sox1, Sox2 and Sox9 is maintained in adult human cerebellar cortex. *Neuroscience Letters* **450**: 114–116.

Alvarez JV, Febbo PG, Ramaswamy S, Loda M, Richardson A, and Frank DA. (2005). Identification of a genetic signature of activated signal transducer and activator of transcription 3 in human tumors. *Cancer Research* **65**: 5054–5062.

Ambrosini G, Adida C, and Altieri DC. (1997). A novel anti-apoptosis gene, survivin, expressed in cancer and lymphoma. *Nat Med* **3**: 917–921.

Androutsellis-Theotokis A, Leker RR, Soldner F, Hoeppner DJ, Ravin R, Poser SW, *et al.* (2006). Notch signalling regulates stem cell numbers in vitro and in vivo. *Nature* **442**: 823–826.

Auernhammer CJ, Bousquet C, and Melmed S. (1999). Autoregulation of pituitary corticotroph SOCS-3 expression: characterization of the murine SOCS-3 promoter. *Proc Natl Acad Sci USA* **96**: 6964–6969.

Avilion AA, Nicolis SK, Pevny LH, Perez L, Vivian N, and Lovell-Badge R. (2003). Multipotent cell lineages in early mouse development depend on SOX2 function. *Genes & Development* **17**: 126–140.

Ball S, Li C, Li P-K, and Lin J. (2011). The Small Molecule, LLL12, Inhibits STAT3 Phosphorylation and Induces Apoptosis in Medulloblastoma and Glioblastoma Cells. *PLoS ONE* **6**: e18820.

Bao S, Wu Q, Mclendon RE, Hao Y, Shi Q, Hjelmeland AB, *et al.* (2006). Glioma stem cells promote radioresistance by preferential activation of the DNA damage response. *Nature* **444**: 756–760.

Beier D, Hau P, Proescholdt M, Lohmeier A, Wischhusen J, Oefner PJ, *et al.* (2007). CD133(+) and CD133(-) glioblastoma-derived cancer stem cells show differential growth characteristics and molecular profiles. *Cancer Research* **67**: 4010–4015.

Ben-Arie N, Bellen HJ, Armstrong DL, McCall AE, Gordadze PR, Guo Q, *et al.* (1997). Math1 is essential for genesis of cerebellar granule neurons. *Nature* **390**: 169–172.

Ben-Porath I, Thomson MW, Carey VJ, Ge R, Bell GW, Regev A, *et al.* (2008). An embryonic stem cell-like gene expression signature in poorly differentiated aggressive human tumors. *Nat Genet* **40**: 499–507.

Berman DM, Karhadkar SS, Hallahan AR, Pritchard JI, Eberhart CG, Watkins DN, *et al.* (2002). Medulloblastoma growth inhibition by hedgehog pathway blockade. *Science* **297**: 1559–1561.

Blazek ER, Foutch JL, and Maki G. (2007). Daoy medulloblastoma cells that express CD133 are radioresistant relative to CD133- cells, and the CD133+ sector is enlarged by hypoxia. *Int. J. Radiat. Oncol. Biol. Phys.* **67**: 1–5.

Bonnet D, and Dick JE. (1997). Human acute myeloid leukemia is organized as a hierarchy that originates from a primitive hematopoietic cell. *Nat Med* **3**: 730–737.

Bourillot P-Y, Aksoy I, Schreiber V, Wianny F, Schulz H, Hummel O, *et al.* (2009). Novel STAT3 target genes exert distinct roles in the inhibition of mesoderm and endoderm differentiation in cooperation with Nanog. *Stem Cells* **27**: 1760–1771.

Calabrese C, Poppleton H, Kocak M, Hogg TL, Fuller C, Hamner B, *et al.* (2007). A Perivascular Niche for Brain Tumor Stem Cells. *Cancer Cell* **11**: 69–82.

Catlett-Falcone R, Landowski TH, Oshiro MM, Turkson J, Levitzki A, Savino R, *et al.* (1999). Constitutive activation of Stat3 signaling confers resistance to apoptosis in human U266 myeloma cells. *Immunity* **10**: 105–115.

Cavallaro M, Mariani J, Lancini C, Latorre E, Caccia R, Gullo F, *et al.* (2008). Impaired generation of mature neurons by neural stem cells from hypomorphic Sox2 mutants. *Development* **135**: 541–557.

Chen J, Li Y, Yu T-S, McKay RM, Burns DK, Kernie SG, *et al.* (2012). A restricted cell population propagates glioblastoma growth after chemotherapy. *Nature* **488**: 522–526.

Chen R, Nishimura MC, Bumbaca SM, Kharbanda S, Forrest WF, Kasman IM, *et al.* (2010). A hierarchy of self-renewing tumor-initiating cell types in glioblastoma. *Cancer Cell* **17**: 362–375.

Chen X, Johns DC, Geiman DE, Marban E, Dang DT, Hamlin G, *et al.* (2001). Krüppel-like factor 4 (gut-enriched Krüppel-like factor) inhibits cell proliferation by blocking G1/S progression of the cell cycle. *J Biol Chem* **276**: 30423–30428.

Cho Y-J, Tsherniak A, Tamayo P, Santagata S, Ligon A, Greulich H, *et al.* (2010). Integrative Genomic Analysis of Medulloblastoma Identifies a Molecular Subgroup That Drives Poor Clinical Outcome. *Journal of Clinical Oncology*.

Chung J, Uchida E, Grammer TC, and Blenis J. (1997). STAT3 serine phosphorylation by ERK-dependent and -independent pathways negatively modulates its tyrosine phosphorylation. *Mol Cell Biol* **17**: 6508–6516.

Cittelly DM, Finlay-Schultz J, Howe EN, Spoelstra NS, Axlund SD, Hendricks P, *et al.* (2013). Progestin suppression of miR-29 potentiates dedifferentiation of breast cancer cells via KLF4. *Oncogene* **32**: 2555–2564.

Clarke MF, Dick JE, Dirks PB, Eaves CJ, Jamieson CHM, Jones DL, *et al.* (2006). Cancer stem

cells--perspectives on current status and future directions: AACR Workshop on cancer stem cells. In: Vol. 66. p 9339–9344.

Clement V, Sanchez P, de Tribolet N, Radovanovic I, and Ruiz i Altaba A. (2007). HEDGEHOG-GLI1 signaling regulates human glioma growth, cancer stem cell self-renewal, and tumorigenicity. *Curr Biol* **17**: 165–172.

Clevers H. (2011). The cancer stem cell: premises, promises and challenges. *Nat Med* **17**: 313–319.

Clifford SC, Lusher ME, Lindsey JC, Langdon JA, Gilbertson RJ, Straughton D, *et al.* (2006). Wnt/Wingless pathway activation and chromosome 6 loss characterize a distinct molecular sub-group of medulloblastomas associated with a favorable prognosis. *Cell Cycle* **5**: 2666–2670.

Coles-Takabe BLK, Brain I, Purpura KA, Karpowicz P, Zandstra PW, Morshead CM, *et al.* (2008). Don't look: growing clonal versus nonclonal neural stem cell colonies. *Stem Cells* **26**: 2938–2944.

Cozzio A, Passegué E, Ayton PM, Karsunky H, Cleary ML, and Weissman IL. (2003). Similar MLL-associated leukemias arising from self-renewing stem cells and short-lived myeloid progenitors. *Genes & Development* **17**: 3029–3035.

Crawford JR, MacDonald TJ, and Packer RJ. (2007). Medulloblastoma in childhood: new biological advances. *Lancet Neurol* **6**: 1073–1085.

Dean M, Fojo T, and Bates S. (2005). Tumour stem cells and drug resistance. *Nat Rev Cancer* **5**: 275–284.

Decker T, and Kovarik P. (2000). Serine phosphorylation of STATs. *Oncogene* **19**: 2628–2637.

Dennis M, Spiegler BJ, Hetherington CR, and Greenberg ML. (1996). Neuropsychological sequelae of the treatment of children with medulloblastoma. *J Neurooncol* **29**: 91–101.

Dick JE. (2009). Looking ahead in cancer stem cell research. *Nat Biotechnol* **27**: 44–46.

Diehn M, Cho RW, Lobo NA, Kalisky T, Dorie MJ, Kulp AN, *et al.* (2009). Association of reactive oxygen species levels and radioresistance in cancer stem cells. *Nature* **458**: 780–783.

Dijkgraaf GJP, Alicke B, Weinmann L, Januario T, West K, Modrusan Z, *et al.* (2011). Small molecule inhibition of GDC-0449 refractory smoothened mutants and downstream mechanisms of drug resistance. *Cancer Research* **71**: 435–444.

Dirks PB. (2008). Brain tumor stem cells: bringing order to the chaos of brain cancer. *Journal of Clinical Oncology* **26**: 2916–2924.

Driessens G, Beck B, Caauwe A, Simons BD, and Blanpain C. (2012). Defining the mode of tumour growth by clonal analysis. *Nature* **488**: 527–530.

Ellis P, Fagan BM, Magness ST, Hutton S, Taranova O, Hayashi S, *et al.* (2004). SOX2, a persistent marker for multipotential neural stem cells derived from embryonic stem cells, the embryo or the adult. *Dev. Neurosci.* **26**: 148–165.

Ellison DW, Clifford SC, Gajjar A, and Gilbertson RJ. (2003). What's new in neuro-oncology? Recent advances in medulloblastoma. *Eur J Paediatr Neurol* **7**: 53–66.

Ellison DW, Dalton J, Kocak M, Nicholson SL, Fraga C, Neale G, *et al.* (2011). Medulloblastoma: clinicopathological correlates of SHH, WNT, and non-SHH/WNT molecular subgroups. *Acta Neuropathol.* **121**: 381–396.

Epling-Burnette PK, Liu JH, Catlett-Falcone R, Turkson J, Oshiro M, Kothapalli R, *et al.* (2001). Inhibition of STAT3 signaling leads to apoptosis of leukemic large granular lymphocytes and decreased Mcl-1 expression. *J Clin Invest* **107**: 351–362.

Eppert K, Takenaka K, Lechman ER, Waldron L, Nilsson B, van Galen P, *et al.* (2011). Stem cell gene expression programs influence clinical outcome in human leukemia. *Nat Med* **17**: 1086–1093.

Favaro R, Valotta M, Ferri ALM, Latorre E, Mariani J, Giachino C, *et al.* (2009). Hippocampal development and neural stem cell maintenance require Sox2-dependent regulation of Shh. *Nat Neurosci* **12**: 1248–1256.

Ferri ALM, Cavallaro M, Braida D, Di Cristofano A, Canta A, Vezzani A, *et al.* (2004). Sox2 deficiency causes neurodegeneration and impaired neurogenesis in the adult mouse brain. *Development* **131**: 3805–3819.

Fogarty MP, Emmenegger BA, Grasfeder LL, Oliver TG, and Wechsler-Reya RJ. (2007). Fibroblast growth factor blocks Sonic hedgehog signaling in neuronal precursors and tumor cells. *Proc Natl Acad Sci USA* **104**: 2973–2978.

Foshay KM, and Gallicano GI. (2008). Regulation of Sox2 by STAT3 initiates commitment to the neural precursor cell fate. *Stem Cells Dev.* **17**: 269–278.

Gage FH, Ray J, and Fisher LJ. (1995). Isolation, characterization, and use of stem cells from the CNS. *Annu. Rev. Neurosci.* **18**: 159–192.

Galli R, Binda E, Orfanelli U, Cipelletti B, Gritti A, De Vitis S, *et al.* (2004). Isolation and characterization of tumorigenic, stem-like neural precursors from human glioblastoma. *Cancer Research* **64**: 7011–7021.

Gangemi RMR, Griffero F, Marubbi D, Perera M, Capra MC, Malatesta P, *et al.* (2009). SOX2 silencing in glioblastoma tumor-initiating cells causes stop of proliferation and loss of tumorigenicity. *Stem Cells* **27**: 40–48.

Gautron L, De Smedt-Peyrusse V, and Layé S. (2006). Characterization of STAT3-expressing cells in the postnatal rat brain. *Brain Res.* **1098**: 26–32.

Ghaleb AM, Katz JP, Kaestner KH, Du JX, and Yang VW. (2007). Krüppel-like factor 4 exhibits antiapoptotic activity following gamma-radiation-induced DNA damage. *Oncogene* **26**: 2365–2373.

Gibson P, Tong Y, Robinson G, Thompson MC, Currle DS, Eden C, *et al.* (2010). Subtypes of medulloblastoma have distinct developmental origins. *Nature* **468**: 1095–1099.

Ginestier C, Hur MH, Charafe-Jauffret E, Monville F, Dutcher J, Brown M, *et al.* (2007). ALDH1 is a marker of normal and malignant human mammary stem cells and a predictor of poor clinical outcome. *Stem Cell* **1**: 555–567.

Goodrich LV, Milenković L, Higgins KM, and Scott MP. (1997). Altered neural cell fates and medulloblastoma in mouse patched mutants. *Science* **277**: 1109–1113.

Gritsko T, Williams A, Turkson J, Kaneko S, Bowman T, Huang M, *et al.* (2006). Persistent activation of stat3 signaling induces survivin gene expression and confers resistance to apoptosis in human breast cancer cells. *Clin Cancer Res* **12**: 11–19.

Guo G, Yang J, Nichols J, Hall JS, Eyres I, Mansfield W, *et al.* (2009). Klf4 reverts developmentally programmed restriction of ground state pluripotency. *Development* **136**: 1063–1069.

Guo W, Lasky JL, Chang C-J, Mosessian S, Lewis X, Xiao Y, *et al.* (2008). Multi-genetic events collaboratively contribute to Pten-null leukaemia stem-cell formation. *Nature* **453**: 529–533.

Gupta PB, Chaffer CL, and Weinberg RA. (2009). Cancer stem cells: mirage or reality? *Nat Med* **15**: 1010–1012.

Hall J, Guo G, Wray J, Eyres I, Nichols J, Grotewold L, *et al.* (2009). Oct4 and LIF/Stat3 Additively Induce Krüppel Factors to Sustain Embryonic Stem Cell Self-Renewal. *Cell Stem Cell* **5**: 597–609.

Hambardzumyan D, Becher OJ, Rosenblum MK, Pandolfi PP, Manova-Todorova K, and Holland EC. (2008). PI3K pathway regulates survival of cancer stem cells residing in the perivascular niche following radiation in medulloblastoma in vivo. *Genes & Development* **22**: 436–448.

Hamilton SR, Liu B, Parsons RE, Papadopoulos N, Jen J, Powell SM, *et al.* (1995). The molecular basis of Turcot's syndrome. *N Engl J Med* **332**: 839–847.

Hanahan D, and Weinberg RA. (2011). Hallmarks of Cancer: The Next Generation. *Cell* **144**: 646–674.

Hatten ME, Alder J, Zimmerman K, and Heintz N. (1997). Genes involved in cerebellar cell specification and differentiation. *Curr. Opin. Neurobiol.* **7**: 40–47.

Hatten ME, and Heintz N. (1995). Mechanisms of neural patterning and specification in the developing cerebellum. *Annu. Rev. Neurosci.* **18**: 385–408.

Hatten ME, and Roussel MF. (2011). Development and cancer of the cerebellum. *Trends Neurosci* **34**: 134–142.

Hatton BA, Villavicencio EH, Tsuchiya KD, Pritchard JI, Ditzler S, Pullar B, *et al.* (2008). The Smo/Smo model: hedgehog-induced medulloblastoma with 90% incidence and leptomeningeal spread. *Cancer Research* **68**: 1768–1776.

Hazan-Halevy I, Harris D, Liu Z, Liu J, Li P, Chen X, *et al.* (2010). STAT3 is constitutively phosphorylated on serine 727 residues, binds DNA, and activates transcription in CLL cells. *Blood*.

Hemmati HD, Nakano I, Lazareff JA, Masterman-Smith M, Geschwind DH, Bronner-Fraser M, *et al.* (2003). Cancerous stem cells can arise from pediatric brain tumors. *Proc Natl Acad Sci USA* **100**: 15178–15183.

Hermann PC, Huber SL, Herrler T, Aicher A, Ellwart JW, Guba M, *et al.* (2007). Distinct populations of cancer stem cells determine tumor growth and metastatic activity in human pancreatic cancer. *Cell Stem Cell* **1**: 313–323.

Hitoshi S, Seaberg RM, Koscik C, Alexson T, Kusunoki S, Kanazawa I, *et al.* (2004). Primitive neural stem cells from the mammalian epiblast differentiate to definitive neural stem cells under the control of Notch signaling. *Genes & Development* **18**: 1806–1811.

Hochedlinger K, Blelloch R, Brennan C, Yamada Y, Kim M, Chin L, *et al.* (2004). Reprogramming of a melanoma genome by nuclear transplantation. *Genes & Development* **18**: 1875–1885.

Holmberg J, He X, Peredo I, Orrego A, Hesselager G, Ericsson C, *et al.* (2011). Activation of neural and pluripotent stem cell signatures correlates with increased malignancy in human glioma. *PLoS ONE* **6**: e18454.

Hong H, Takahashi K, Ichisaka T, Aoi T, Kanagawa O, Nakagawa M, *et al.* (2009). Suppression of induced pluripotent stem cell generation by the p53-p21 pathway. *Nature* **460**: 1132–1135.

Hoshino M, Nakamura S, Mori K, Kawauchi T, Terao M, Nishimura YV, *et al.* (2005). Ptf1a, a bHLH transcriptional gene, defines GABAergic neuronal fates in cerebellum. *Neuron* **47**: 201–213.

Hu Y, and Smyth GK. (2009). ELDA: extreme limiting dilution analysis for comparing depleted and enriched populations in stem cell and other assays. *J. Immunol. Methods* **347**: 70–78.

Huse JT, and Holland EC. (2010). Targeting brain cancer: advances in the molecular pathology of malignant glioma and medulloblastoma. *Nat Rev Cancer* **10**: 319–331.

Ichiba M, Nakajima K, Yamanaka Y, Kiuchi N, and Hirano T. (1998). Autoregulation of the Stat3 gene through cooperation with a cAMP-responsive element-binding protein. *J Biol Chem* **273**: 6132–6138.

Irizarry RA, Ladd-Acosta C, Wen B, Wu Z, Montano C, Onyango P, *et al.* (2009). The human colon cancer methylome shows similar hypo- and hypermethylation at conserved tissue-specific CpG island shores. *Nat Genet* **41**: 178–186.

Ishikawa F, Yoshida S, Saito Y, Hijikata A, Kitamura H, Tanaka S, *et al.* (2007). Chemotherapy-resistant human AML stem cells home to and engraft within the bone-marrow endosteal region. *Nat Biotechnol* **25**: 1315–1321.

Joo KM, Kim SY, Jin X, Song SY, Kong D-S, Lee J-I, *et al.* (2008). Clinical and biological implications of CD133-positive and CD133-negative cells in glioblastomas. *Lab. Invest.* **88**: 808–815.

Jordan CT. (2009). Cancer stem cells: controversial or just misunderstood? *Cell Stem Cell* **4**: 203–205.

Katz JP, Perreault N, Goldstein BG, Lee CS, Labosky PA, Yang VW, *et al.* (2002). The zinc-finger transcription factor Klf4 is required for terminal differentiation of goblet cells in the colon. *Development* **129**: 2619–2628.

Kawamura T, Suzuki J, Wang YV, Menendez S, Morera LB, Raya A, *et al.* (2009). Linking the p53 tumour suppressor pathway to somatic cell reprogramming. *Nature* **460**: 1140–1144.

Kawauchi D, Robinson G, Uziel T, Gibson P, Rehg J, Gao C, *et al.* (2012). A Mouse Model of the Most Aggressive Subgroup of Human Medulloblastoma. *Cancer Cell* **21**: 168–180.

Kelly PN, Dakic A, Adams JM, Nutt SL, and Strasser A. (2007). Tumor growth need not be driven by rare cancer stem cells. *Science* **317**: 337.

Kho AT, Zhao Q, Cai Z, Butte AJ, Kim JYH, Pomeroy SL, *et al.* (2004). Conserved mechanisms across development and tumorigenesis revealed by a mouse development perspective of human cancers. *Genes & Development* **18**: 629–640.

Kim J, Chu J, Shen X, Wang J, and Orkin SH. (2008a). An extended transcriptional network for pluripotency of embryonic stem cells. *Cell* **132**: 1049–1061.

Kim J, Woo AJ, Chu J, Snow JW, Fujiwara Y, Kim CG, *et al.* (2010). A Myc Network Accounts for Similarities between Embryonic Stem and Cancer Cell Transcription Programs. *Cell* **143**: 313–324.

Kim JB, Sebastiano V, Wu G, Araúzo-Bravo MJ, Sasse P, Gentile L, *et al.* (2009). Oct4-induced pluripotency in adult neural stem cells. *Cell* **136**: 411–419.

Kim JB, Zaehres H, Wu G, Gentile L, Ko K, Sebastiano V, *et al.* (2008b). Pluripotent stem cells induced from adult neural stem cells by reprogramming with two factors. *Nature* **454**: 646–650.

Kim JYH, Nelson AL, Algon SA, Graves O, Sturla LM, Goumnerova LC, *et al.* (2003). Medulloblastoma tumorigenesis diverges from cerebellar granule cell differentiation in patched heterozygous mice. *Dev Biol* **263**: 50–66.

Kool M, Korshunov A, Remke M, Jones DTW, Schlanstein M, Northcott PA, *et al.* (2012). Molecular subgroups of medulloblastoma: an international meta-analysis of transcriptome, genetic aberrations, and clinical data of WNT, SHH, Group 3, and Group 4 medulloblastomas. *Acta Neuropathol.* **123**: 473–484.

Kool M, Koster J, Bunt J, Hasselt NE, Lakeman A, van Sluis P, *et al.* (2008). Integrated genomics identifies five medulloblastoma subtypes with distinct genetic profiles, pathway signatures and clinicopathological features. *PLoS ONE* **3**: e3088.

Krivtsov AV, Twomey D, Feng Z, Stubbs MC, Wang Y, Faber J, *et al.* (2006). Transformation from committed progenitor to leukaemia stem cell initiated by MLL-AF9. *Nature* **442**: 818–822.

Krizhanovsky V, and Lowe SW. (2009). Stem cells: The promises and perils of p53. *Nature* **460**: 1085–1086.

Kumar SM, Liu S, Lu H, Zhang H, Zhang PJ, Gimotty PA, *et al.* (2012). Acquired cancer stem cell phenotypes through Oct4-mediated dedifferentiation. *Oncogene*.

Lang J-Y, Shi Y, and Chin YE. (2012). Reprogramming cancer cells: back to the future. : 1–2.

Lapidot T, Sirard C, Vormoor J, Murdoch B, Hoang T, Caceres-Cortes J, *et al.* (1994). A cell initiating human acute myeloid leukaemia after transplantation into SCID mice. *Nature* **367**: 645–648.

Lau J, Schmidt C, Markant SL, Taylor MD, Wechsler-Reya RJ, and Weiss WA. (2012). Matching mice to malignancy: molecular subgroups and models of medulloblastoma. *Childs Nerv Syst* **28**: 521–532.

Lee A, Kessler JD, Read T-A, Kaiser C, Corbeil D, Huttner WB, *et al.* (2005). Isolation of neural stem cells from the postnatal cerebellum. *Nat Neurosci* **8**: 723–729.

Lee J, Kotliarova S, Kotliarov Y, Li A, Su Q, Donin NM, *et al.* (2006). Tumor stem cells derived from glioblastomas cultured in bFGF and EGF more closely mirror the phenotype and genotype of primary tumors than do serum-cultured cell lines. *Cancer Cell* **9**: 391–403.

Leis O, Eguiara A, Lopez-Arribillaga E, Alberdi MJ, Hernandez-Garcia S, Elorriaga K, *et al.* (2011). Sox2 expression in breast tumours and activation in breast cancer stem cells. *Oncogene*.

Li C, Heidt DG, Dalerba P, Burant CF, Zhang L, Adsay V, *et al.* (2007). Identification of pancreatic cancer stem cells. *Cancer Research* **67**: 1030–1037.

Li H, Collado M, Villasante A, Strati K, Ortega S, Cañamero M, *et al.* (2009). The Ink4/Arf locus is a barrier for iPS cell reprogramming. *Nature* **460**: 1136–1139.

Li L, Connelly MC, Wetmore C, Curran T, and Morgan JI. (2003). Mouse embryos cloned from brain tumors. *Cancer Research* **63**: 2733–2736.

Li X, Lewis MT, Huang J, Gutierrez C, Osborne CK, Wu M-F, *et al.* (2008). Intrinsic resistance

of tumorigenic breast cancer cells to chemotherapy. *J. Natl. Cancer Inst.* **100**: 672–679.

Li Y, McClintick J, Zhong L, Edenberg HJ, Yoder MC, and Chan RJ. (2005). Murine embryonic stem cell differentiation is promoted by SOCS-3 and inhibited by the zinc finger transcription factor Klf4. *Blood* **105**: 635–637.

Lin CY (2012) Developmental Origins of Aggressive Medulloblastoma (Doctoral Dissertation). Retrieved from ProQuest Dissertations and Theses (Accession Order No.3543074)

Lin CY, Lovén J, Rahl PB, Paranal RM, Burge CB, Bradner JE, *et al.* (2012). Transcriptional Amplification in Tumor Cells with Elevated c-Myc. *Cell* **151**: 56–67.

Liu J, Li JW, Gang Y, Guo L, and Li H. (1999). Expression of leukemia-inhibitory factor as an autocrinal growth factor in human medulloblastomas. *J Cancer Res Clin Oncol* **125**: 475–480.

Lo H-W, Cao X, Zhu H, and Ali-Osman F. (2008). Constitutively activated STAT3 frequently coexpresses with epidermal growth factor receptor in high-grade gliomas and targeting STAT3 sensitizes them to Iressa and alkylators. *Clin Cancer Res* **14**: 6042–6054.

Louis DN, Ohgaki H, Wiestler OD, Cavenee WK, Burger PC, Jouvet A, *et al.* (2007). The 2007 WHO classification of tumours of the central nervous system. *Acta Neuropathol.* **114**: 97–109.

Luo J, Solimini NL, and Elledge SJ. (2009). Principles of cancer therapy: oncogene and non-oncogene addiction. *Cell* **136**: 823–837.

MacDonald TJ, Brown KM, LaFleur B, Peterson K, Lawlor C, Chen Y, *et al.* (2001). Expression profiling of medulloblastoma: PDGFRA and the RAS/MAPK pathway as therapeutic targets for metastatic disease. *Nat Genet* **29**: 143–152.

Marino S. (2005). Medulloblastoma: developmental mechanisms out of control. *Trends in molecular medicine* **11**: 17–22.

Marión RM, Strati K, Li H, Murga M, Blanco R, Ortega S, *et al.* (2009). A p53-mediated DNA damage response limits reprogramming to ensure iPS cell genomic integrity. *Nature* **460**: 1149–1153.

McMahon AP, and Bradley A. (1990). The Wnt-1 (int-1) proto-oncogene is required for development of a large region of the mouse brain. *Cell* **62**: 1073–1085.

Medema JP. (2013). Cancer stem cells: the challenges ahead. *Nat Cell Biol* **15**: 338–344.

Meletis K, Wirta V, Hede S-M, Nistér M, Lundeberg J, and Frisén J. (2006). p53 suppresses the self-renewal of adult neural stem cells. *Development* **133**: 363–369.

Moon J-H, Heo JS, Kim JS, Jun EK, Lee JH, Kim A, *et al.* (2011). Reprogramming fibroblasts into induced pluripotent stem cells with Bmi1. *Nature Publishing Group* **21**: 1305–1315.

Nakahara Y, Northcott PA, Li M, Kongkham PN, Smith C, Yan H, *et al.* (2010). Genetic and

epigenetic inactivation of Kruppel-like factor 4 in medulloblastoma. *Neoplasia* **12**: 20–27.

Nakamura Y, Sakakibara SI, Miyata T, Ogawa M, Shimazaki T, Weiss S, *et al.* (2000). The bHLH gene hes1 as a repressor of the neuronal commitment of CNS stem cells. *Journal of Neuroscience* **20**: 283–293.

Nelson EA, Walker SR, Kepich A, Gashin LB, Hideshima T, Ikeda H, *et al.* (2008). Nifuroxazide inhibits survival of multiple myeloma cells by directly inhibiting STAT3. *Blood* **112**: 5095–5102.

Nishi M, Sakai Y, Akutsu H, Nagashima Y, Quinn G, Masui S, *et al.* (2013). Induction of cells with cancer stem cell properties from nontumorigenic human mammary epithelial cells by defined reprogramming factors. *Oncogene*.

Niwa H, Burdon T, Chambers I, and Smith A. (1998). Self-renewal of pluripotent embryonic stem cells is mediated via activation of STAT3. *Genes & Development* **12**: 2048–2060.

Niwa H, Ogawa K, Shimosato D, and Adachi K. (2009). A parallel circuit of LIF signalling pathways maintains pluripotency of mouse ES cells. *Nature* **460**: 118–122.

Northcott PA, Hielscher T, Dubuc A, Mack S, Shih D, Remke M, *et al.* (2011a). Pediatric and adult sonic hedgehog medulloblastomas are clinically and molecularly distinct. *Acta Neuropathol.* **122**: 231–240.

Northcott PA, Jones DTW, Kool M, Robinson GW, Gilbertson RJ, Cho Y-J, *et al.* (2012). Medulloblastomics: the end of the beginning. *Nat Rev Cancer* **12**: 818–834.

Northcott PA, Korshunov A, Witt H, Hielscher T, Eberhart CG, Mack S, *et al.* (2011b). Medulloblastoma Comprises Four Distinct Molecular Variants. *Journal of Clinical Oncology* **29**: 1408–1414.

Oliver TG, Read TA, Kessler JD, Mehmeti A, Wells JF, Huynh TTT, *et al.* (2005). Loss of patched and disruption of granule cell development in a pre-neoplastic stage of medulloblastoma. *Development* **132**: 2425–2439.

O'Brien CA, Pollett A, Gallinger S, and Dick JE. (2007). A human colon cancer cell capable of initiating tumour growth in immunodeficient mice. *Nature* **445**: 106–110.

Passegué E, Jamieson CHM, Ailles LE, and Weissman IL. (2003). Normal and leukemic hematopoiesis: are leukemias a stem cell disorder or a reacquisition of stem cell characteristics? *Proc Natl Acad Sci USA* **100 Suppl 1**: 11842–11849.

Pastrana E, Silva-Vargas V, and Doetsch F. (2011). Eyes wide open: a critical review of sphere-formation as an assay for stem cells. *Cell Stem Cell* **8**: 486–498.

Pei Y, Moore CE, Wang J, Tewari AK, Eroshkin A, Cho Y-J, *et al.* (2012). An Animal Model of MYC-Driven Medulloblastoma. *Cancer Cell* **21**: 155–167.

Peterson KA, Nishi Y, Ma W, Vedenko A, Shokri L, Zhang X, *et al.* (2012). Neural-specific Sox2 input and differential Gli-binding affinity provide context and positional information in Shh-directed neural patterning. *Genes & Development* **26**: 2802–2816.

Po A, Ferretti E, Miele E, De Smaele E, Paganelli A, Canettieri G, *et al.* (2010). Hedgehog controls neural stem cells through p53-independent regulation of Nanog. *EMBO J* **29**: 2646–2658.

Pomeroy SL, Tamayo P, Gaasenbeek M, Sturla LM, Angelo M, McLaughlin ME, *et al.* (2002). Prediction of central nervous system embryonal tumour outcome based on gene expression. *Nature* **415**: 436–442.

Qin S, Liu M, Niu W, and Zhang C-L. (2011). Dysregulation of Kruppel-like factor 4 during brain development leads to hydrocephalus in mice. *Proc Natl Acad Sci USA* **108**: 21117–21121.

Quintana E, Shackleton M, Sabel MS, Fullen DR, Johnson TM, and Morrison SJ. (2008). Efficient tumour formation by single human melanoma cells. *Nature* **456**: 593–598.

Rane SG, and Reddy EP. (2000). Janus kinases: components of multiple signaling pathways. *Oncogene* **19**: 5662–5679.

Read T-A, Fogarty MP, Markant SL, Mclendon RE, Wei Z, Ellison DW, *et al.* (2009). Identification of CD15 as a Marker for Tumor-Propagating Cells in a Mouse Model of Medulloblastoma. *Cancer Cell* **15**: 135–147.

Reya T, Morrison SJ, Clarke MF, and Weissman IL. (2001). Stem cells, cancer, and cancer stem cells. *Nature* **414**: 105–111.

Reynolds A, Leake D, Boese Q, Scaringe S, Marshall WS, and Khvorova A. (2004). Rational siRNA design for RNA interference. *Nat Biotechnol* **22**: 326–330.

Reynolds BA, and Weiss S. (1996). Clonal and population analyses demonstrate that an EGF-responsive mammalian embryonic CNS precursor is a stem cell. *Dev Biol* **175**: 1–13.

Reynolds BA, Tetzlaff W, and Weiss S. (1992). A multipotent EGF-responsive striatal embryonic progenitor cell produces neurons and astrocytes. *J Neurosci* **12**: 4565–4574.

Ricci-Vitiani L, Lombardi DG, Pilozzi E, Biffoni M, Todaro M, Peschle C, *et al.* (2007). Identification and expansion of human colon-cancer-initiating cells. *Nature* **445**: 111–115.

Ris MD, Walsh K, Wallace D, Armstrong FD, Holmes E, Gajjar A, *et al.* (2013). Intellectual and Academic Outcome Following Two Chemotherapy Regimens and Radiotherapy for Average-Risk Medulloblastoma: COG A9961. *Pediatr Blood Cancer*.

Roberts PJ, and Der CJ. (2007). Targeting the Raf-MEK-ERK mitogen-activated protein kinase cascade for the treatment of cancer. *Oncogene* **26**: 3291–3310.

Romer JT, Kimura H, Magdaleno S, Sasai K, Fuller C, Baines H, *et al.* (2004). Suppression of

the Shh pathway using a small molecule inhibitor eliminates medulloblastoma in Ptc1(+/-)p53(-/-) mice. *Cancer Cell* **6**: 229–240.

Rowland BD, and Peeper DS. (2006). KLF4, p21 and context-dependent opposing forces in cancer. *Nat Rev Cancer* **6**: 11–23.

Rowland BD, Bernards R, and Peeper DS. (2005). The KLF4 tumour suppressor is a transcriptional repressor of p53 that acts as a context-dependent oncogene. *Nat Cell Biol* **7**: 1074–1082.

Rudin CM, Hann CL, Laterra J, Yauch RL, Callahan CA, Fu L, *et al.* (2009). Treatment of medulloblastoma with hedgehog pathway inhibitor GDC-0449. *N Engl J Med* **361**: 1173–1178.

Sasai K, Romer JT, Lee Y, Finkelstein D, Fuller C, McKinnon PJ, *et al.* (2006). Shh pathway activity is down-regulated in cultured medulloblastoma cells: implications for preclinical studies. *Cancer Research* **66**: 4215–4222.

Schaefer LK, Ren Z, Fuller GN, and Schaefer TS. (2002). Constitutive activation of Stat3alpha in brain tumors: localization to tumor endothelial cells and activation by the endothelial tyrosine kinase receptor (VEGFR-2). *Oncogene* **21**: 2058–2065.

Schepers AG, Snippert HJ, Stange DE, van den Born M, van Es JH, van de Wetering M, *et al.* (2012). Lineage Tracing Reveals Lgr5+ Stem Cell Activity in Mouse Intestinal Adenomas. *Science* **337**: 730–735.

Schüller U, Heine VM, Mao J, Kho AT, Dillon AK, Han Y-G, *et al.* (2008). Acquisition of Granule Neuron Precursor Identity Is a Critical Determinant of Progenitor Cell Competence to Form Shh-Induced Medulloblastoma. *Cancer Cell* **14**: 123–134.

Segre JA, Bauer C, and Fuchs E. (1999). Klf4 is a transcription factor required for establishing the barrier function of the skin. *Nat Genet* **22**: 356–360.

Sengupta A, Banerjee D, Chandra S, Banerji SK, Ghosh R, Roy R, *et al.* (2007). Deregulation and cross talk among Sonic hedgehog, Wnt, Hox and Notch signaling in chronic myeloid leukemia progression. *Leukemia*.

Shackleton M, Quintana E, Fearon ER, and Morrison SJ. (2009). Heterogeneity in cancer: cancer stem cells versus clonal evolution. *Cell* **138**: 822–829.

Sherry M, Reeves A, Wu J, and Cochran B. (2009). STAT3 is required for proliferation and maintenance of multipotency in glioblastoma stem cells. *Stem Cells*.

Shields JM, Christy RJ, and Yang VW. (1996). Identification and characterization of a gene encoding a gut-enriched Krüppel-like factor expressed during growth arrest. *J Biol Chem* **271**: 20009–20017.

Singh SK, Clarke ID, Terasaki M, Bonn VE, Hawkins C, Squire J, *et al.* (2003). Identification of a cancer stem cell in human brain tumors. *Cancer Research* **63**: 5821–5828.

Singh SK, Hawkins C, Clarke ID, Squire JA, Bayani J, Hide T, *et al.* (2004). Identification of human brain tumour initiating cells. *Nature* **432**: 396–401.

Sottile V, Li M, and Scotting PJ. (2006). Stem cell marker expression in the Bergmann glia population of the adult mouse brain. *Brain Res.* **1099**: 8–17.

Spike BT, and Wahl GM. (2011). p53, Stem Cells, and Reprogramming: Tumor Suppression beyond Guarding the Genome. *Genes & Cancer* **2**: 404–419.

Stecca B, and Ruiz i Altaba A. (2009). A GLI1-p53 inhibitory loop controls neural stem cell and tumour cell numbers. *EMBO J* **28**: 663–676.

Stephens JM, Lumpkin SJ, and Fishman JB. (1998). Activation of signal transducers and activators of transcription 1 and 3 by leukemia inhibitory factor, oncostatin-M, and interferon-gamma in adipocytes. *J Biol Chem* **273**: 31408–31416.

Suh H, Consiglio A, Ray J, Sawai T, D'Amour KA, and Gage FH. (2007). In Vivo Fate Analysis Reveals the Multipotent and Self-Renewal Capacities of Sox2+ Neural Stem Cells in the Adult Hippocampus. *Cell Stem Cell* **1**: 515–528.

Sun Y, Kong W, Falk A, Hu J, Zhou L, Pollard S, *et al.* (2009). CD133 (Prominin) negative human neural stem cells are clonogenic and tripotent. *PLoS ONE* **4**: e5498.

Suslov ON, Kukekov VG, Ignatova TN, and Steindler DA. (2002). Neural stem cell heterogeneity demonstrated by molecular phenotyping of clonal neurospheres. *Proc Natl Acad Sci USA* **99**: 14506–14511.

Sutter R, Shakhova O, Bhagat H, Behesti H, Sutter C, Penkar S, *et al.* (2010). Cerebellar stem cells act as medulloblastoma-initiating cells in a mouse model and a neural stem cell signature characterizes a subset of human medulloblastomas. *Oncogene*: 1–12.

Swartling FJ, Grimmer MR, Hackett CS, Northcott PA, Fan Q-W, Goldenberg DD, *et al.* (2010). Pleiotropic role for MYCN in medulloblastoma. *Genes & Development* **24**: 1059–1072.

Tabori U, Baskin B, Shago M, Alon N, Taylor MD, Ray PN, *et al.* (2010). Universal poor survival in children with medulloblastoma harboring somatic TP53 mutations. *Journal of Clinical Oncology* **28**: 1345–1350.

Takahashi K, and Yamanaka S. (2006). Induction of pluripotent stem cells from mouse embryonic and adult fibroblast cultures by defined factors. *Cell* **126**: 663–676.

Takanaga H, Tsuchida-Straeten N, Nishide K, Watanabe A, Aburatani H, and Kondo T. (2009). Gli2 is a novel regulator of sox2 expression in telencephalic neuroepithelial cells. *Stem Cells* **27**: 165–174.

Taupin P, Ray J, Fischer WH, Suhr ST, Hakansson K, Grubb A, *et al.* (2000). FGF-2-responsive neural stem cell proliferation requires CCg, a novel autocrine/paracrine cofactor. *Neuron* **28**: 385–397.

Taylor MD, Northcott PA, Korshunov A, Remke M, Cho Y-J, Clifford SC, *et al.* (2012). Molecular subgroups of medulloblastoma: the current consensus. *Acta Neuropathol.* **123**: 465–472.

Thomas KR, and Capecchi MR. (1990). Targeted disruption of the murine int-1 proto-oncogene resulting in severe abnormalities in midbrain and cerebellar development. *Nature* **346**: 847–850.

Thomas PR, Deutsch M, Kepner JL, Boyett JM, Krischer J, Aronin P, *et al.* (2000). Low-stage medulloblastoma: final analysis of trial comparing standard-dose with reduced-dose neuraxis irradiation. *J Clin Oncol* **18**: 3004–3011.

Tropepe V, Sibilia M, Ciruna BG, Rossant J, Wagner EF, and Van Der Kooy D. (1999). Distinct neural stem cells proliferate in response to EGF and FGF in the developing mouse telencephalon. *Dev Biol* **208**: 166–188.

Turkson J, Bowman T, Adnane J, Zhang Y, Djeu JY, Sekharam M, *et al.* (1999). Requirement for Ras/Rac1-mediated p38 and c-Jun N-terminal kinase signaling in Stat3 transcriptional activity induced by the Src oncoprotein. *Mol Cell Biol* **19**: 7519–7528.

Uchida N, Buck DW, He D, Reitsma MJ, Masek M, Phan TV, *et al.* (2000). Direct isolation of human central nervous system stem cells. *Proc Natl Acad Sci USA* **97**: 14720–14725.

Utikal J, Polo JM, Stadtfeld M, Maherali N, Kulalert W, Walsh RM, *et al.* (2009). Immortalization eliminates a roadblock during cellular reprogramming into iPS cells. *Nature* **460**: 1145–1148.

Varnat F, Siegl-Cachedenier I, Malerba M, Gervaz P, and Ruiz i Altaba A. (2010). Loss of WNT-TCF addiction and enhancement of HH-GLI1 signalling define the metastatic transition of human colon carcinomas. *EMBO Mol Med* **2**: 440–457.

Ventura A, Meissner A, Dillon CP, McManus M, Sharp PA, Van Parijs L, *et al.* (2004). Cre-lox-regulated conditional RNA interference from transgenes. *Proc Natl Acad Sci USA* **101**: 10380–10385.

Villalva C, Martin-Lannerée S, Cortes U, Dkhissi F, Wager M, Le Corf A, *et al.* (2011). STAT3 is essential for the maintenance of neurosphere-initiating tumor cells in patients with glioblastomas: a potential for targeted therapy? *Int J Cancer* **128**: 826–838.

Visvader JE, and Lindeman GJ. (2008). Cancer stem cells in solid tumours: accumulating evidence and unresolved questions. *Nat Rev Cancer* **8**: 755–768.

Visvader JE, and Lindeman GJ. (2012). Cancer Stem Cells: Current Status and Evolving Complexities. *Stem Cell* **10**: 717–728.

Walkley CR, Olsen GH, Dworkin S, Fabb SA, Swann J, McArthur GA, *et al.* (2007). A microenvironment-induced myeloproliferative syndrome caused by retinoic acid receptor gamma deficiency. *Cell* **129**: 1097–1110.

Wang J, Pham-Mitchell N, Schindler C, and Campbell IL. (2003). Dysregulated Sonic hedgehog signaling and medulloblastoma consequent to IFN-alpha-stimulated STAT2-independent production of IFN-gamma in the brain. *J Clin Invest* **112**: 535–543.

Wang J, Rao S, Chu J, Shen X, Levasseur DN, Theunissen TW, *et al.* (2006). A protein interaction network for pluripotency of embryonic stem cells. *Nature* **444**: 364–368.

Wang VY, and Zoghbi HY. (2001). Genetic regulation of cerebellar development. *Nat. Rev. Neurosci.* **2**: 484–491.

Ward RJ, Lee L, Graham K, Satkunendran T, Yoshikawa K, Ling E, *et al.* (2009). Multipotent CD15+ cancer stem cells in patched-1-deficient mouse medulloblastoma. *Cancer Research* **69**: 4682–4690.

Wechsler-Reya R, and Scott MP. (2001). The developmental biology of brain tumors. *Annu. Rev. Neurosci.* **24**: 385–428.

Wechsler-Reya RJ, and Scott MP. (1999). Control of neuronal precursor proliferation in the cerebellum by Sonic Hedgehog. *Neuron* **22**: 103–114.

Wetmore C, Eberhart DE, and Curran T. (2001). Loss of p53 but not ARF accelerates medulloblastoma in mice heterozygous for patched. *Cancer Research* **61**: 513–516.

Wicha MS, Liu S, and Dontu G. (2006). Cancer stem cells: an old idea--a paradigm shift. *Cancer Research* **66**: 1883–90– discussion 1895–6.

Wierenga ATJ, Vogelzang I, Eggen BJL, and Vellenga E. (2003). Erythropoietin-induced serine 727 phosphorylation of STAT3 in erythroid cells is mediated by a MEK-, ERK-, and MSK1-dependent pathway. *Experimental Hematology* **31**: 398–405.

Wong DJ, Liu H, Ridky TW, Cassarino D, Segal E, and Chang HY. (2008). Module map of stem cell genes guides creation of epithelial cancer stem cells. *Cell Stem Cell* **2**: 333–344.

Wu X, Northcott PA, Dubuc A, Dupuy AJ, Shih DJH, Witt H, *et al.* (2013). Clonal selection drives genetic divergence of metastatic medulloblastoma. *Nature* **482**: 529–533.

Yang F, Jove V, Xin H, Hedvat M, Van Meter TE, and Yu H. (2010a). Sunitinib Induces Apoptosis and Growth Arrest of Medulloblastoma Tumor Cells by Inhibiting STAT3 and AKT Signaling Pathways. *Molecular Cancer Research* **8**: 35–45.

Yang F, Van Meter TE, Buettner R, Hedvat M, Liang W, Kowolik CM, *et al.* (2008a). Sorafenib inhibits signal transducer and activator of transcription 3 signaling associated with growth arrest and apoptosis of medulloblastomas. *Molecular Cancer Therapeutics* **7**: 3519–3526.

Yang J, van Oosten AL, Theunissen TW, Guo G, Silva JCR, and Smith A. (2010b). Stat3 activation is limiting for reprogramming to ground state pluripotency. *Cell Stem Cell* **7**: 319–328.

Yang Z-J, Ellis T, Markant SL, Read T-A, Kessler JD, Bourboulas M, *et al.* (2008b).

Medulloblastoma can be initiated by deletion of Patched in lineage-restricted progenitors or stem cells. *Cancer Cell* **14**: 135–145.

Yauch RL, Dijkgraaf GJP, Alicke B, Januario T, Ahn CP, Holcomb T, *et al.* (2009). Smoothened mutation confers resistance to a Hedgehog pathway inhibitor in medulloblastoma. *Science* **326**: 572–574.

Yokogami K, Wakisaka S, Avruch J, and Reeves SA. (2000). Serine phosphorylation and maximal activation of STAT3 during CNTF signaling is mediated by the rapamycin target mTOR. *Curr Biol* **10**: 47–50.

Yoshimatsu T, Kawaguchi D, Oishi K, Takeda K, Akira S, Masuyama N, *et al.* (2006). Non-cell-autonomous action of STAT3 in maintenance of neural precursor cells in the mouse neocortex. *Development* **133**: 2553–2563.

Yu F, Li J, Chen H, Fu J, Ray S, Huang S, *et al.* (2011). Kruppel-like factor 4 (KLF4) is required for maintenance of breast cancer stem cells and for cell migration and invasion. *Oncogene* **30**: 2161–2172.

Yu F, Yao H, Zhu P, Zhang X, Pan Q, Gong C, *et al.* (2007). let-7 regulates self renewal and tumorigenicity of breast cancer cells. *Cell* **131**: 1109–1123.

Yu H, and Jove R. (2004). The STATs of cancer--new molecular targets come of age. *Nat Rev Cancer* **4**: 97–105.

Yuan X, Curtin J, Xiong Y, Liu G, Waschsmann-Hogiu S, Farkas DL, *et al.* (2004). Isolation of cancer stem cells from adult glioblastoma multiforme. *Oncogene* **23**: 9392–9400.

Zeltzer PM, Boyett JM, Finlay JL, Albright AL, Rorke LB, Milstein JM, *et al.* (1999). Metastasis stage, adjuvant treatment, and residual tumor are prognostic factors for medulloblastoma in children: conclusions from the Children's Cancer Group 921 randomized phase III study. *J Clin Oncol* **17**: 832–845.

Zhang M, Behbod F, Atkinson RL, Landis MD, Kittrell F, Edwards D, *et al.* (2008). Identification of tumor-initiating cells in a p53-null mouse model of breast cancer. *Cancer Research* **68**: 4674–4682.

Zhang P, Andrianakos R, Yang Y, Liu C, and Lu W. (2010). Kruppel-like Factor 4 (Klf4) Prevents Embryonic Stem (ES) Cell Differentiation by Regulating Nanog Gene Expression. *Journal of Biological Chemistry* **285**: 9180–9189.